ROOM AND PILLARS DESIGN FOR PHETCHABOON COAL MINE PROJECT

Sa-Nguan Choochang

A Thesis Submitted in Partial Fulfillment of the Requirements for the

Degree of Master of Engineering in Geotechnology

Suranaree University of Technology

Academic Year 2013

การออกแบบเหมืองถ่านหินใต้ดิน ชนิดห้องและเสาค้ำยัน
โครงการเหมืองถ่านหินเพชรบูรณ์

นายสงวน ชูช้าง

วิทยานิพนธ์นี้เป็นส่วนหนึ่งของการศึกษาตามหลักสูตรปริญญาวิศวกรรมศาสตรมหาบัณฑิต
สาขาวิชาเทคโนโลยีธรณี
มหาวิทยาลัยเทคโนโลยีสุรนารี
ปีการศึกษา 2556

ROOM AND PILLARS DESIGN FOR PHETCHABOON COAL MINE PROJECT

Suranaree University of Technology has approved this thesis submitted in partial fulfillment of the requirements for a Master's Degree.

Thesis Examining Committee

_____

(Dr. Prachya Tepnarong)

Chairperson

_____

(Prof. Dr. Kittitep Fuenkajorn)

Member (Thesis Advisor)

_____

(Dr. Decho Phueakphum)

Member

_____

(Prof. Dr. Sukit Limpijumnong)

Vice Rector for Academic Affairs and Innovation

_____

(Assoc. Prof. Flt. Lt. Dr. Kontorn Chamniprasart)

Dean of Institute of Engineering

สงวน ชูช้าง : การออกแบบเหมืองถ่านหินใต้ดิน ชนิดห้องและเสาค้ำยัน โครงการเหมืองถ่านหินเพชรบูรณ์ (ROOM AND PILLARS DESIGN FOR PHETCHABOON COAL MINE PROJECT) อาจารย์ที่ปรึกษา : ศาสตราจารย์ ดร.กิตติเทพ เฟื่องขจร, 123 หน้า.

การออกแบบด้านกลศาสตร์หินของเหมืองอุโมงค์ถ่านหินชนิดห้องและเสาค้ำยัน โครงการเหมืองถ่านหินเพชรบูรณ์ (PCB coal mine project) จังหวัดเพชรบูรณ์ บริเวณภาคกลางตอนบนของประเทศไทย เป็นการศึกษาวิจัยเพื่อสนองและหาแนวทางการแก้ไขปัญหาการผลิตถ่านหิน เพื่อป้อนให้แก่โรงงานอุตสาหกรรมซีเมนต์ ชั้นถ่านหินแห่งนี้เกิดอยู่ในช่วงอายุเพอร์เมี่ยนที่ถูกปิดทับด้วยหินปูนที่ระดับลึกจากผิวดิน 5-90 เมตร ซึ่งมีความหนาประมาณ 10-30 เมตร ในการขุดและเคลื่อนย้ายหน้าดินที่เป็นหินปูนเนื้อแข็งออกเพื่อเปิดทำเป็นเหมืองถ่านหินชนิดเหมืองเปิดมีต้นทุนการผลิตที่สูงมาก การออกแบบเหมืองใต้ดินผลิตถ่านหินชนิดห้องและเสาค้ำยันในขั้นแรก มีจุดประสงค์เพื่อออกแบบ เสาค้ำยันในชั้นถ่านหินที่มีความเอียงตัวประมาณ 36 องศาให้มีความปลอดภัย ห้องและเสาค้ำยันมีทั้งหมด 11 ระดับโดยเริ่มตั้งแต่ความลึก 2 เมตร ถึงลึกสุด 58 เมตร ห้องผลิตถ่านหินได้ขุดเข้าไปในมวลหินที่มีความไม่ต่อเนื่องทั้งหมด 3 แนว การวิเคราะห์ความมีเสถียรภาพโดยหลักของ Obert and Duval สำหรับการออกแบบเสาค้ำยันและเกณฑ์ของ Hoek and Brown สำหรับการออกแบบอุโมงค์แบบขนานของโครงการเหมืองถ่านหิน PCB ได้แสดงผลลัพธ์ที่สอดคล้องกับผลการออกแบบ และเมื่อเปรียบเทียบกับมาตราฐาน ตัวแปรเชิงประจักษ์ของเหมืองโชรามอน และ มูลโล่ ประเทศอัฟริกาใต้ ที่มีผลการศึกษาวิจัยความปลอดภัยเท่ากับ 1.60 พบว่าโครงการเหมืองถ่านหิน PCB มีความปลอดภัยมากกว่า 1.60 ในบริเวณที่อยู่ระดับความลึก 50 เมตร การวิเคราะห์แนวแตกของหินตามหลังคาอุโมงค์พบว่ามีโอกาศที่จะเกิดหินร่วงแบบรูปลิ่มเข้ามาภายในห้อง และจากแบบจำลองทางคอมพิวเตอร์ แสดงให้เห็นการยุบตัวของพื้นผิวบางส่วนภายหลังการขุดเจาะใต้ดิน

สาขาวิชา เทคโนโลยีธรณี ลายมือชื่อนักศึกษา _____

ปีการศึกษา 2556 ลายมือชื่ออาจารย์ที่ปรึกษา_____

SA-NGUAN CHOOCHANG : ROOM AND PILLARS DESIGN FOR PHETCHABOON COAL MINE PROJECT. THESIS ADVISOR : PROF. KITTITEP FUENKAJORN, Ph.D., P.E., 123 PP.

COAL/ROOM AND PILLAR/OPEN PIT/UNDERGROUNG MINING

The geomechanical design room and pillar coal mine project (PCB) at Phetchaboon provinces, upper part of middle region of Thailand, is studied to produce solid energy to support cement plant. The coal is deposited in Permian age and coal seams are under competent limestone with depths ranging from 5 to 90 m and 10-30 m apparent thickness. Hard rock overburden gives high cost for removal for open pit mine method. The primary underground mining design by room and pillar method is proposed to the design the safe pillar support in the coal seam. The coal seam inclines with dip angle of 36 degrees. The room and pillar are designed for 11 levels. They are starting at depth of 2 m to 58 m. Openings will be cut into the main three discontinuity sets of rock mass. The factor safety (FS) analysis of the Obert and Duval criterion for pillar and Hoek and Brown criterion for parallel tunnel at PCB coal mine project shows favorable results. When compared with the empirical standard at 1.60 factor of safety of Salamon and Munro in South Africa, PCB coal pillar has the factors of safety above 1.60 at depth about 50 m. The safety analysis for wedge failure indicates the probability of rock fall in the room. The computer simulation for subsidence shows some surface displacement after mining.

School of Geotechnology Student's Signature_____

Academic Year 2013 Advisor's Signature_____

ACKNOWLEDGEMENTS

The author wishes to acknowledge the support from the Suranaree University of Technology (SUT) who has provided funding for this research.

Grateful thanks and appreciation are given to Prof. Dr. Kittitep Fuenkajorn, thesis advisor, who lets the author work independently, but gave a critical review of this research. Many thank are also extended to Dr. Prachya Tepnarong and Dr. Decho Phueakphum, who served on the thesis committee and commented on the manuscript. Grateful thanks are given to all staffs of Geomechanics Research Unit, Institute of Engineering who supported my work

Finally, I most gratefully acknowledge my parents and friends for all their supported throughout the period of this research.

Sa-Nguan Choochang

TABLE OF CONTENTS

Page

TABLE OF CONTENTS (Continued)

Page

TABLE OF CONTENTS (Continued)

Page

TABLE OF CONTENTS (Continued)

Page

TABLE OF CONTENTS (Continued)

Page

TABLE OF CONTENTS (Continued)

Page

LIST OF TABLES

Table **Page**

LIST OF TABLES (Continued)

Table **Page**

LIST OF FIGURES

Figure **Page**

LIST OF FIGURES (Continued)

Figure **Page**

LIST OF FIGURES (Continued)

Figure **Page**

SYMBOLS AND ABBREVIATIONS

∂c	=	Maximum pillar strength
∂p	=	Average pillar stress for square pillars
∂ps	=	Average pillar stress
Ap	=	Width of the room
At	=	Width of the pillar
Bo	=	Width of the room
Bp	=	Width of the pillar
c	=	Cohesion
D_b	=	Block diameter
D_e	=	Equivalent dimension
DP	=	Drill hole
E_{mass}	=	Deformation modulus of the rock mass
f_σ	=	Massivity parameter
GSI	=	Geological strength index
H	=	Seam height
jA	=	joint alteration
J_a	=	Joint alternation number
JC	=	Joint conditions
jL	=	joint length

SYMBOLS AND ABBREVIATIONS (Continued)

J_n	=	Joint set number
JP	=	Jointing parameter combines by empirical relations JC
J_r	=	Joint roughness number
J_w	=	Joint water reduction number SRF
K	=	Constant principally for coal mines
Ko	=	Ratio between or the coefficient of geostatic stress
L	=	Extent of the mined area
P	=	Tension force
R	=	Ratio of the area extracted to the total area of the ore body mined
RMi	=	Rock mass index
RMR	=	Rock mass rating system
RQD	=	Percentage of core recovered in intact pieces of 100 mm or more in length in the total length of a borehole
RQD	=	Rock quality designation
SRF	=	Stress reduction factor
UCS	=	Uniaxial compressive strength of intact rock
V_b	=	Block volume
z	=	Depth to the mining horizon
τ	=	pillar shear strength stress

SYMBOLS AND ABBREVIATIONS (Continued)

ϕ	=	Internal friction angle
σ_{pa}	=	Average pillar stress for square pillar

CHAPTER I

INTRODUCTION

1.1 Background of problems and significance of the study

Phetsabun coal mine project is located 150 km from Saraburi to Phetsabun, belonging on high way number 21. It was govern by Lamtanen village, Nongphai district. Coal deposit was new discovery by geologist from Lanna Lignite Company on 2005. It was detailed geological exploration by core drilling campaign by geologist of Siam City Cement Company on 2008.Coal was deposited in limestone Permian age with competent limestone at depths ranging between 5 and 90 m. This is positive significant for coal production by room-and-pillar tunnel, because hard rock overburden given very high cost for removal. The results from feasibility study suggest that the coal has economic potential to develop using a room-and-pillar mining method. The geotechnical for room-and-pillar design is relied on the exploratory data, by geological field mapping, facture analysis, core drilling and rock mechanics laboratory testing. (See figure 1.1)

Rock mass classification systems are a useful tool for the preliminary design stage of the project. To classify the rock mass quality, rock mass classification systems, such as rock mass rating system (RMR), NGI tunneling quality index (Q system), rock mass index (RMi), and geological strength index (GSI) are utilized. Their rating values are used to estimate tunnel support systems and to evaluate the rock mass parameters. These empirical methods have been originally obtained from many tunneling case studies. They have been applied to many construction tunnel designs.

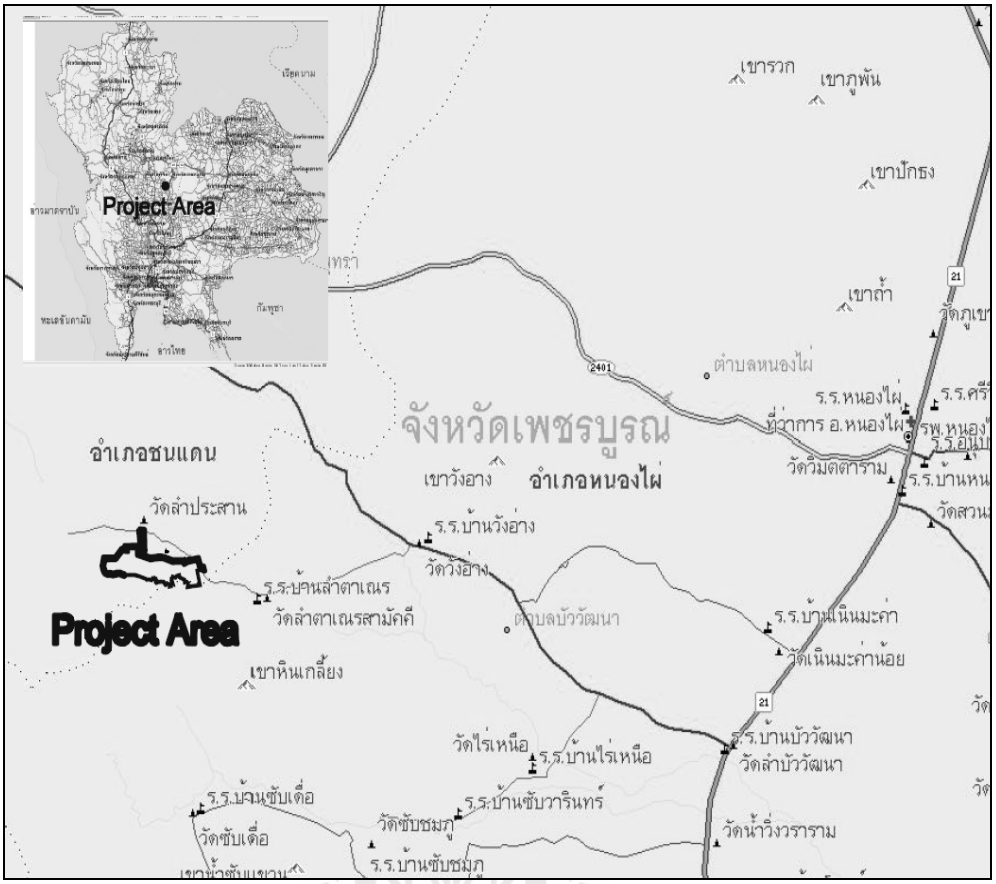

Figure 1.1 Location map of the project area (Scale 1:5000)

However, these empirical methods cannot adequately calculate stress redistributions, support performance and deformations around a tunnel. Therefore, 2D finite element software, such as UDEC, will be used for the numerical simulations. The rock mass parameters evaluated by empirical equations are utilized as input data for numerical modeling (using UDEC). The comparison will be made the results obtained from empirical methods with numerical method to assess the support systems.

1.2 Research objectives

The objective of this research is the design and tunnel support by room and pillar method for mine production at PCB coal mine project. The objective of design is to extract the maximum amount of ore that is compatible with safe working conditions and will be complying with six principles and geological and rock mechanics in this area. The principle of designs are independent, minimum uncertainly, simplify, state of the art, optimization and construct ability. The bottom line of this research is comparisons of possibility between computer simulation and empirical design.

1.3 Research methodology

This research consists of nine main tasks; literature review, Geological data Collection, Rock Mechanic Lab Test, Rock Mass Classification Room and Pillar design Computer Simulation, Comparison, Discussion and Conclusion .The last is thesis writing and presentation. The work plan is illustrated in the Figure 1.2 and has some more detail as follow these;

1.3.1 Literature review

Literature review will be carried out to study the room and pillar design, The imply of PCB coal mine project, case study in room and pillar tunnel and rock mass classification systems. The stability analysis, support estimation design of underground excavation, numerical modeling are includes in room and pillar designs. The sources of information are from journals, technical reports and conference papers. A summary of the literature review will be given in the thesis.

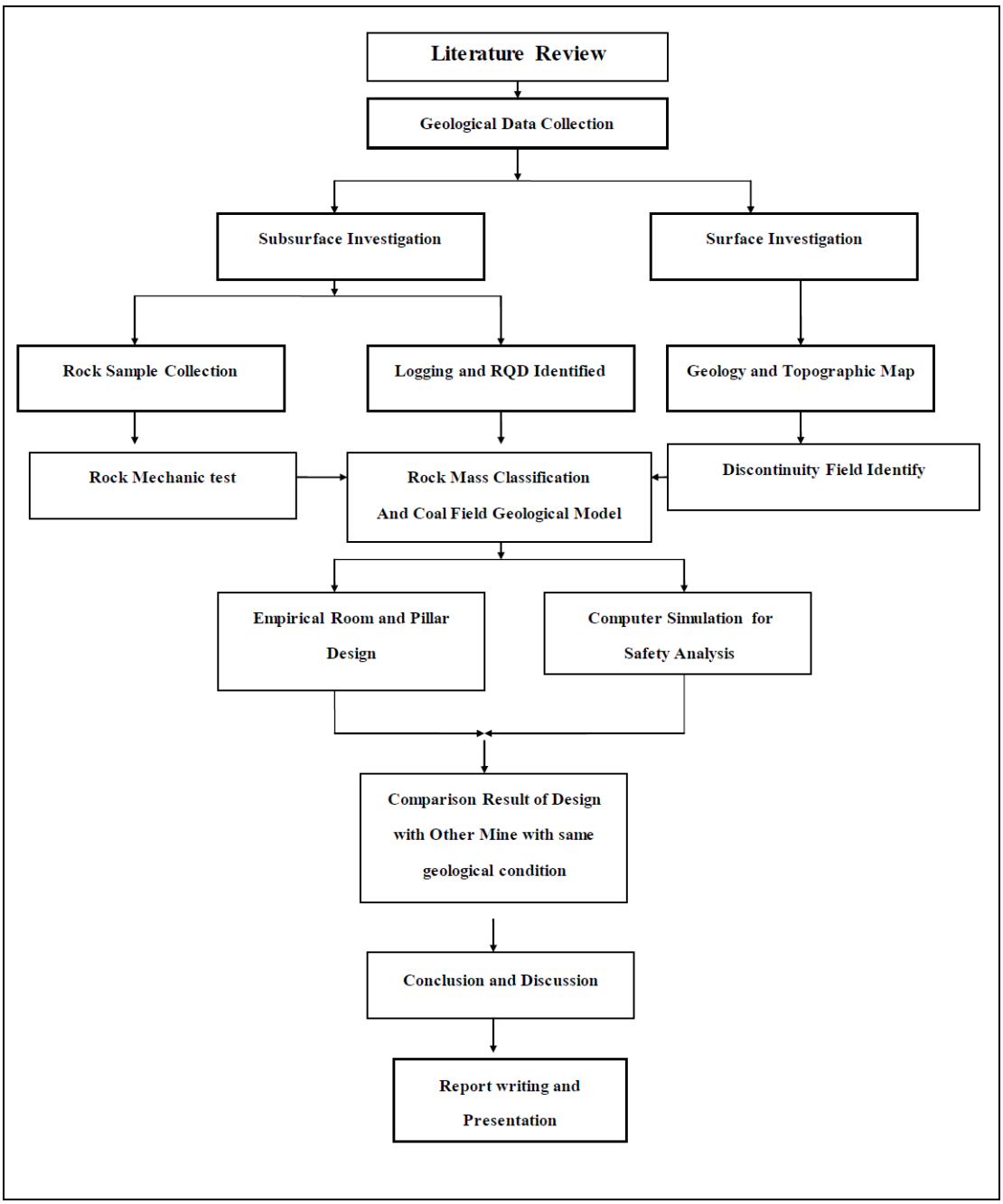

Figure 1.2 Chart of activity for research methodology

1.3.2 Geological Data Collection

Department of geology, Siam City Cement Company Office carried out the preliminary geological investigation in 2004 and 2009. The investigations

have been performed. The geotechnical evaluation of the PCB coal mine project team is relied in the surface and subsurface exploratory data, field mapping and laboratory test results.

1.3.3 Rock Mechanic Lab Test

Three core rock types from the PCB coal mine project will be used as rock samples. A minimum of 150 rock samples of Limestone and coal will be preparing comply with ASTM standard. They used in the rock mechanic testing for essential engineering property identified such as elastic modulus, Passion ratio, Shear strength Uniaxial strength and Triaxial compression strength.

1.3.4 Rock Mass Classification

Rock mass classification has the detail methodology in literature review. It used to evaluate the quality and expected behavior of rock masses based on the most important parameters that influence the rock mass quality (Basarir, Ozsan and Karakus, 2005). The result of rock mass classification becomes effective parameters for the application of the tunnel stability and design. In order to evaluate the rock mass quality, the empirical methods will be applied including rock mass rating (RMR), NGI tunneling quality index (Q system), Geological strength index (GSI) and rock mass index (RMi)

1.3.5 Room and Pillar Design

Room and pillar design has the detail methodology in literature review. The design principles will also include minimum uncertainty, simplicity, application of the state-of-the-art, optimization of the design solutions and constructability. Empirical design will perform by use character of PCB geological and rock mass quality. The principal design will calculate by rock quality RMR and Q System.

Methodology of underground mine is room and pillar method. Conceptual will use limestone is roof of room, coal will be pillar.

1.3.6 Computer Simulation

Computer simulation will use FLAC3D has been widely used in the simulation of geological materials and geotechnical engineering with nonlinearity, large deformation and instability, especially the plastic flow of the materials reaching the yield limit and the gradual destruction together with caving of tracking materials. FLAC3D modeling is based on the principle of the use of Mohr-Coulomb yield criterion to determine the damage of rock mass and reflect the strain-softening model, after the destruction of coal deformation with the development gradually reducing the residual strength of character. Based on the geological conditions and mining technology of the mining face.

The level model is established along strike length, inclined length and height. The bottom and the side border in the model use displacement constraints, and the vertical loads are imposed on the top of model to simulate the weight of overlying strata. The mechanical parameters for numerical simulation model follow with lithological column of coal resource combined with the several of physical and mechanical strength test results. The mechanical test results are Density Bulk Modulus, Shear Modulus, Cohesion, Friction Angle, and Tensile Strength were put forward a calculation scheme. The conclusion of numerical simulation is the working face advances forecast unstable suddenly and prevent roof accident.

1.3.7 Comparison of Design.

Results obtained from empirical methods design in this research will be comparisons of the design results with other mine sites that have similar geological and topographic environments to optimize the final design.

1.3.8 Discussion and Conclusion

All research activities, methods, and results will be documented and complied in the thesis. The research or findings will be published in the conferences, proceedings or journals.

1.3.9 Thesis Writing and Presentation

All aspects of the theoretical and experimental studies mentioned will be documented and incorporated into the thesis.

1.4 Scope and limitations of the study

The scope and limitations of the research include as follows.

1) The area of coal resources for this research is PCB coal mine project. It was organizing and operates by Siam City Cement Company. It located in Lamtanen village, Nong Pai district, and Phetchaboon province. This project is handling by thesis owner.

2) The coal geology and geological structures will be collected from surface and subsurface investigations by geologist of the project.

3) The rock for engineering property will collect from core in exploration drill holes and will be rock mechanic test at Suranaree University implying with ASTM standard.

4) The tunnel design for this coal mine will be room and pillar method. It will design both of computer simulation and empirical imply with coal geological and rock mechanic data.

5) The results of design will be comparisons with other mine sites that have similar geological and topographic environments to optimize the final design.

1.5 Thesis contents

Chapter I introduces the thesis by briefly describing the background of problems and significance of the study. The research objectives, methodology, scope and limitations are identified. **Chapter II** summarizes results of the literature review. **Chapter III** describes the geological data collection. **Chapter IV** presents the characterizations of rock mass class by using rock mass classification systems. **Chapter V** perform the primary underground coal mine by room and pillar method and numerical analysis factor of safety with support design. **Chapter VI** compares the result of design with other project, which same geological data condition. **Chapter VII** concludes the research results, and provides recommendations for future research studies

CHAPTER II

LITERATURE REVIEW

2.1 Introduction

This chapter summarizes the results of literature review carried out to improve an understanding of stability analysis and support design of portal, adit and vertical shaft. Topics relevant to this study involve rock mass classification systems, such as rock mass rating (RMR), NGI tunneling quality index (Q system), geological strength index (GSI), rock mass index (RMi), numerical modeling (UDEC) and published papers.

2.2 Rock mass classification systems

The rock mass characterization processes are normally used to assess the rock mass quality in accordance with the existing engineering rock mass classification systems. The result becomes effective parameters for the application of the tunnel stability and design. In any analysis of rock mass behavior that includes deformation modulus is an important input parameter. Field tests to determine this parameter directly are time consuming, expensive and the reliability of the results of these tests is sometimes questionable. Consequently, several authors have proposed empirical relationships for estimating the value of an isotropic rock mass deformation modulus based on empirical rock mass classification schemes (Hoek and Diederichs, 2005). The four methods of quantitative rock mass classifications (RMR, Q, RMi and GSI) will be applied.

2.2.1 Rock mass rating system (RMR)

Bieniswski (1973) initially developed the rock mass rating system (RMR), otherwise known as the geomechanics classification. It was modified over the years as more case histories, became available and to conform to international standards and procedures (Bieniawski, 1979).

Bieniawski provided the system as the most common quantitative method for describing the quality of the rock mass for tunneling. Uniaxial compressive strength of intact rock (UCS), rock quality designation (RQD), and spacing of discontinuities, conditions of discontinuities, ground water condition and orientation of discontinuities are utilized parameters. After the determination of the important ratings of the each parameter, they are summed to describe the basic RMR rating of the rock mass. In tunneling, the rating must be made adjustment for the discontinuity orientation. Bieniawski (1989) has provided guidelines for the selection of rock support for horseshoe shaped tunnels excavated by the drill-and-blast technique, shown in Table 2.1.

In many designing the primary support and final lining for a tunnel, the deformations of the rock mass surrounding the tunnel are important and a numerical analysis of these deformations requires an estimate of the rock mass deformation modulus. Based on the RMR rating value, many researchers have proposed different empirical equations to calculate the rock mass deformation modulus as follows:

Bieniawski (1978) has defined E_{mass} as:

$$E_{mass} = 2RMR\text{-}100 \text{ (GPa)} \qquad \text{For RMR} > 50 \qquad (2.1)$$

Serafim and Pereira (1983) have proposed:

$$E_{mass} = 10^{\left(\frac{RMR-10}{40}\right)} \text{ (GPa)} \qquad \text{For RMR} < 50 \qquad (2.2)$$

Read et al. (1999) has proposed the following equation:

$$E_{mass} = 0.1\left(\frac{RMR}{10}\right)^3 \text{ (GPa)} \qquad (2.3)$$

where E_{mass} is the deformation modulus of the rock mass.

Table 2.1 Guidelines for excavation and support of 10 m span rock tunnels in Accordance with the RMR system (After Bieniawski, 1989).

Rock mass class	Excavation	Rock bolts (20 mm diameter, fully grouted)	Shotcrete	Steel sets
I - Very good rock *RMR*: 81-100	Full face, 3 m advance.	Generally no support required except spot bolting.		
II - Good rock *RMR*: 61-80	Full face , 1-1.5 m advance. Complete support 20 m from face.	Locally, bolts in crown 3 m long, spaced 2.5 m with occasional wire mesh.	50 mm in crown where required.	None.
III - Fair rock *RMR*: 41-60	Top heading and bench 1.5-3 m advance in top heading. Commence support after each blast. Complete support 10 m from face.	Systematic bolts 4 m long, spaced 1.5 - 2 m in crown and walls with wire mesh in crown.	50-100 mm in crown and 30 mm in sides.	None.
IV - Poor rock *RMR*: 21-40	Top heading and bench 1.0-1.5 m advance in top heading. Install support concurrently with excavation, 10 m from face.	Systematic bolts 4-5 m long, spaced 1-1.5 m in crown and walls with wire mesh.	100-150 mm in crown and 100 mm in sides.	Light to medium ribs spaced 1.5 m where required.
V – Very poor rock *RMR*: < 20	Multiple drifts 0.5-1.5 m advance in top heading. Install support concurrently with excavation. Shotcrete as soon as possible after blasting.	Systematic bolts 5-6 m long, spaced 1-1.5 m in crown and walls with wire mesh. Bolt invert.	150-200 mm in crown, 150 mm in sides, and 50 mm on face.	Medium to heavy ribs spaced 0.75 m with steel lagging and forepoling if required. Close invert.

2.2.2 NGI tunneling quality index (Q system)

The Q system of rock mass classification was developed in Norway by Barton, Lien, and Lunde (1974), all of the Norwegian Geotechnical Institute. Its development represented a major contribution to the subject of rock mass classification for a number of reasons: the system was proposed based on the analysis of 212 tunnel case histories from Scandinavia, it is a quantitative classification system, and it is an engineering system facilitating the design of tunnel supports. The Q system is based on a numerical assessment of the rock mass quality using six different parameters:

1) RQD
2) Number of joint sets
3) Roughness of the most unfavorable joint or discontinuity
4) Degree of alteration or filling along the weakest joint.
5) Water inflow.
6) Stress condition

These six parameters are combined to express the ground quality with respect to stability and rock support in underground openings in the following equation:

$$Q = \frac{RQD}{J_n} \cdot \frac{J_v}{J_a} \cdot \frac{J_w}{SRF} \tag{2.4}$$

where RQD is rock quality designation, J_n is joint set number, J_r is joint roughness number, J_a is joint alternation number, J_w is joint water reduction number and SRF is

stress reduction factor. The rock quality can range from Q = 0.001 to Q = 1000 on a logarithmic rock mass quality scale.

Barton et al. (1974), relating the Q index with the stability and support requirements of underground excavations, have defined an additional parameter that is called the Equivalent Dimension D_e of excavation. This dimension is obtained by dividing the span, diameter or wall height of excavation by a quantity called the excavation support ratio, ESR. Hence:

$$D_e = \frac{\text{Excavation span, diameter or height (m)}}{\text{Excavation Support Ratio, ESR}} \tag{2.5}$$

The value of ESR is the so-called excavation support ratio. It ranges between 0.5 and 5. For the diversion tunnel, the excavation support ratio, ESR is defined as 1.6. The value of ESR is related to the intended use of the excavation and to the degree of security, which is influence on the support system to be installed to maintain the stability of the excavation. The equivalent dimension, D_e, plotted against the value of Q is used to define a number of support categories in a chart published in the original paper (Barton et al., 1974). This chart has later been updated to directly give the support. Grimstad and Barton (1993) made another update to reflect the increasing use of steel fiber, reinforced shotcrete in underground excavation support, shown in Figure 2.1.

The Q-values and support in Figure 2.1 are related to the total amount of support (temporary and permanent) in the roof. The diagram is based on numerous tunnel support cases. Wall support can also be found by applying the wall height and the following adjustments to Q:

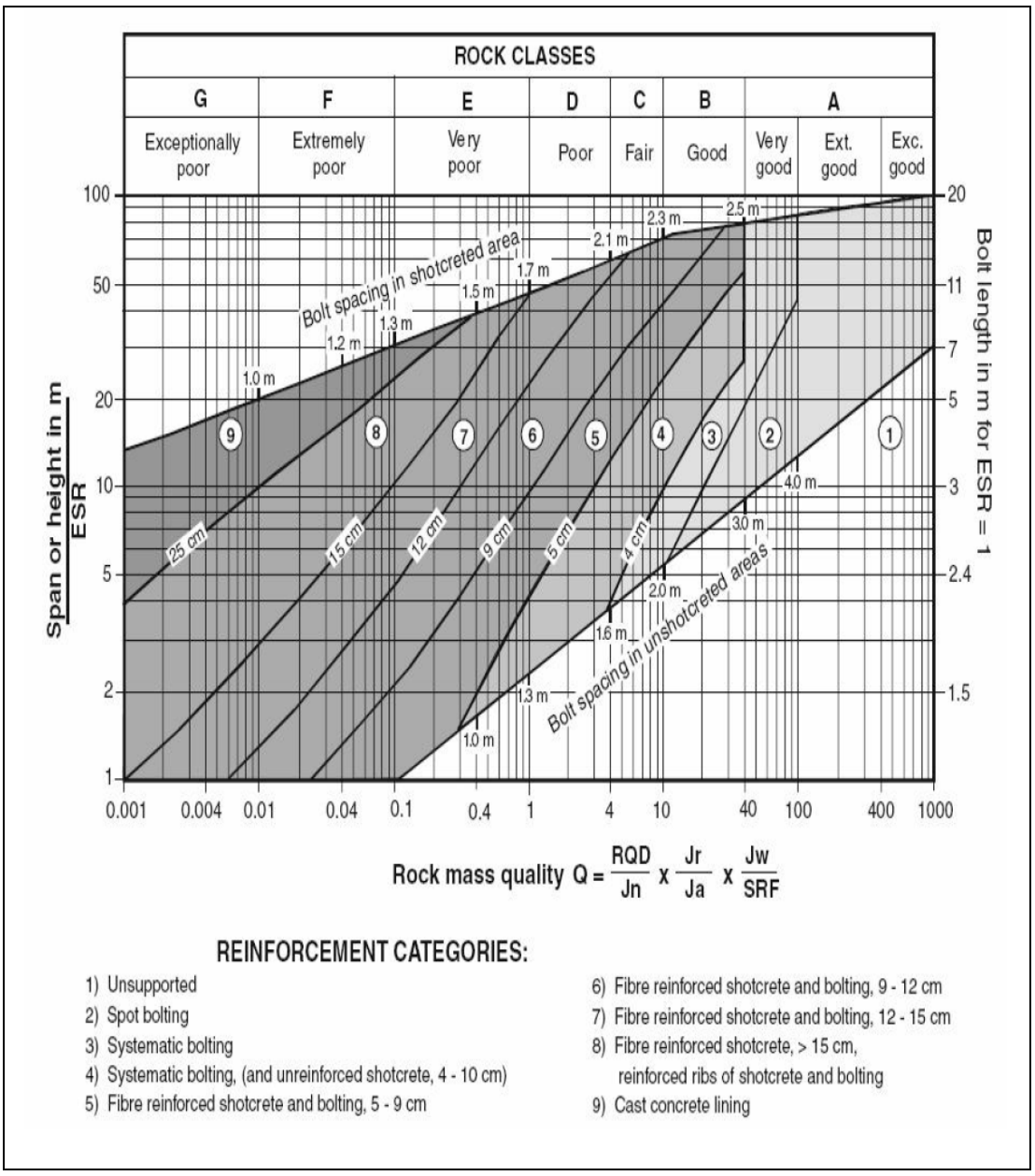

Figure 2.1 Estimated support categories based on the tunneling quality index Q (After Grimstad and Barton, 1993, reproduced from Palmstrom and Broch, 2006).

For $Q > 10$	use	$Q_{wall} = 5Q$	(2.6)
For $0.1 < Q < 10$	use	$Q_{wall} = 2.5Q$	(2.7)
For $Q < 0.1$	use	$Q_{wall} = Q$	(2.8)

The use of the Q classification system can be of considerable benefit during the feasibility and preliminary design stages of a project, when very little detailed information on the rock mass and its stress and hydrologic characteristics is available (Palmstrom and Broch, 2006).

Quantitative classification systems are used to estimate the deformation modulus of rock masses, E_m. Simple equations have been presented from the Q-system as follow:

Grimstad and Barton (1993) have proposed the equation for Q > 1:

$$E_m = 25 \log Q \quad \text{(GPa)} \tag{2.9}$$

E_m was expressed as below by Barton (2002).

$$E_m = 10\, Q_c^{1/3} = 10\, (Q \times \frac{\sigma_c}{100})^{1/3} \tag{2.10}$$

where Q_c is the normalization of Q-value and σ_c is uniaxial compressive strength of intact rock.

2.2.3 Rock mass index (RMi)

The rock mass index (RMi) was first presented by Palmström in 1995 and has been further developed and presented in several papers. It is a volumetric parameter indicating the approximate uniaxial compressive strength of a rock mass. The RMi value is applied as input for estimating rock support and input to other rock engineering methods Palmström (2009). The RMi system has some input parameters similar to those of the Q system. Thus, the joint and jointing features are almost the same.

The input parameters used can be determined by commonly used field observations and measurements. The RMi value can be calculated as follow:

For Jointed rock:

$$RMi = \sigma_c \times JP \tag{2.11}$$

where σ_c is uniaxial compressive strength of the intact rock, JP is the jointing parameter combines by empirical relations JC (joint conditions) and V_b (block volume) in the following exponential equation derived from strength tests on large jointed rock samples:

$$JP = 0.2\ \sqrt{JC}\ \ V_b^{D} \qquad (D = 0.37\ JC^{-0.2}) \tag{2.12}$$

Where JC = jR × jL/jA (jR = the joint roughness, jA = the joint alteration, and jL = the joint length). For massive rock,

$$RMi = \sigma_c \times f_\sigma \text{ (applied for cases where } f_\sigma > JP) \tag{2.13}$$

Where f_σ is called the massivity parameter, given as $f_\sigma = \sigma_c\ (0.05/D_b)^{0.2}$ (D_b = block diameter). In most cases, $f_\sigma \approx 0.5$.

The RMi requires more calculations than the RMR and the Q system, but the spreadsheets have been developed (see www.rockmass.net) from which the RMi value and the type(s) and amount of rock support can be found directly. For the estimation of RMi value and RMi support design, RMi-calc., version 2 and RMi support, version 3.1 will be used (www.rockmass.net).

2.2.4 Geological strength index (GSI)

The geological strength index (GSI) is a system of rock mass characterization that has been developed in engineering rock mechanics to meet the need for reliable input data, particularly those related to rock mass properties required as inputs into numerical analysis or closed form solutions for designing tunnels, slopes or foundations in rocks. The rock mass characterization is straightforward and it is based upon the visual impression of the rock structure, in terms of blockiness, and

Table 2.2 The modified quantitative GSI system (Sonmez, H. and Ulusay, R., 1999)

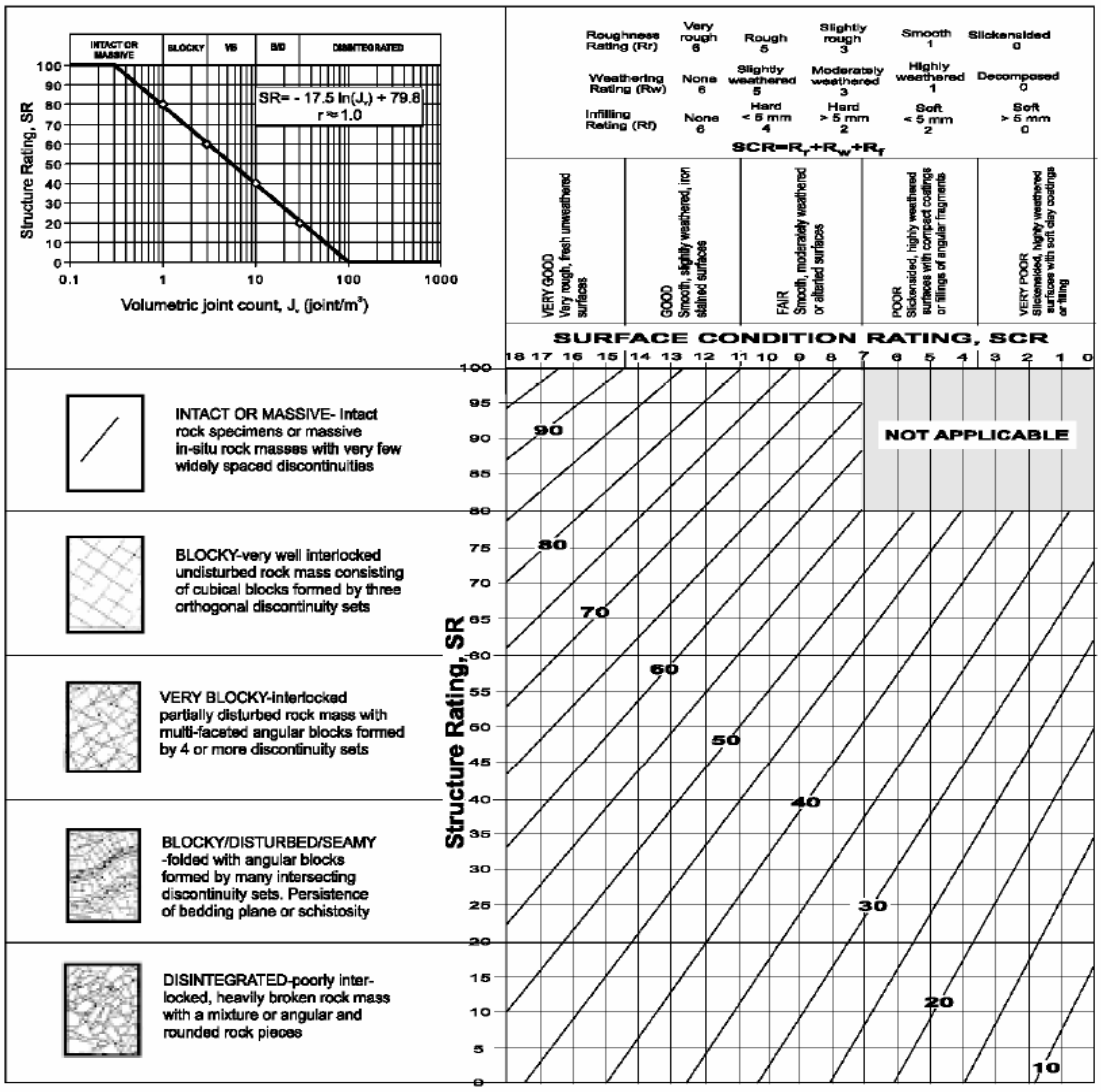

The surface condition of the discontinuities was indicated by joint roughness and alteration. The combination of these two parameters provides a practical basis for describing a wide range of rock mass types, with diversified rock structure ranging from very tightly interlocked strong rock fragments to heavily crushed rock masses. Based on the rock mass description the value of GSI is estimated from the contours.

Table 2.3 Field estimates of uniaxial compressive strength of intact rock (Marinos and Hoek, 2000)

Grade*	Term	Uniaxial Comp. Strength (MPa)	Point Load Index (MPa)	Field estimate of strength	Examples
R6	Extremely Strong	> 250	>10	Specimen can only be chipped with a geological hammer	Fresh basalt, chert, diabase, gneiss, granite, quartzite
R5	Very strong	100 - 250	4 - 10	Specimen requires many blows of a geological hammer to fracture it	Amphibolite, sandstone, basalt, gabbro, gneiss, granodiorite, peridotite , rhyolite, tuff
R4	Strong	50 - 100	2 - 4	Specimen requires more than one blow of a geological hammer to fracture it	Limestone, marble, sandstone, schist
R3	Medium strong	25 - 50	1 - 2	Cannot be scraped or peeled with a pocket knife, specimen can be fractured with a single blow from a geological hammer	Concrete, phyllite, schist, siltstone
R2	Weak	5 - 25	**	Can be peeled with a pocket knife with difficulty, shallow indentation made by firm blow with point of a geological hammer	Chalk, claystone, potash, marl, siltstone, shale, rocksalt,
R1	Very weak	1 - 5	**	Crumbles under firm blows with point of a geological hammer, can be peeled by a pocket knife	Highly weathered or altered rock, shale
R0	Extremely Weak	0.25 - 1	**	Indented by thumbnail	Stiff fault gouge

* Grade according to Brown (1981).
** Point load tests on rocks with a uniaxial compressive strength below 25 MPa are likely to yield highly ambiguous results.

Due to lack of the parameters to describe surface conditions of the discontinuities and the rock mass structure in the GSI system, two terms namely, structure rating (SR) based on volumetric joint count (j_v) and surface condition rating, (SCR) estimated from the input parameters (e.g., roughness, weathering and infilling) were suggested by Sonmez and Ulusay (1999), shown in Table 2.3.

Table 2.4 Values of the constant m_i for intact rock (Marinos and Hoek, 2000)

	Rock type	Class	Group	Texture			
				Coarse	Medium	Fine	Very fine
SEDIMENTARY		Clastic		Conglomerates * Breccias *	Sandstones 17 ± 4	Siltstones 7 ± 2 Greywackes (18 ± 3)	Claystones 4 ± 2 Shales (6 ± 2) Marls (7 ± 2)
		Non-Clastic	Carbonates	Crystalline Limestone (12 ± 3)	Sparitic Limestones (10 ± 2)	Micritic Limestones (9 ± 2)	Dolomites (9 ± 3)
			Evaporites		Gypsum 8 ± 2	Anhydrite 12 ± 2	
			Organic				Chalk 7 ± 2
METAMORPHIC		Non Foliated		Marble 9 ± 3	Hornfels (19 ± 4) Metasandstone (19 ± 3)	Quartzites 20 ± 3	
		Slightly foliated		Migmatite (29 ± 3)	Amphibolites 26 ± 6	Gneiss 28 ± 5	
		Foliated**			Schists 12 ± 3	Phyllites (7 ± 3)	Slates 7 ± 4
IGNEOUS		Plutonic	Light	Granite 32 ± 3 Granodiorite (29 ± 3)	Diorite 25 ± 5		
			Dark	Gabbro 27 ± 3 Norite 20 ± 5	Dolerite (16 ± 5)		
		Hypabyssal		Porphyries (20 ± 5)		Diabase (15 ± 5)	Peridotite (25 ± 5)
		Volcanic	Lava		Rhyolite (25 ± 5) Andesite 25 ± 5	Dacite (25 ± 3) Basalt (25 ± 5)	
			Pyroclastic	Agglomerate (19 ± 3)	Breccia (19 ± 5)	Tuff (13 ± 5)	

* Conglomerates and breccias may present a wide range of m_i values depending on the nature of the cementing material and the degree of cementation, so they may range from values similar to sandstone, to values used for fine grained sediments (even under 10).
** These values are for intact rock specimens tested normal to bedding or foliation. The value of mi will be significantly different if failure occurs along a weakness plane.

The basic input consists of estimates or measurements of the uniaxial compressive strength (σ_c) and a material constant (m_i) that is related to the frictional

properties of the rock. Ideally, these basic properties should determine by laboratory testing as described by Hoek and Brown (1997) but, in many cases, the information is required before laboratory tests have been completed and the condition that the laboratory testing is not available. To meet this need, Marions and Hoek (2000) reproduced the tables that can be used to estimate values for these parameters are reproduced in Tables 2.3 and 2.4.

Using the GSI system, provided the UCS value is known the rock mass deformation modulus E_m for $\sigma_{ci} \leq 100$ MPa is estimated in GPa from the following equation (Hoek et al, 2002).

$$E_m \text{ (GPa)} = (1- \frac{D}{2}) \sqrt{\frac{\sigma_{ci}}{100}} \times 10^{\left(\frac{GSI-10}{40}\right)} \quad (2.14)$$

For $\sigma_{ci} > 100$ MPa, use equitation 15.

$$E_m \text{ (GPa)} = (1- \frac{D}{2}) \times 10^{\left(\frac{GSI-10}{40}\right)} \quad (2.15)$$

The original equation proposed by Hoek and Brown has been modified, by the inclusion of the factor D, to allow for the effects of blast damage and stress relaxation.

2.3 Deere's rock quality designation (RQD)

In 1964, Deere proposed a quantitative index of rock mass quality based upon core recovery by diamond drilling, but it was not until 1967 that the concept was presented for the first time in a published form Deere et al. (1967). It has come to be

very widely used and has been shown to be particularly useful in classifying rock masses for the selection of tunnel support.

The RQD is defined as the percentage of core recovered in intact pieces of 100 mm or more in length in the total length of a borehole (After Deere, 1989). Hence:

$$\text{RQD (\%)} = 100 \times \frac{\text{Length of core in pieces} \geq 100\,\text{mm}}{\text{Length of borehole}} \tag{2.16}$$

Palmstrom (1982) has suggested that when core is unavailable, the RQD can be estimated from the number of joints (discontinuities) per unit volume with the following equation:

$$\text{RQD} = 115 - 3.3J_v \tag{2.17}$$

where J_v is the total number of joints per cubic meter (volumetric joint count). The RQD is used as a standard parameter in drill core logging and forms a basic element of the two major rock mass classification systems such as rock mass rating system (RMR) and NGI tunneling quality index (Q system).

2.4 Room and Pillar Design

The applications of pillar mining have been discussed by Hamrin (1982) and Hittman Associates (Anon., 1976) among others. Suitable conditions include ore bodies that are horizontal or have a dip of less than 30°. A major requirement is that the hanging wall is relatively competent over a short period of time, or is capable of support by rock bolts that are used extensively in room and pillar mining. The method

is particularly suited to bedded deposits of moderate thickness (6 to 20 ft, or 2 to 6 m) such as coal (the main application) salt, potash, and limestone.

2.4.1 Pillar Stress

The major recent work on stresses acting on pillars has been carried out by Coates (1981). He started with the simplest and traditional statement of average pillar stress, known as the tributary area method. This assumes that each of the pillars left during excavation supports all the overlying strata that are "tributary" to their location. Then the average pillar stress for square pillars with rooms of consistent width is

$$\sigma_{pa} = \sigma_2 \frac{(B_p + B_o)}{B_p} \tag{2.18}$$

Where *Bp* and *Bo* are width of the pillar and room, respectively (Fig.1), and is the geostatic or pre mining stress acting normal to the plane of excavation. If this is horizontal, then

$$\sigma_2 = yz \tag{2.19}$$

Where rock average unit weight and z is depth to the mining horizon. This can be stated more simply for the common case of rectangular or irregular shaped pillars in terms of the extraction ratio *R*, where *R* = is the ratio of the area extracted to the total area of the ore body mined. Since 1 – *R* = Eq. 2.18 can be more generally stated.

$$\sigma_{pa} = \sigma_z \left(\frac{1}{1 - R} \right) \tag{2.20}$$

This approach assumes that the mined area is extensive and shallow, that the mined rock is horizontally stratified, and that the pillars are equidimensional. It specifically ignores the relative extent and depth of the mined area, the stress component parallel to the plane of mining, the relative deformation properties of pillar, roof, and floor rocks, and the positions of the pillars in the mining zone. Taking some of these into account, Coates (1981) obtained a more general solution, principally for deep, long, mine pillars but applicable generally, by solving the statically indeterminate net deflection of the roof and floor rocks resulting from mining. Then the solution for average pillar stress becomes

$$\sigma_{pa} = \sigma_z \left\{ \frac{\left[2R - K_o \frac{H}{L} \left(\frac{1-2v_w}{1-v_w} \right) - \frac{v_p}{1-v_p} k_o \frac{H}{L} \frac{E_w}{E_p} \right]}{\frac{H}{L} \frac{E_w}{E_p} + 2(1-R)\left(1+\frac{1}{N} \right) + 2\frac{RB}{L} \frac{(1-2v_w)}{(1-v_w)}} \right\} \tag{2.21}$$

Where *H* is seam height; *L* is the extent of the mined area; *Ko* is the ratio between or the coefficient of geostatic stress; and *Ew*, *Ep, vw*, and *vp* are the elastic constants of the wall (roof and floor) and pillar materials.

This is a two-dimensional elastic solution in plane strain and requires, strictly speaking, a length/width ratio of about 3 or more to be applicable. An analytical three-dimensional approach is not feasible, although finite element and boundary element methods (see for instance Tang and Peng, 1988) can be used to give a numerical solution.

Coates' (1981) approach is helpful in that it can be used to illustrate simply several of the fundamental characteristics of strata and geometry that affect pillar stresses. Some of these are illustrated in Figure 2.2. For instance, as the *Ew /Ep*

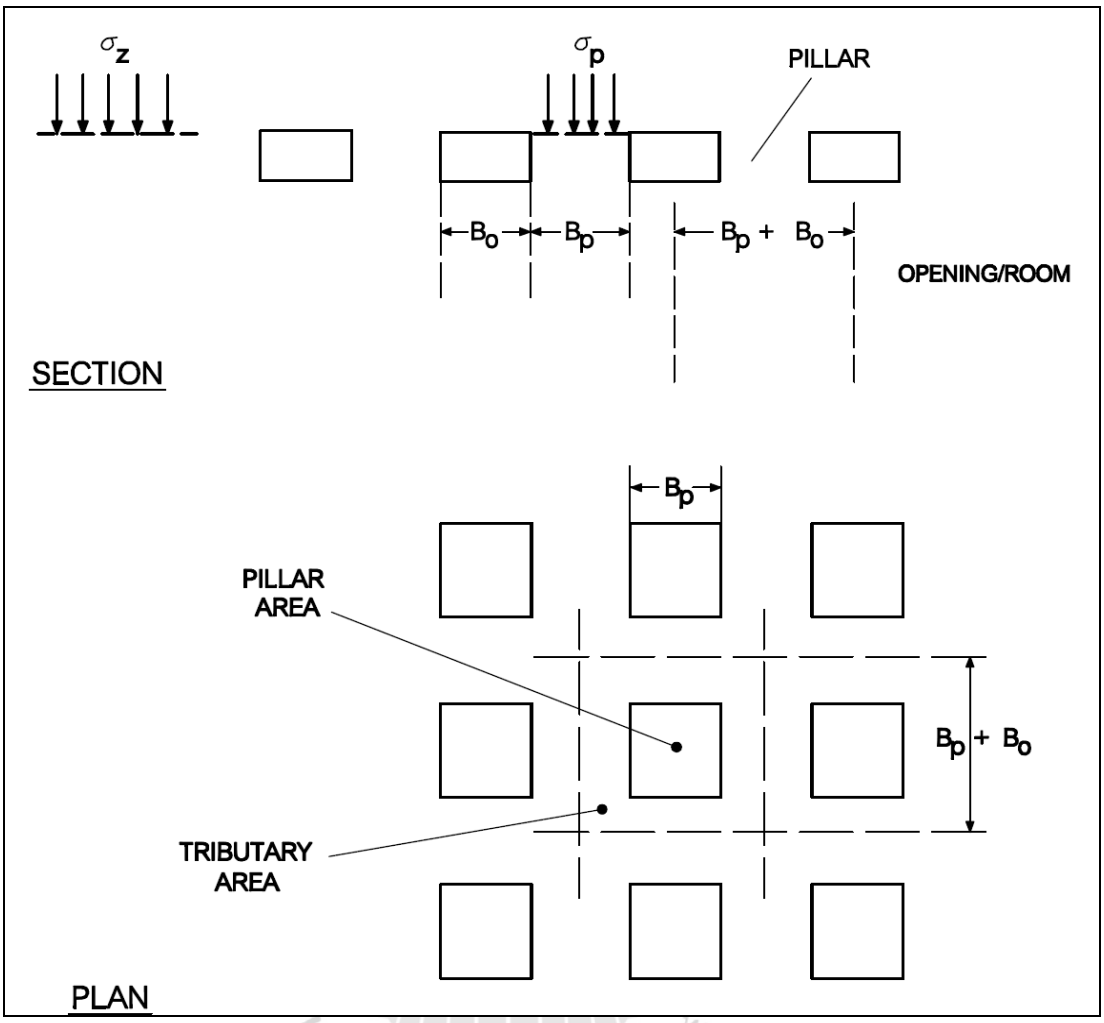

Figure 2.2 Section and plans of rooms and pillars

ratio rises so the pillar stress is reduced from a magnitude close to (the extraction ratio has been chosen as 80%) to a level of for *H/L* = *B/L* = 0.1. This illustrates the bridging effect of the stiffer roof and floor layers and the tendency to transfer stress to the side abutment. Similarly, as *L* is decreased the pillar stress is reduced from a maximum magnitude of to zero and *H/L* = 0.4 for a *Ew /Ep*, ratio of 6.Again this can be attributed to bridging at low spans. As a further illustration using fixed values for

Ew /Ep,H/L, B/L, there is considerable variation between the tributary area calculation (Eqs. 1 and 4) for stress at increasing extraction ratios.

It should be emphasized that this is used as an illustration, and that measurements of *average* pillar stresses are very in frequent. In fact, a review of the literature shows virtually no reliable measurements of average stress, principally because such measurements are difficult to obtain. One of the more interesting sets of data is by Orawecz (1977) from work in South African coal mines. He describes two case histories in which surface settlements and underground displacements were measured using leveling and anchors in boreholes drilled from the surface to the seam level and below. The seams were at average depths of 131 ft (40 m) and 223 ft (68 m). The purpose of the measurements was to test an analog model, and satisfactory simulation allowed computation of pillar stresses from observed seam deformations.

The pillar geometries and data on the mining and instrumentation layouts are illustrated in Figs. 3 and 4 these are quite close to the pillar stresses computed from the tributary area equation (Eq.2.22). In these cases, the *Ew /Ep* and *H/L* ratios were, respectively, 3 and 0.01 and 2 and 0.05, and it can be seen from Figure 2.3 that such a result would be expected. It is interesting to note the reduced pressure on the pillars adjacent to the rib side, and also the relatively low level of the abutment stress. The former would be expected; the latter is rather surprising and implies some weakening of the abutment.

$$\frac{\sigma_p}{\sigma_z} = \frac{\left(2R - 0.5H/L\right) - \left(0.5H/LXE_o/E_p\right)}{H/LXE_w/E_p + 2\left(1-R\right) + RB/L} \tag{2.22}$$

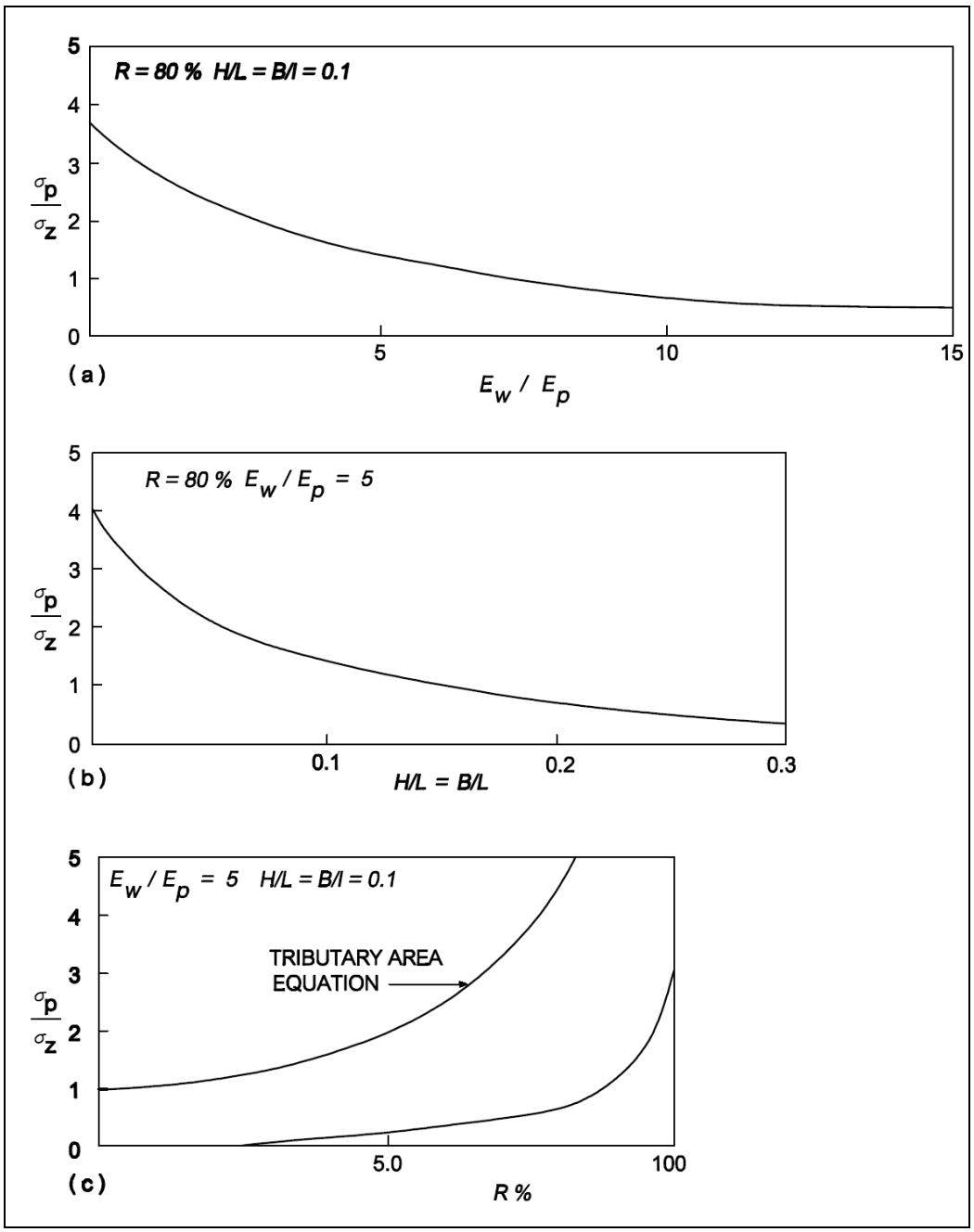

Figure2.3 Estimates of pillar stress as a proportion of vertical stress putting *K0* = 1, *vp* = *vw* = 0.33, and *N* large

The concept of average pillar stress is not a good one, since pillar stresses are not evenly distributed. This can be illustrated simply by stress analysis. A simple two-dimensional boundary element program developed by Bray and Hocking among

others, is included in Hoek and Brown (1981). This can be used, after modification, to calculate stresses around an opening or openings in a homogeneous, isotropic, linearly elastic material, under conditions of plane strain in an infinite medium subjected to various combinations of uniform field stresses or external loadings.

Typical solutions are given in Hoek and Brown, and the solutions for square and rectangular openings. This takes the stress distribution and assumes initially two square rooms of dimension at a distance 4a apart. Then the minor principal stress or confining stress in the pillar between the two can be projected on to a graph of minor principal stress against pillar width, to give the minor principal stress distribution and the average minor principal stress. This can be computed for pillars of any width and the resultant distribution can be used to compute the ultimate pillar strength using the strength envelope of the rock or coal in the form.

$$\sigma_{lf} = \sigma_{cf} + K_p \sigma_3 \tag{2.23}$$

Then can be compared with the pillar stress computed from the tributary area Eq. 5.1.1 to obtain an estimate of safety factor.

2.4.2 Pillar Strength

There is a large literature on pillar strength, much of it empirical. The most complete work is by Salamon and Monro (1967), and the best summaries by Bieniawski (1981) and Tsur- Lavie and Denekamp (1982). The basic problem with pillar strength is that in a brittle rock, strength is dependent upon the size, and to a lesser extent, the shape of a test specimen. This means that the conventional method of pillar design, relating rock strength to pillar stress through a factor of safety is

unacceptable in brittle rocks, although it may be acceptable in more ductile rocks. The reason for this is evident: if failure occurs in a brittle manner, the strain energy stored in a pillar will be released from a volume onto a shear or tensile failure plane, where it will be distributed as surface energy per unit area of fracture surface; a constant for a particular rock.

This is the basis of the Griffith failure criterion and is explained in Farmer (1985). Since energy is proportional to the square of stress, this means that strength will be inversely proportional to the square root of the dimension of the rock specimen, an observation confirmed experimentally by Bieniawski (1981) and Singh (1981) for various rocks including coal. In terms of pillar and rock strength, this can be expressed

$$\frac{\sigma_{pf}}{\sigma_{cf}} = \left(\frac{L_s}{L_p}\right)^{1/2} = \left(\frac{V_s}{V_p}\right)^{1/6} = \left(\frac{V_s}{V_p}\right)^{0.17} \quad (2.24)$$

Where L and V represent dimension and volume, respectively, and the subscripts s and p refer to the laboratory specimen for strength testing and the pillar, respectively. In the ductile case, the energy is not transferred onto fracture surfaces but evenly distributed in the specimen or pillar. Then the exponent approaches unity. Thus, in the case of wide pillars, and pillars in pseudo-ductile rocks such as rock salt can be modified. The relevance of Eq. 6 can, however, be confirmed by the empirical work of Hardy and Agapito (1977) on oil shale pillars in western Colorado. They proposed a general pillar formula which is recommended for all brittle rocks—that is, where the pillars fail in tension or shear—in the form,

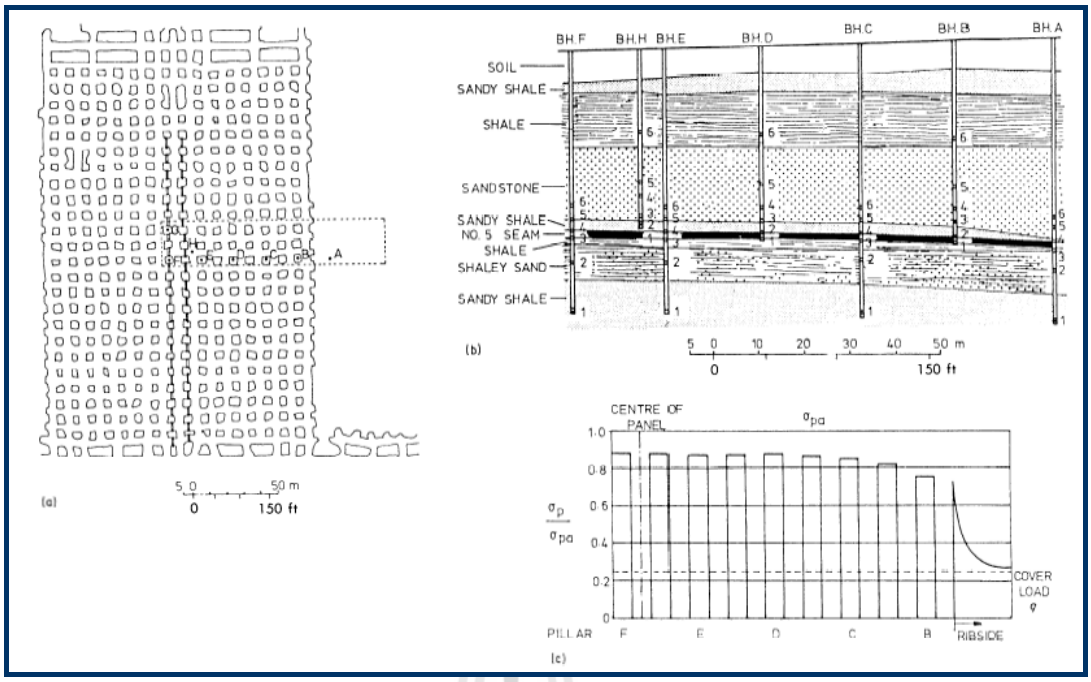

Figure2.4 Estimation of pillar stress as a proportion of pillar stress computed from tributary area theory from experiments by Oravecz (1977) in No. 5 seam at Colliery A., South Africa. Data: average depth to mid-seam 40.3m; seam height 1.5m; pillar width5.2m; room width 5.5m; percentage extraction 76.4%; panel width 176.2m (est.); deformation modulus, seam (est.) 1.54 GNm–2; deformation modulus strata (est.) 4.43 GNm–2; Poisson's ratio (est.) 0.15. Conversion factors: 1 ft = 0.3048 m, 106 psi = 6.894 GNm–2.

$$\frac{\sigma_{pf}}{\sigma_{cf}} = \left(\frac{V_s}{V_p}\right)^{0.118} \left[\left(\frac{B_p}{H_p}\right) \Big/ \left(\frac{B_s}{H_s}\right)\right]^{0.833} \tag{2.25}$$

Where B and H are pillar and specimen width and height, respectively. There are, of course, limitations for this approach, one of which would probably be the pillar width/height ratio. If this is less than 1, and particularly if the rock is ductile, the volume

exponent will increase. For the record, although the above method is strongly recommended, it is useful also to include the conventional representations of pillar design equations, often called the Holland- Gaddy (Holland, 1964) equation in the United States, which take the form,

$$\sigma_{pf} = \sigma_{cf\left(a+b\frac{B}{H}\right)} \tag{2.26}$$

$$\sigma_{pf} = K\frac{B^{a}}{H^{B}} \tag{2.27}$$

In this case, is uniaxial compressive strength of a cube of specified dimension; *a* and *b* are dimensionless constants, usually chosen so that *a* + *b* = *b are* dimensionless constants; and *K* = is a constant principally for coal mines. All of the constants are effectively shape factors. The basic problem is that in either equation is essentially the laboratory value, and a factor of safety, usually not included in the equation, is needed to allow for size effects and ensure safe design. Quoted values of this "safety factor" are difficult to find.

Wilson (1983) suggests 5 for coal, but incorrectly recommends 1 for strong massive unjointed rock and 6 to 7 for weak rock—quite the reverse of the probable actual values. Where the economic success or failure of an operation depends on correct estimation of extraction ratio, a more accurate approach is required and Eq. (2.27) is recommended as a starting point. This represents a safety factor of 4 to 5 for most rocks and pillar shapes.

2.4.3 Barrier Pillar Design

Room and pillar mines are usually developed in a series of rectangular panels separated by barrier pillars. There is no specific design method for these pillars, but where the roof is not caved or where pillars are left in place, design of barrier pillars assumes greater importance. Figure 2.5 shows that pillar stress is not necessarily evenly distributed, and where the roof and floor rocks are stiffer than the pillar rocks, stress with be transferred to an abutment. There is also the probability that deterioration or over mining of highly stressed pillars may lead to a reduction in load capacity of individual (or groups of) pillars, and transfer of load to other pillars that may lead to progressive failure. This is one of the most common causes of extensive pillar collapse (Mottahed and Szeki, 1982, describe a total mine collapse), and barrier pillars can control this.

Wilson (1983) analyzed this problem and suggested, for coal mines, barrier pillar widths of 1/10th of the working depth, but his approach, although applied to room and pillar workings, was designed principally to reduce entry damage in longwall entry chain pillars. A more satisfactory approach may be to consider pillar yield. Hudson, Brown, and Fairhurst (1971) in a series of tests on marble, which can be repeated on coal, showed that a pillar behaved in a yielding rather than a brittle manner if its height/width ratio was less than 1/3. The implication is that below this ratio, a pillar will deform rather than fracture, resisting rapid collapse. A yielding, barrier pillar of 3 to 4 times the excavation height can, therefore, be recommended, particularly at greater mining depths.

2.4.4 Support Design

Where a bolt is used to restrain a single block in the roof of an entry, the volume and hence the weight of the block and where necessary its direction of sliding can be determined by Stereo graphic analysis of the kinetics of sliding. This method is

outlined in Farmer and Shelton (1980) and in Farmer (1985).Methods of support based on the common requirement that bolt spacing should be half the bolt lengths are discussed in the same sources.

In coal mining, the design of bolts is usually based on Panek's (1962a,b) analysis. The most simple assumption for design purposes is to consider a sagging roof plate or beam of thickness *L,* span *B,* and length *X,* supported by rows of bolts with separation *a* between rows and spacing *S.* Then the bolt tension force *P* to support the roof will be given by:

$$p = \frac{{}_{y} BXL}{\left(\frac{x}{a}+1\right)\left(\frac{B}{S}+1\right)} \qquad (2.29)$$

Where λ is unit weight of the roof-rock. This equation, suggested by Obert and Duvall (1967), is valid if the roof above the excavation is completely suspended by bolts. For an assumed bolt load, it can also be used to estimate spacing and the number of rows. It represents the upper limit of bolt force since it ignores the important supporting effect of the abutments. It also ignores the interaction of a series of roof beds.

A more accurate approximation can be obtained by considering the effects of friction between beds and also by considering the roof span as a series of thin beams, fixed at each side of the opening. Panek (1962a,b; 1964) in a series of seminal papers considered this condition both experimentally by centrifugal testing and analytically, and developed the monograph illustrated in Fig 4, which has been used extensively in mine design. It is explained in detail by Panek and McCormick (1973) in the *SME* Mining Engineering Handbook.

The basic variable is a reinforcement factor RF that is used to evaluate the interbed friction effect due to bolting. The roof is considered as a series of beds of equal thickness, of the same material, and without bonding between them. The bolts are assumed normal to the beds and tensioned to give normal compressive loading across the beds. Then

$$RF = \left(1 + \frac{\Delta\sigma_f}{\sigma_{fs}}\right)^{-1} \tag{2.30}$$

Where $\frac{\Delta\sigma_f}{\sigma_{fs}}$ the decrease in bending stress from frictional resistance is induced

By bolting, expressed as a ratio of the maximum bending stress in the unbolted strata, and is given by the empirical equation:

$$\frac{\Delta\sigma_f}{\sigma_{fs}} = \frac{3}{8}\mu(aB)^{-0.5}\left[\frac{B}{S}p\left(\frac{L}{t}-1\right)+\frac{1}{y}\right]^{0.33} \tag{2.31}$$

Where μ is the interbred coefficient of friction, *a* is spacing between rows, *B* is span, *S* is bolt spacing, *t* is average roof layer thickness, *P* is assumed bolt tension, and *L* is assumed equal to bolt length or supported thickness. For typical thin-bedded mine roof strata, *RF* should be greater than 2, and bolt spacing must by law be less than 5 ft (1.5 m). Spacing of 4 ft (1.2 m) is more common. Based on Eqs. 12, and 5.1.12, Panek's well-known monogram (Figure.5.) allows rapid estimation of *RF* for a bolted roof, and forms a basis for rapid rock bolt pattern design.

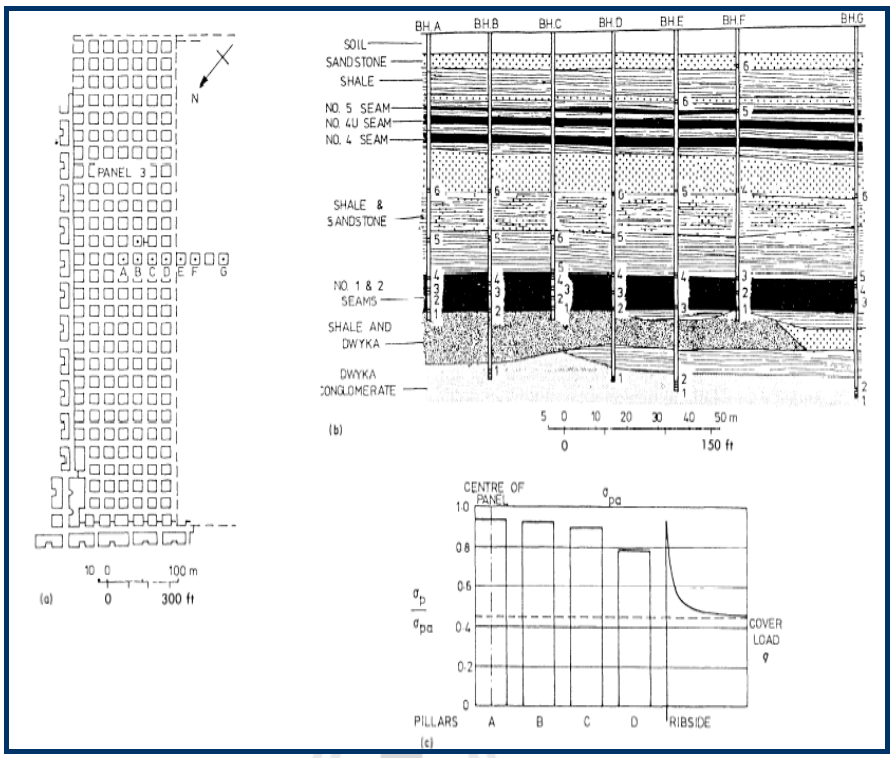

Figure2.5 Estimation of pillar stress as a proportion of pillar stress computed from tributary area theory, from experiments by Oravecz (1977) in No. 2 seam at Colliery B., S. Africa. Data: average depth to mid-seam 66.7m; seam height 5.5m; pillar width 13.7m; room width 6.1 m; percentage extraction 52.1%; panel width 144.8m; deformation modulus, seam (est.) 3.92 GNm–2; deformation modulus, strata (est.) 6.27 GNm–2; Poisson's ratio (est.) 0.15. Conversion factors: 1 ft = 0.3048 m, 106 psi = 6.894 GNm–2.

2.5 Review of paper

2.5.1 Technology Study on Pillar Stability of Wongawilli Area in Shallow Close

Distance Coal Seams

In order to ensure the lower working face safety production under

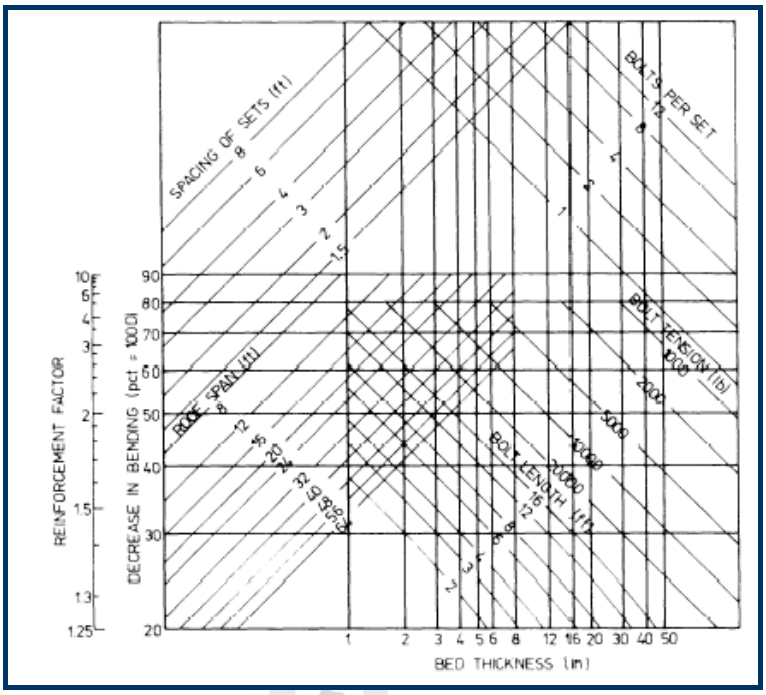

Figure 2.6 Monograph to determine the friction effect for bolting in mine roof

Wongawilli mining area pillars in shallow close distance coal seams in Bulianta coalmine, the influence of Wongawilli coal pillars' stability in upper coal seam on lower working face is studied by three-dimensional simulation and field measurement. The results of finite element software FLAC3D, shows that, the maximal vertical stress in Wongawilli coal pillars is 32 MPa, and the stress concentration factor is 4.8. The results of on-site surface subsidence and rock pressure appearance shows that, the surface subsidence value corresponding to Wongawilli coal pillars is much less than old gob area, and the rock pressure appearance of mining face is always normal, so the result indicates that Wongawilli coal pillars are not unstable and the safety of extraction of 32301 working face is ensured. The research achievement would provide technique support for safety mining under similar condition in Shendong mining district.

2.5.2 Tunneling Underground Space Center, Department of Environment, Land and Geotechnology Engineering, Politecnico di Torino, Italy

The geomechanical and stability design of underground granite mine located in Canal San Bovo (Trento district, Northeastern Italy) was described. The exploitation of the granite, which is used in the ceramic industry, was carried out by the rooms and rib pillars method. The rooms are 12 m wide while the pillars **are** 11 m wide and they cross the main discontinuity set of the rock mass in the perpendicular direction. To verify the stability condition of an underground mine, it is necessary to canny out the calculations that are able to check both the local and global stability of the rock mass. In the studied example, this approach has been applied with the development of analytical and numerical parametric analyses and it has permitted to get the best orientation and to design the size of rooms and pillars.

2.5.3 The strength of hard-rock pillars failures in Canadian

Observations of pillar failures in Canadian hard-rock mines indicate that the dominant mode of failure is progressive slabbing and spalling. Empirical formulas developed for the stability of hard-rock pillars suggest that the pillar strength is directly related to the pillar width-to-height ratio and that failure is seldom observed in pillars where the width-to-height ratio is greater than 2. Two- dimensional element analyses using conventional Hoek-Brown parameters for typical hard-rock pillars (Geological Strength Index of 40, 60 and 80) predicted rib-pillar failure envelopes that did not agree with the empirical pillar-failure envelopes. It is suggested that the conventional Hoek and Brown failure envelopes over predict the strength of hard-rock pillars because the failure process is fundamentally controlled by a

cohesion-loss process in which the frictional strength component is not mobilized. Two- dimensional elastic analyses were carried out using the Hoek-Brown brittle parameters which only relies on the cohesive strength of the rock mass. The predicted pillar strength curves were generally found to be in agreement with the observed empirical failure envelopes.

2.5.4 Stability and Subsidence Assessment over Shallow Abandoned Room and Pillar Limestone Mines Netherlands and in Belgium.

In the region of Maastricht, both in The Netherlands and in Belgium, many areas are underlain by abandoned room and pillar mines, which have been excavated in weak limestone to produce building stone. Several of these mines are kept open now to serve as an important tourist attraction. However, there have been both local and large-scale collapses up to the present, resulting in extensive surface subsidence, faulting, and sinkhole formation. For many mines the stability needs continuous attention. Depending on rock overburden thickness, mine span and density of joints, different collapse and subsidence mechanisms can apply. This contribution describes these mechanisms and then concentrates on how to assess the potential of a large-scale pillar collapse of a room and pillar mine. This quantitative assessment is based on short- and long-term laboratory tests on model pillars, numerical experiments and numerous field observations, taken during more than 20 years. Only taking the stability of individual pillars into account cannot assess the collapse potential of a mine. Particularly large-scale pillar stability, which considers the load carrying capacity of all pillars together, and general mine stability, which concerns the arching. Capacity of the overburden, are important. In the recent past, the method was applied successfully to several mines, in order to investigate the necessity of

underground support measures to protect existing infrastructure and planned infrastructural projects. It is expected that at least a major part of the method applies to shallow room and pillar mines in other regions and rock types.

2.5.5 Pillar design by combining finite element methods, neural networks and Reliability: a case study of in China

This paper presents a mine pillar design approach by combining finite element methods (FEMs), neural networks (NN) and reliability analysis. This practical approach is presented by examining an actual cylindrical mine pillar in a copper mine and taking into account uncertainties in ore pillar material parameters including modulus, Poisson's ratio, density and uniaxial compressive strength. The ore pillar had to be able to safely and effectively support a drilling room that occupied an open space of 3.8m high and 55m long and 20m wide and at a depth of 360m below ground surface. Three-dimensional FEM was used to simulate the mining operations and to estimate average pillar compressive stress at each operation step. A pillar performance function was established in implicit form taking into account pillar strength and pillar dimension. NN was incorporated in the FEM to substantially reduce the number of finite element calculations in establishment of the relationship between pillar compressive stress and basic random variables. Trained NN was then used to generate a database for the implicit performance function. The database was used to determine the reliability index and failure probability for each trial pillar diameter. Relationship between pillar reliability index and each of the coefficients of variation of the basic random variables was used for optimal design of pillar diameter. The optimal pillar design was used in the mining construction and functioned well.

CHAPTER III

GEOLOGICAL DATA COLLECTION

3.1 Introduction

The objective of this study is to collect geologies data for engineering design and stability analysis of the mine openings and pillar support. The main design requirement is to extract the maximum tonnage of the ore while maintaining mechanical stability of the mine area and minimizing the environmental impact (surface subsidence). The principle of tunnel design was including the minimum uncertainty, simplicity, application of the state-of-the-art, optimization of the design solutions and constructability.

The Siam City Cement Public Company (SCCC) has initiated and developed a Phetchaboon Coal Mine project (PCB) in a newly found coal resource to supply the energy to the cement plant operation. The study area is located in Lamtanen village, Nongphai district, Phetchaboon province. The coal is classified as anthracite in Permian age deposited with competent limestone at depths ranging between 5 and 90 m (Figure 3.1). The results from feasibility study suggest that the coal has economic potential to develop using a room-and-pillar mining method.

3.2 Elevation and Ground Water Table

PCB coal mine deposit has maximum elevation at 235 m (msl). Flat land background surround coal deposit is 200 m. Ground water table was measurement

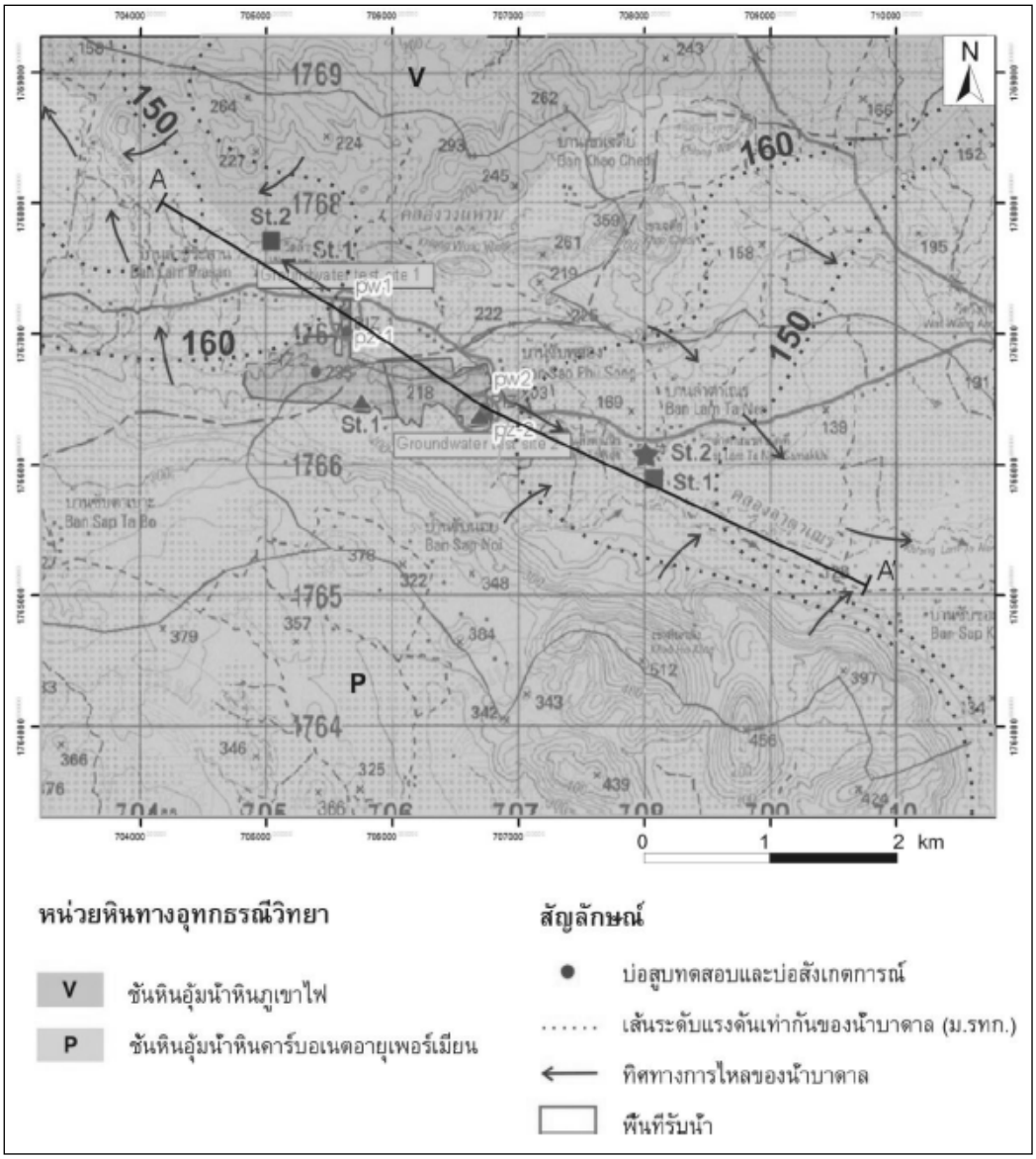

Figure 3.1 Topographic map showing the elevation from mean sea level at PCB coal mine deposit and water well for ground water study from water well at background area is 30 m depth from ground surface. It is 170 m elevation from mean sea level. Ground water table was below coal mine surface at elevation 65 m (msl). The topographic of coal deposit is medium high relief of limestone hill above ground water table with flow rate 18Cu_m/h.

Table 3.1 List of water wells for ground water study**.**

Name	Rock type Aquifer	Well Type	Well Size	UTM Corrodinate		Depth of water well	Depth Ground Water Table
			Inch	North	East	m	m
PW-1	Vocalnic	Pump well	6	1767153	705638	30	11.5
PW-2	Carbonate	Pump well	6	1766442	706740	30	14.5
Pizo-1	Vocalnic	Observe well	3	1767154	705628	30	12.5
Pizo-2	Carbonate	Observe well	3	1766442	706738	30	14.5

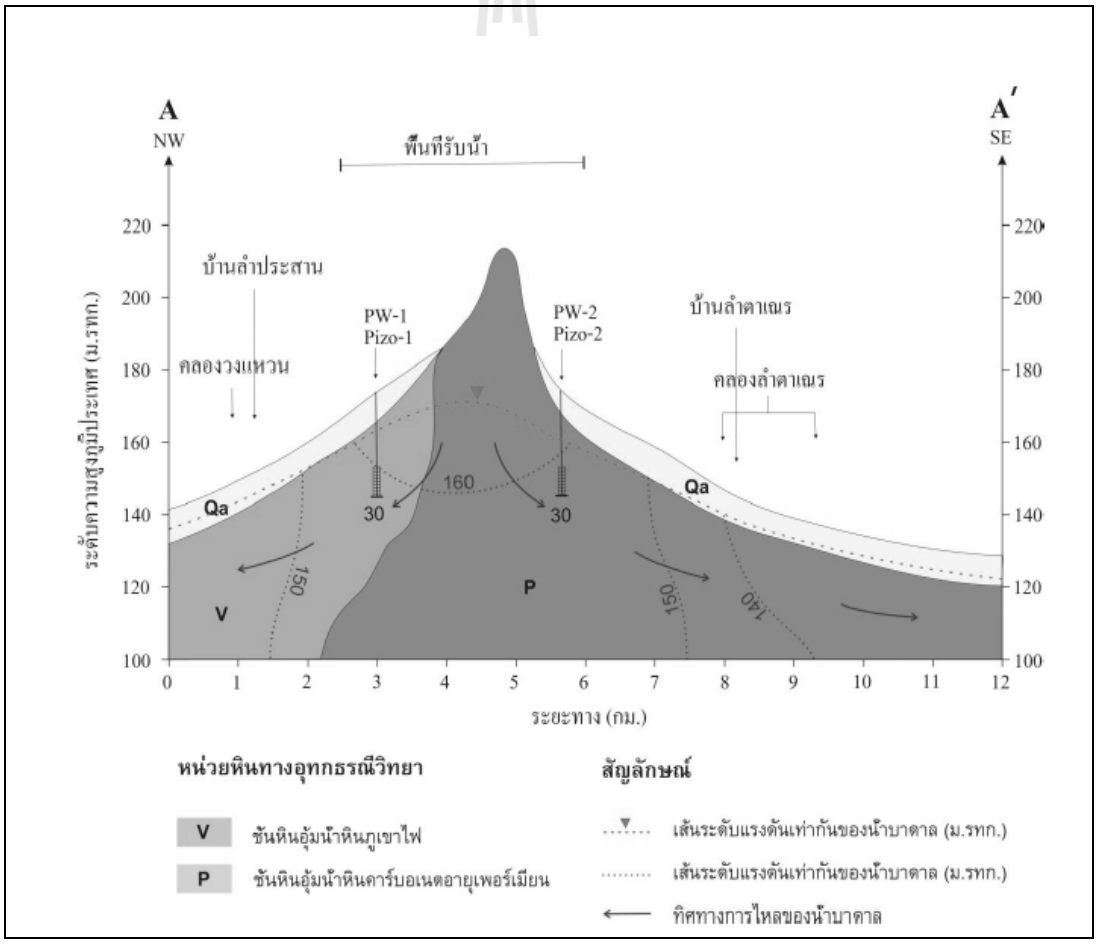

Figure 3.2 Cross section along East West passing coal deposit for showing ground water table and flow direction.

Table 3.2 Results of pumping test by specific capacity and water flow rate

Name	Pumping Test	Rate Of Pumping Test	Water depth			Specific Capacity	Water Flow Rate
			Before pump	Decrease distance	After pump	Pumping Rate/Distance Decrease	Steady state 6 Hour
		Cu_m/H	m	m	m	Cu-m/m	Cu-m/m
PW-1	Constant rate	4.80	4.80	11.80	16.60	0.41	4.80
		3.27	4.80	4.10	8.90		
	Step drawdown	4.80	4.80	12.13	16.93		
PW-2	Constant rate	18.00	10.14	2.67	12.81	3.80	18.00
		10.00	9.92	2.50	12.42		
	Step drawdown	15.00	10.10	2.10	12.20		
		18.00	10.14	2.67	12.81		

3.3 Geological of coal deposit

Phetchaboon coal resource is a new occurrence in Thailand. The coal field distribute between the coordinate of vertical grid 705,000 to 710,000 and horizontal grid 1,767,600 to 1,767,500. Coal was deposited in limestone and mudstone of the Lower Permian age. It has two main seams, 10-30 m appearance thickness, 0.50 m depth at sub crop, 258/50 (Strike/dip angle) except the east area 245/42. Confirm by drilling hole on year 2009, coal seam continuous extend to more than 90 m of depth and has open pit mine able reserve 1.77 million tons at pit limit 50 m.

3.4 Lithostratigraphic

Rock formation at PCB coal deposit comprises 6 units. They sequent from young to old are: top soil, Lime mud over burden, upper coal seam, lime mud Interburden, lower coal seam, lime mud basement. For each rock unit see lithological Colum in Figure 3.5.

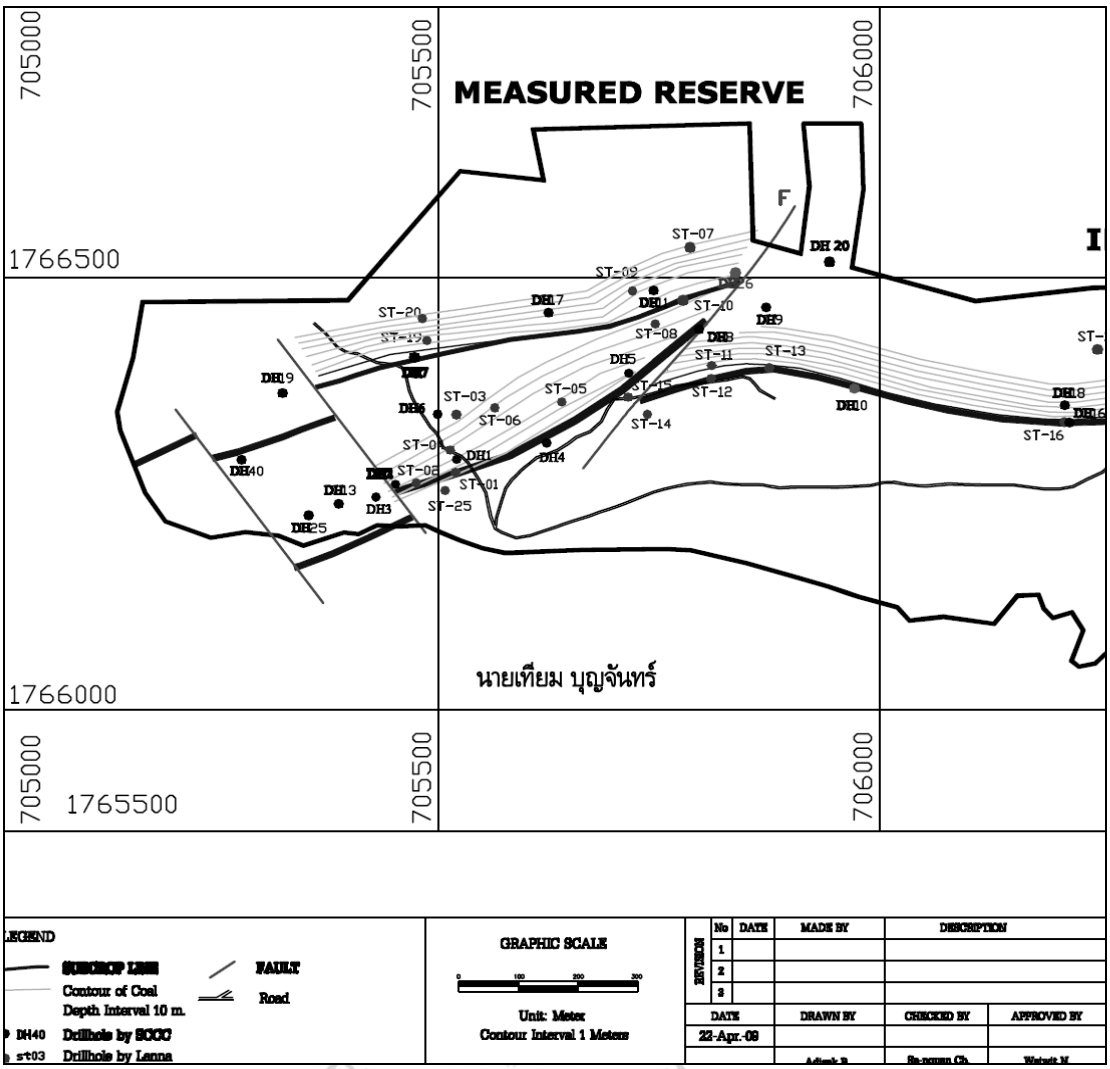

Figure 3.3 Location of core drilling holes for coal seam identify and rock mechanic study.

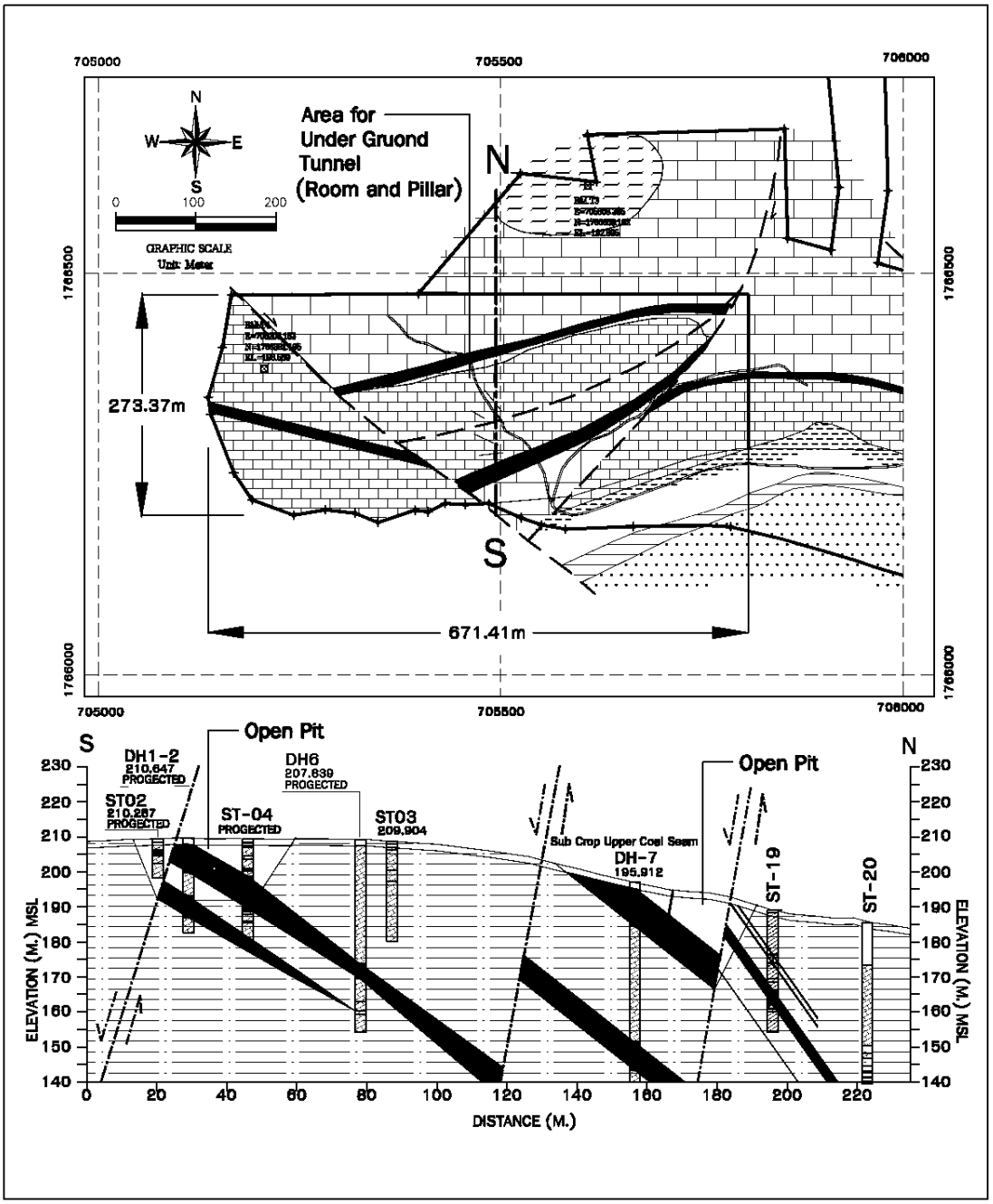

Figure 3.4 Geological map and cross-section at study area (PCB coal mine deposit**)**

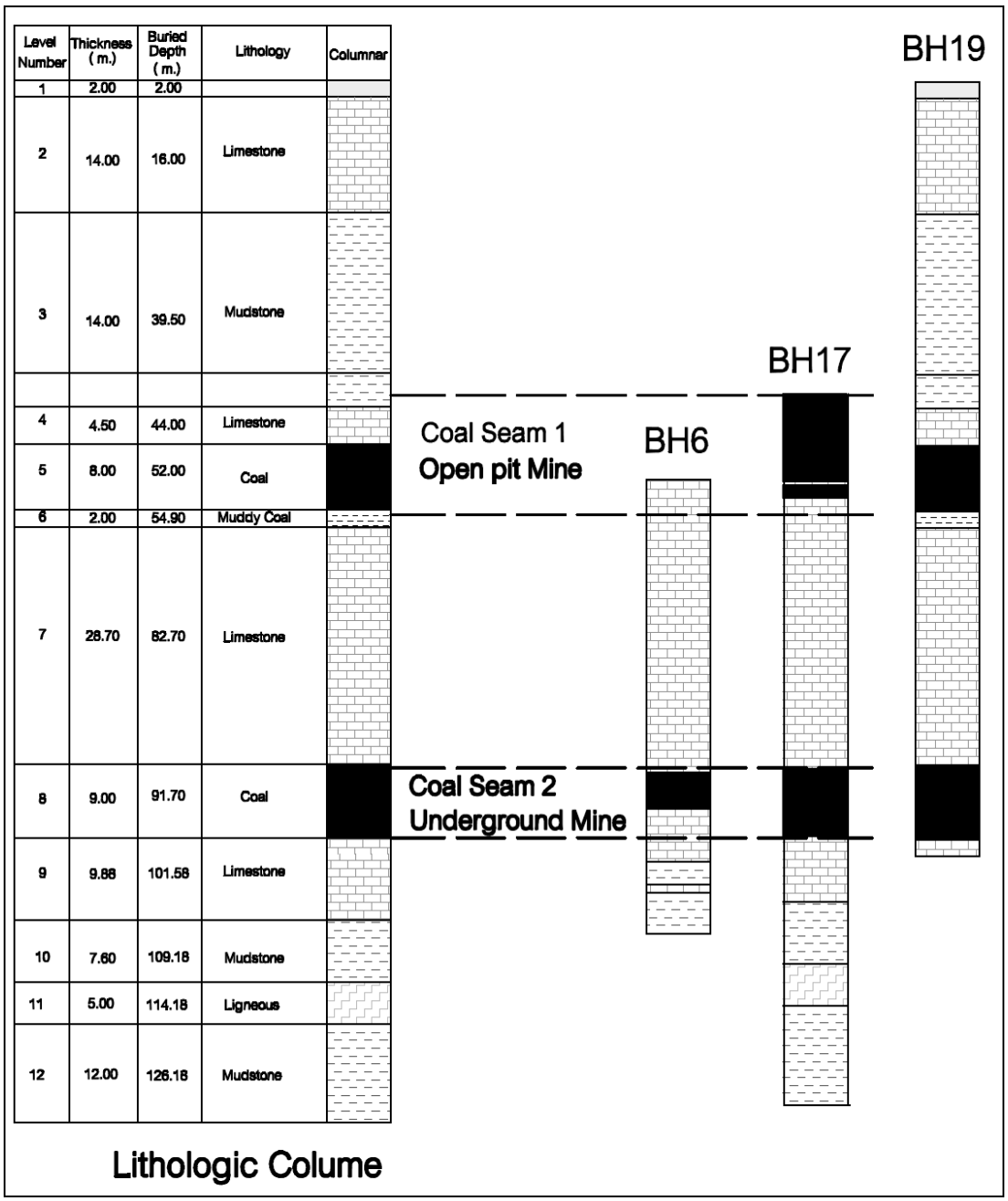

Figure 3.5 Lithological stratigraphy columns at PCB coal mine deposit

Table 3.3 Geological map and cross-section of PCB coal mine deposit

No.	Name	UTM Coordinate (Indial Thai)		Inclination	Elevation	TD.	1st Coal Thickness(m)						2st Coal Thickness(m)				1ST+2nd	Dip Angle	Remark
		North	East		m (MSL)	(m)	O/B	Start	Stop	Layer	Parting	Total	Start	Stop	Layer	Total	m		
1	DH1	1,766,293.26	705,522.25	90°	212.08	16.00							7.50	16.00	8.50	8.50	8.50	36.00	
3	DH2	1,766,259.48	705,455.37	90°	206.27	35.00							9.20	25.60	16.40		17.60	30.00	
													31.80	33.00	1.20	17.60			
5	DH4	1,766,306.99	705,616.22	90°	215.45	29.00							0.00	15.00	15.00		26.00	50.00	
													18.00	29.00	11.00	26.00			
6	DH5	1,766,403.82	705,716.62	90°	199.20	37.00							6.10	12.30	6.20		10.30	28.00	
													24.20	28.30	4.10	10.30			
33	DH6	1,766,318.67	705,479.78	90°	207.84	55.00							35.40	39.80	4.40	4.40	4.40	33.00	
8	DH7	1,766,396.99	705,471.28	90°	195.91	86.00	0.00	0.00	12.50	12.50		12.50	45.30	53.50	8.20	8.20	20.70	38.00	
9	DH8	1,766,432.81	705,772.21	90°	189.99	31.50							2.50	5.00	2.50	2.50	2.50	35.00	
11	DH10	1,766,365.91	705,971.80	90°	199.25	23.00	4.60	4.60	9.00	4.40		4.40	non	non			4.40	45.00	
12	DH11	1,766,478.67	705,734.94	90°	190.77	34.00							6.00	8.70	2.70		12.30	30.00	Apparent Thicknessn
													13.00	18.00	5.00	12.30			
													20.90	25.50	4.60				
13	DH13	1,766,228.59	705,369.08	90°	202.77	20.00	2.00	2.00	9.00	7.00		7.00					7.00		
14	DH14	1,766,372.57	706,313.60	90°	186.96	29.00	11.00	11.50	14.50	3.00		10.80					10.80	32.00	
								17.50	19.00	1.50	3.00								
								20.70	27.00	6.30	1.70								
16	DH16	1,766,340.95	706,194.14	90°	189.87	23.00	4.00	4.00	15.50	11.50		11.50					11.50	35.00	
17	DH17	1,766,450.97	705,592.33	90°	207.83	85.00	21.00	21.00	26.00	5.00		5.00	37.40	50.00	12.60		24.50	35.00	
													57.00	62.30	5.30	19.50			
													73.40	75.00	1.60				
19	DH19	1,766,383.82	705,301.54	90°	192.81	91.00	44.00	44.00	52.00			8.00	82.70	91.70	9.00	9.00	17.00	40.00	
32	DH40	1,766,327.37	705,273.61	90°	194.67	84.80							66.00	72.00	6.00	6.00			
Max					**215.45**	**91.00**	**44.00**	**44.00**	**52.00**	**12.50**	**3.00**	**12.50**	**82.70**	**91.70**	**16.40**	**26.00**	**26.00**	**50.00**	
Average					**199.44**	**45.29**	**12.37**	**13.92**	**20.50**	**6.40**	**2.35**	**8.46**	**29.80**	**36.71**	**6.91**	**11.30**	**12.68**	**35.92**	
Min					**186.96**	**16.00**	**0.00**	**0.00**	**9.00**	**1.50**	**1.70**	**4.40**	**0.00**	**5.00**	**1.20**	**2.50**	**2.50**	**28.00**	

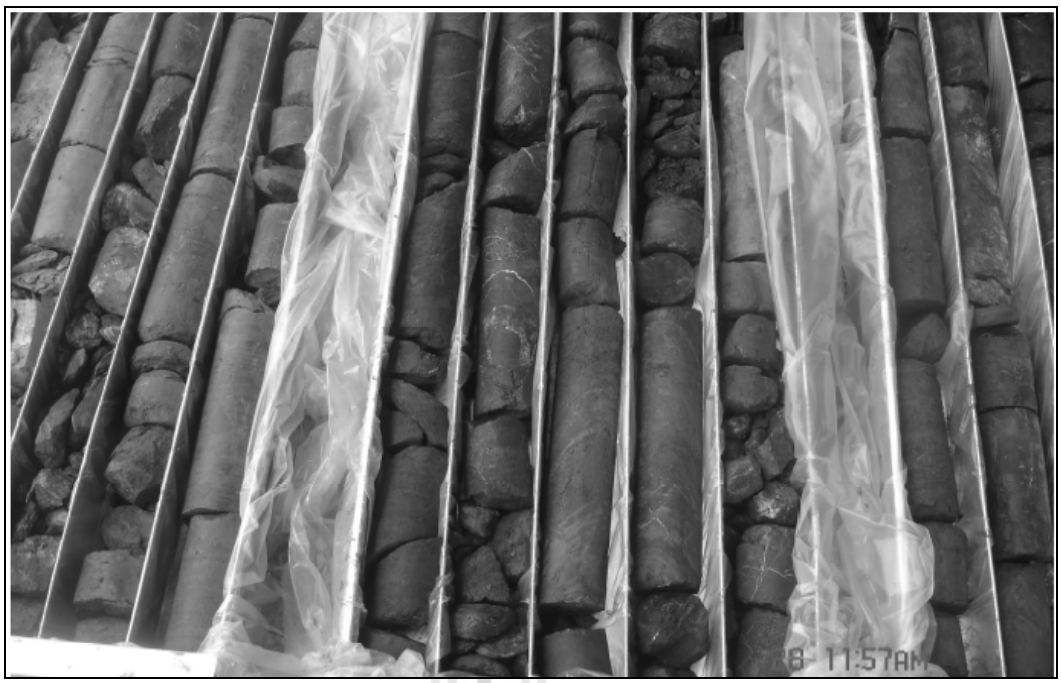

Figure 3.6 Core sampling from drilling whole DH 19_2007

Figure 3.7 Coal core samples from PCB coal mine deposit

Figure 3.8 Bedding limestone and mudstone and dipping plan.

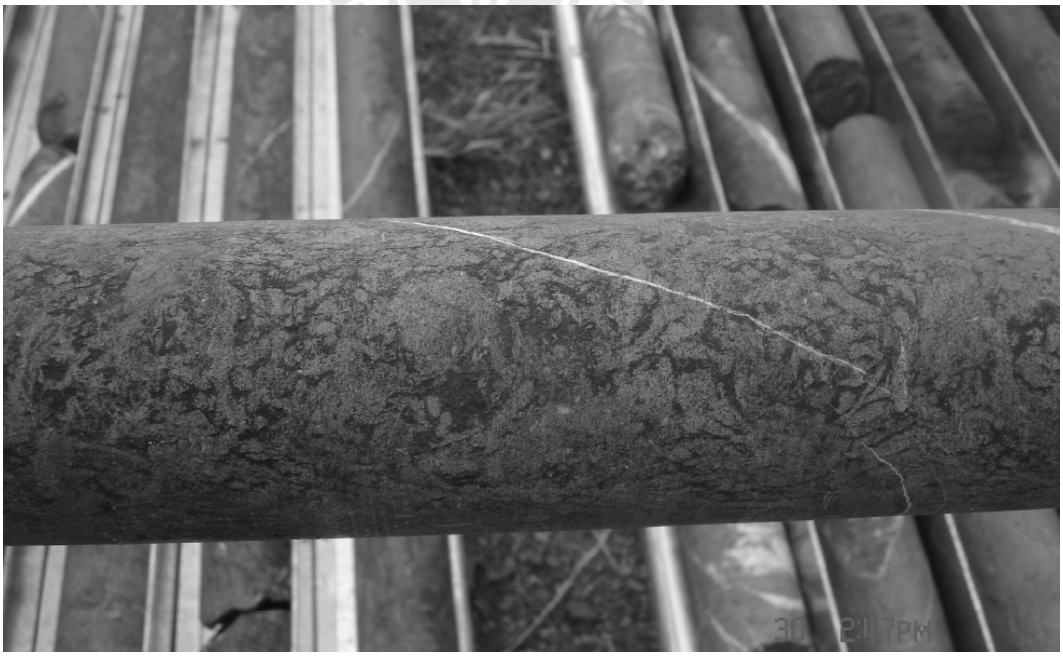

Figure 3.9 Limestone with fossil found from the cores.

3.5 Geological Structure

Geological data collection is carried out to fracture analysis and classify the rock mass as accurately as possible. The integrated engineering geological data collection was used to design room and pillar of underground coal mine and anticipate any serve geological condition, which can give rise to problem during the excavation of the opening. Referring to the results of representative joint analysis at project area.(figure 3.14). It has major of strike and dip direction in 354/69 and two miner 080/26 and 254/42. The bedding plan of coal seam is 245 / 42 degree and two miners of fracture are fault plan. The results of dipping angle by joint analysis are implying to 6 degrees difference from cross section measurement.

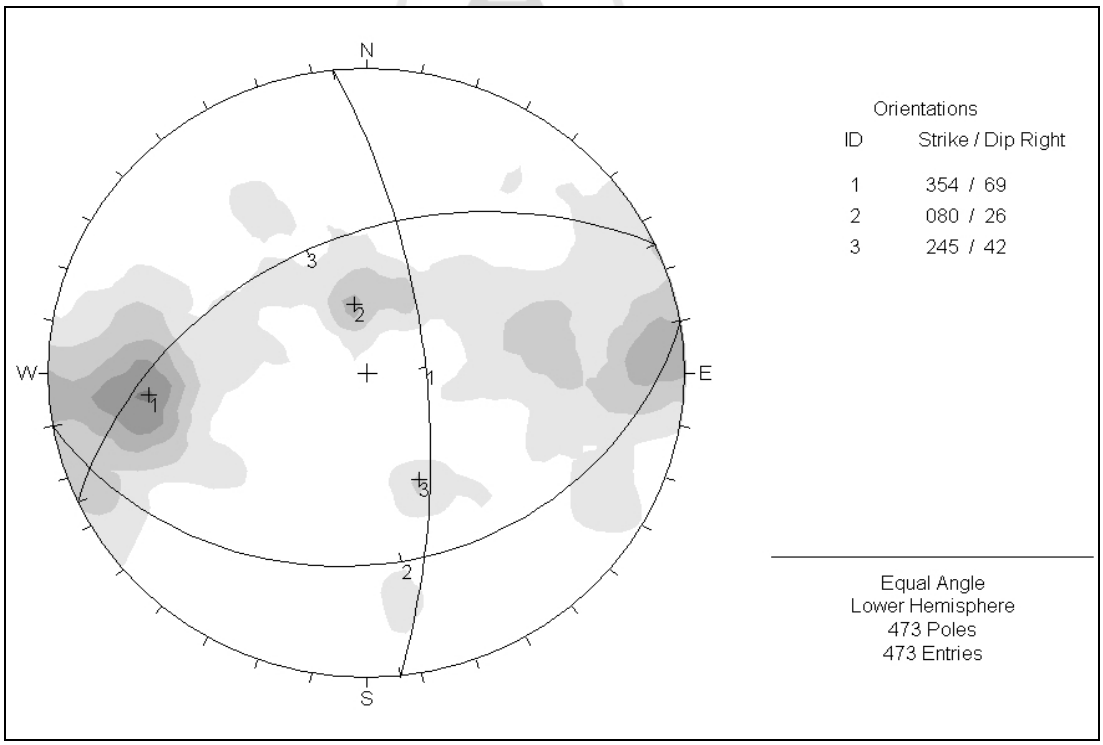

Figure 3.10 Representative fractures at PCB coal mine project. Attitude 245/42 is bedding plan

3.6 Engineering Geology

Core specimens at specific depth from each bore hole are requested by the company for the each specific test. Standard testing methods and quantity of specimens are tabulated in Table 1.

Table 3.4 List of sample for rock mechanic test

No	DH	Sample NO.	Depth Interval of sample		Length	Rock Type	Testing request
			from	to	(m.)		
1	DH-17	DH-17/1	14.22	14.63	0.41	Upper Limestone	Direct shear Test
2	DH-17	DH-17/2	17.65	18.00	0.35	Upper Limestone	Uniaxial Test
3	DH-17	DH-17/3	15.50	15.60	0.10	Upper Limestone	Tilt Test
4	DH-17	DH-17/4	16.40	16.50	0.10	Upper Limestone	Tilt Test
5	DH-17	DH-17/5	27.32	27.72	0.40	Upper Limestone	Triaxil Test
6	DH-17	DH-17/6	33.55	33.89	0.34	Upper Limestone	Uniaxial Test 1
7	DH-17	DH-17/7	34.65	35.00	0.35	Upper Limestone	Direct shear Test 1
8	DH-17	DH-17/8	35.00	35.40	0.40	Upper Limestone	Triaxil Test 1
9	DH-17	DH-17/9	50.00	50.45	0.45	Inter burden Muddy coal	Uniaxial Test 1
10	DH-17	DH-17/10	50.45	50.72	0.27	Inter burden Muddy coal	Direct shaer test 1
11	DH-17	DH-17/11	51.05	51.50	0.45	Inter burden Muddy coal	Triaxial test 1
12	DH-17	DH-17/12	56.15	56.43	0.28	Inter burden Muddy coal	
13	DH-17	DH-17/13	75.55	75.72	0.17	Lower Muddy coal	Uniaxial Test 1
14	DH-17	DH-17/14	75.72	76.00	0.28	Lower Muddy coal	Direct shaer test 1
15	DH-17	DH-17/15	76.38	76.58	0.20	Lower Muddy coal	
16	DH-19	DH-19/1	7.52	7.90	0.38	Upper Limestone	Uniaxial Test 1
17	DH-19	DH-19/2	12.30	12.60	0.30	Upper Limestone	Direct shaer test 1
18	DH-19	DH-19/3	12.60	12.85	0.25	Upper Limestone	Triaxial test 1
19	DH-19	DH-19/4	26.28	26.60	0.32	Upper Mudstone	Uniaxial Test 1
20	DH-19	DH-19/5	30.45	30.68	0.23	Upper Mudstone	Direct shaer test 1
21	DH-19	DH-19/6	32.45	32.70	0.25	Upper Mudstone	Triaxial test 1
22	DH-19	DH-19/7	39.50	39.88	0.38	Upper Limestone	
23	DH-19	DH-19/8	41.20	41.55	0.35	Upper Limestone	Uniaxial Test 1
24	DH-19	DH-19/9	41.65	41.98	0.33	Upper Limestone	Direct shaer test 1
25	DH-19	DH-19/10	42.00	42.30	0.30	Upper Limestone	Triaxial test 1
26	DH-19	DH-19/11	42.30	42.80	0.50	Upper Limestone	
27	DH-19	DH-19/12	52.15	52.55	0.40	Muddy coal under 1st coal	Triaxil test 1
28	DH-19	DH-19/13	54.45	54.82	0.37	Muddy coal under 1st coal	Direct shaer test 1
29	DH-19	DH-19/14	57.20	57.60	0.40	Middle Limestone	Uniaxial Test 1
30	DH-19	DH-19/15	57.60	58.00	0.40	Middle Limestone	Direct shaer test 1
31	DH-19	DH-19/16	63.44	63.90	0.46	Middle Limestone	Triaxial test 1
32	DH-19	DH-19/17	64.38	64.80	0.42	Middle Limestone	
33	DH-19	DH-19/18	71.00	71.40	0.40	Middle Limestone	Uniaxial Test 1
34	DH-19	DH-19/19	82.00	82.50	0.50	Middle Limestone	Direct shaer test 1
35	DH-19	DH-19/20	81.00	81.25	0.25	Middle Limestone	Triaxial test 1

Table 3.5 Standard testing methods and quantity

No.	Descriptive	Standard	Quantity
1	Uniaxial compressive strength	ASTM D2938-95	9
2	Triaxial compressive strength	ASTM D2664-95a	31
3	Direct shear strength	ASTM D5607-95	36
4	Los Angeles abrasion	ASTM C131-69	5
5	Tilt test		2

3.6.1 Direct shear strength test (ASTM D5607-95)

A selected specimen is cut and trimmed to from top and bottom pieces. The specimen shall have a thickness approximately 20.00 mm in order to fit into a shear box. The shear planes of both pieces were lapped to get a smooth flat surface. Since the shear box diameter of a bit larger than diameter of the specimens, thus adapter rings were used to ensure proper fitting. The specimen diameter was measured and placed in the shear box. Place the upper platen on the specimen and align properly. A normal load was applied on the top of platen given predetermined normal stress on the test. Unlock the frames that hold the test specimen. Then shear force was applied continuously at a constant rate. The shear force, horizontal and vertical displacements were recorded with data logger(30-WF-6016). The specimen was sheared to at least 7 mm displacement. Photographs of each specimen were taken before and after testing. At least three sub specimens at different normal stresses should be tested. The shear stress – displacement curve of each normal stress level was plot. Then, a maximum shear stress at failure of each test was selected. Pair of normal and shear stress at failure from three specimens is plotted, and shear failure envelope is determined. Shear strength parameter could be obtained as cohesion (c)

and internal friction angle (ϕ) from the envelope. These parameters are residual shear, since the shear test is performed on smooth surface.

3.6.2 Los angles abrasion test (ASTM C131-69)

Aggregates of grading A and B for limestone and mudstone core specimens are selected respectively for the tests according to availability of core specimens. The core specimens were broken into aggregates and then dried at 110 ± 5˚C, and cooled to room temperature. Then separate the aggregate on the required sieve sizes, and given mass on each sieve size fraction to its specific grading. Weight the aggregate to the nearest 1 g. Place prepared aggregate and abrasive charge in the Los Angeles Abrasive Testing Machine. Start the testing machine and allow operating for the required number of revolutions. When the testing machine has completed rotating the required number of revolutions, Separate the test specimen on the 4.75 mm sieve, then sieve the passing 4.75 mm material on the 1.70-mm sieve. Combine the material retained on the 4.75 and 1.70 mm sieves. Weigh and record these values to the nearest 1 gram, calculate the grading of the test specimen and the percent wear at the number of revolutions tested.

3.6.3 Tilt test

Tilt test suggested by Barton (1982) in performed for determination of discontinuity internal friction angle. The specimen from DH-17/3 and DH-17/4 were selected and requested for the tilt test by the company. Place the lower piece of specimen on tilting board; adjust the discontinuity surface parallel to the plate. The roughness of the discontinuity plane is observed, and then put the upper piece over the surface. Then, the board was tilted slowly till sliding of the upper piece occurred. The

tilt angle which represents the base friction angle of discontinuity plane was measured.

3.6.4 Results of Laboratory testing

The uniaxial compressive strength (UCS) at natural moisture content of the rocks from DH-17 and DH-19 are tabulated in Table 2. The results indicate pale grey limestone having UCS range between 72-171 MPa (moderate to high strength) while dark limestone with fine sand size lamina having the UCS range from 35-59 MPa (low to moderate strength). Mudstones or muddy coals establish low to moderate strength similar to dark lamina limestone with the UCS in the range of 35-69 MPa. Dark mudstone with weak fractures gives UCS in the range of 2-24 MPa which is in a very low strength. Details strength classification according to Deer and Miller (1996) are listed in Table 3.

Results of confining and axial stresses of each sub-specimen from triaxial compressive test are listed in Table 4.6. The peak shear strength parameters (cohesion, c and internal friction angle,ϕ) determining from the tests is also included. The limestone cores (pale grey and some calcite fill) give wide range strength parameters with c = 13.58-26.08 MPa and ϕ = 29.5 - 50.67 degrees. The limestone of dark colure, fine grain sand with some muddy coal laminar also give a similar wide variation in shear strength parameters as: c = 0.52 – 32.11 MPa and ϕ = 22.44- 51.52 degrees.

The results indicate the influences of calcites veins, impurities, fractures and laminations on the wide variations peak shear strength. Therefore, the strength could not be defined from depth or types of the rocks themselves. However, average peak shear strength parameters determined from all tests data of both

limestone types are approximately c = 9 MPa and ϕ = 45 degree. The results of triaxial test on mudstone and muddy coal core specimens are tabulated in Table 6. The shear strength parameters of mudstones are c = 5.75 - 9.60 MPa and ϕ = 39.98 – 54.81 degrees while the average strength parameters are c = 7.9 MPa and ϕ = 44.58 degrees.

Residual shear strength parameters of the three rock types from bore holes DH-17 and DH-19 are illustrated in Table 7-9. Pale grey limestone with calcite veins give ϕr = 31.10-32.84 degree with no apparent cohesion. The dark limestone core specimens show some apparent cohesion, c = 2.82 -49.59 kPa (kN/m^2) with ϕr = 31.40-36.54 degrees with average c = 16.82 kPa and ϕr = 34.79^o. Residual strength parameters of mudstone are c = 1.63-59.93 kPa and ϕr = 32.87-38.10 degrees with average c = 34.36 MPa and ϕ = 35.76 degrees.

Internal friction angles of the limestone joint planes from DH-17/3 and DH-17/4 obtained from the tilt tests 35.76^o and 35.76o respectively (Table 10). According to the observation the joint planes are having some roughness. Therefore, the base friction angle of the joint planes is higher than the residual fiction angle of limestone from direct shear tests.

The results of Los angles abrasion test of rock from DH-17 and DH-27 including percent of wear, uniformity and moisture contents of aggregates are depicted in Table 11. Limestone aggregate of grading A have percent of wear range from 22.57 to 24.46 with uniformity 0.26-0.28. The mudstone aggregate of grading B has a percentage of wear 20.97 with the uniformity 0.24. The uniformity of both limestone and mudstones aggregates are slightly higher than 0.20 indicate slightly non

– homogeneous of the aggregates. However, the percentage of wear of both rock types is not over the range of construction specifications.

The uniaxial compressive strength (UCS) at natural moisture content of the rocks from DH-17 and DH-19 are tabulated in Table 2. The results indicate pale grey limestone having UCS range from 72-171 MPa (moderate to high strength) while dark limestone with fine sand size lamina having the UCS range from 35-59 MPa (low to moderate strength). Mudstones or muddy coals establish low to moderate strength similar to dark lamina limestone with the UCS in the range of 35-69 MPa. Dark mudstone with weak fractures gives UCS in the range of 2-24 MPa which is in a very low strength. Details strength classification according to Deer and Miller (1996) are listed in Table 3.

Results of confining and axial stresses of each sub-specimen from triaxial compressive test are listed in Table 4-6.The peak shear strength parameters (cohesion, c and internal friction angle,ϕ) determining from the tests are also included. The limestone cores (pale grey and some calcite fill) give wide range strength parameters with c = 13.58-26.08 MPa and ϕ = 29.5 - 50.67 degrees. Limestone is dark grey, fine grain sand with some muddy coal laminar also give a similar wide variation in shear strength parameters as c = 0.52 – 32.11 MPa and ϕ = 22.44- 51.52 degrees. The results indicate the influences of calcites veins, impurities, fractures and laminations on the wide variations peak shear strength.

Therefore, the strength could not be defined from depth or types of the rocks themselves. However, average peak shear strength parameters determined from all tests data of both limestone types are approximately c = 9 MPa and ϕ = 45 degree. The results of triaxial test on mudstone and muddy coal core specimens are tabulated

in table 6. The shear strength parameters of mudstones are c = 5.75 - 9.60 MPa and ϕ = 39.98 – 54.81 degrees while the average strength parameters are c = 7.9 MPa and ϕ = 44.58 degrees.

Residual shear strength parameters of the three rock types from bore holes DH-17 and DH-19 are illustrated in Table 7-9. Pale grey limestone with calcite veins give ϕr = 31.10-32.84 degree with no apparent cohesion. The dark limestone core specimens show some apparent cohesion, c = 2.82 -49.59 kPa (kN/m^2) with ϕr = 31.40-36.54 degrees with average c = 16.82 kPa and ϕr = 34.79^o. Residual strength parameters of mudstone are c = 1.63-59.93 kPa and ϕr = 32.87-38.10 degrees with average c = 34.36 MPa and ϕ = 35.76 degrees.

3.6.5 Data collection for detail study

Rock mechanic was test by over view. It target to provide for many job, such as slope stability design, room and pillar design, open pit mining, road hauling and other. For this study target for underground mine by room and pillar method. Geological and rock mechanic data was select only special involve the room and pillar design and factor of safety analysis. These data will be referenced in this case. Geological data was selected are UCS limestone at DH 6 study area by uniaxial compressive strength test, UCS Coal seam by point lode index test, Cohesion and internal fiction angle of coal and limestone by triaxial testing and shear strength by direct shear test.

Table 3.6 Coal uniaxial compressive strength

Sample No	diameter (mm)	Surface area	Diametric Core Test	Point Load Strength Index, I_s	K	UCS(∂c)	Load Foce
	mm	mm^2	De^2	Mpa		(MPa)	N
DH07-UC-PT-01	47.95	1,806.52	2,299.20	0.80	24.00	19.20	1,839.36
DH07-UC-PT-02	47.40	7,061.25	8,987.04	1.20	24.00	28.80	10,784.45
DH07-UC-PT-03	47.20	7,001.78	8,911.36	1.30	24.00	31.20	11,584.77
DH07-UC-PT-04	47.30	7,031.48	8,949.16	1.20	24.00	28.80	10,738.99
DH07-UC-PT-05	47.35	7,046.36	8,968.09	0.80	24.00	19.20	7,174.47
DH07-UC-PT-06	46.99	6,939.62	8,832.24	3.50	24.00	84.00	30,912.84
DH07-UC-PT-08	47.10	6,972.15	8,873.64	1.90	24.00	45.60	16,859.92
DH07-UC-PT-09	47.20	7,001.78	8,911.36	2.60	24.00	62.40	23,169.54
DH07-UC-PT-10	47.44	7,073.17	9,002.21	2.80	24.00	67.20	25,206.20
DH07-LC-PT-01	50.60	8,046.85	10,241.44	0.30	24.00	7.20	3,072.43
DH07-LC-PT-02	51.00	8,174.57	10,404.00	0.30	24.00	7.20	3,121.20
DH07-LC-PT-03	51.30	8,271.03	10,526.76	0.40	24.00	9.60	4,210.70
DH07-LC-PT-04	51.10	8,206.66	10,444.84	0.10	24.00	2.40	1,044.48
DH07-LC-PT-05	50.85	8,126.56	10,342.89	0.10	24.00	2.40	1,034.29
DH07-LC-PT-06	50.95	8,158.55	10,383.61	0.10	24.00	2.40	1,038.36
DH07-LC-PT-07	50.85	8,126.56	10,342.89	0.20	24.00	4.80	2,068.58
DH07-LC-PT-08	51.35	8,287.16	10,547.29	0.20	24.00	4.80	2,109.46
DH07-LC-PT-09	51.00	8,174.57	10,404.00	0.10	24.00	2.40	1,040.40
DH07-LC-PT-10	38.40	4,634.33	5,898.24	0.70	24.00	16.80	4,128.77
DH07-LC-PT-11	48.50	7,392.79	9,409.00	0.40	24.00	9.60	3,763.60
Min				0.10	24.00	2.40	1,034.29
Mean				**0.95**	**24.00**	**22.80**	**8,245.14**
Max				3.50	24.00	84.00	30,912.84
SD				1.01	0.00	24.23	9044.51

Table 3.7 Limestone uniaxial compressive strength (UCS)

Sample No.	Depth	Diameter	Length	Density	σ_c (MPa)	E	ν
	m	mm	mm	g/cc	Mpa	Gpa	
DH7-LS-UCS-01	42.00-42.15	47.26	118.82	2.73	34.2	-	-
DH7-LS-UCS-02	42.20-42.40	47.2	118.58	2.66	34.2	-	-
DH7-LS-UCS-03	41.70-41.85	47.16	120.2	2.67	40.1	-	-
DH7-LS-UCS-04	41.40-41.60	47.16	118.54	2.62	37.2	-	-
DH7-LS-UCS-10	29.00-29.15	47.6	119.4	2.68	42.1	-	-
DH7-LS-UCS-05	29.50-29.65	47.66	120.7	2.67	34.6	22.7	0.16
DH7-LS-UCS-07	28.00-28.20	47.66	120.72	2.66	41.9	20.4	0.12
DH7-LS-UCS-08	28.40-28.55	47.56	118	2.68	40.1	23.9	0.11
DH7-LS-UCS-09	28.56-28.70	47.58	121.3	2.69	30.2	25.7	0.14
DH7-LS-UCS-11	30.05-30.15	47.38	115.9	2.55	31.7	18.2	0.2
Min		47.16	115.90	2.55	30.20	18.20	0.11
Mean		**47.42**	**119.22**	**2.66**	**36.63**	**22.18**	**0.15**
Max		47.66	121.30	2.73	42.10	25.70	0.20
SD		0.21	1.61	0.05	4.26	11.85	0.08

Table 3.8 Direct shear strength of rock core specimens for limestone pale gray, some calcites fill

No.	Sample No.	Depth (m.)	Rock Type	σ_n (kN/m^2)	σ_p (kN/m^2)	c (kN/m^2)	ϕ_r (Deg.)
1	DH-17/2-1			443.04	358.6		31.11
2	DH-17/2-2	17.65-18.00	Limestone	883.87	672.53		
3	DH-17/2-3			1379.81	1035.6		
4	DH-17/2-4			1765.55	1287.3		
1	DH-19/3-1			443.04	489.48		
2	DH-19/3-2	56.15-56.43	Limestone	883.87	699.47		
3	DH-19/3-3			1379.81	882.22		32.84
4	DH-19/3-4			1765.55	1030.77		
1	DH-17/6-1			448.67	318.35		
2	DH-17/6-2	33.55-33.89	Limestone	895.12	513.32		
3	DH-17/6-3			1397.37	803.98	4.15	31.4
4	DH-17/6-4			178801	1145.65		
1	DH-19/15-1			460.28	358		
2	DH-19/15-2	57.60-58.00	Limestone	918.27	770.29	49.59	36.02
3	DH-19/15-3			1433.51	1061.39		
4	DH-19/15-4			1834.25	1387.63		
1	DH-19/20-1			441.18	349.11		
2	DH-19/20-2	81.00-81.25	Limestone	880.17	609.79	2.82	36.54
3	DH-19/20-3			1374.04	1058.68		
4	DH-19/20-4			1758.15	1294.43		
Max						49.59	36.54
Mean						**18.85**	**33.58**
Min						2.82	31.11
SD						26.63	2.56

Table 3.9 Cohesion and internal fiction angle of coal and limestone by triaxial testing

No.	Sample no	Depth (m.)	Rock type	Length (mm)	Diameter (mm)	Density (g/cc)	Axial Load (kN)	σ_3 (MPa)	σ_1 (MPa)	c (MPa)	ϕ (Deg.)	Remark
1	DH-17/1-1		Limestone				115.8	1	65.62	26.07	29.49	Test by KKU
2	DH-17/1-2	14.22-14.63					207.3	3	117.48			
3	DH-17/1-3						216.9	6	122.92			
4	DH-17/5-3	27.32-27.72					213.3	15	125.06			
5	DH-19/1-1						114.4	1	64.02	13.58	50.67	
6	DH-19/1-2	7.52-7.90					130.3	3	72.92			
7	DH-19/1-3						283	6	158.37			
8	DH-19/2-2	12.30-12.60					327.1	15	184.59			
9	DH-17/8-1		Limestone finegrain sand and muddy coal and coal laminar				72.4	1	41.2	12.11	46.24	
10	DH-17/8-2	35.00-35.40					161.7	3	92.02			
11	DH-17/8-3						143.4	6	81.55			
12	DH-17/7-1	34.65-35.00					328.8	20	187.12			
13	DH-19/16-1						65.8	1	38.25	32.11	22.45	
14	DH-19/16-2	63.44-63.90					162.4	3	94.41			
15	DH-19/16-3						205.6	6	119.52			
16	DH-19/16-4						239	20	138.94			
17	DH-07-C-TR-04	12.70-12.85	Limestone	100.07	47.32	2.39		0.30	53.00	11.44	40.0	Test by SUT
18	DH-07-C-TR-01	14.50-14.70		99.82	47.16	2.5		0.60	56.90			
19	DH-07-C-TR-02	44.30-44.50		102.44	47.08	2.53		1.00	59.90			
20	DH-07-C-TR-07	43.10-43.25		102.56	47.26	2.57		1.70	68.30			
21	DH-07-C-TR-03	44.00-44.20		99.88	47	2.62		2.00	71.90			
Max				102.56	47.32	2.62		20.00	187.12	32.11	50.67	
Average				**100.95**	**47.16**	**2.52**		**5.50**	**95.90**	**19.06**	**37.77**	
Min				99.82	47.00	2.39		0.30	38.25	11.44	22.45	
SD				1.41	0.13	0.09		6.35	44.46	9.43	11.69	

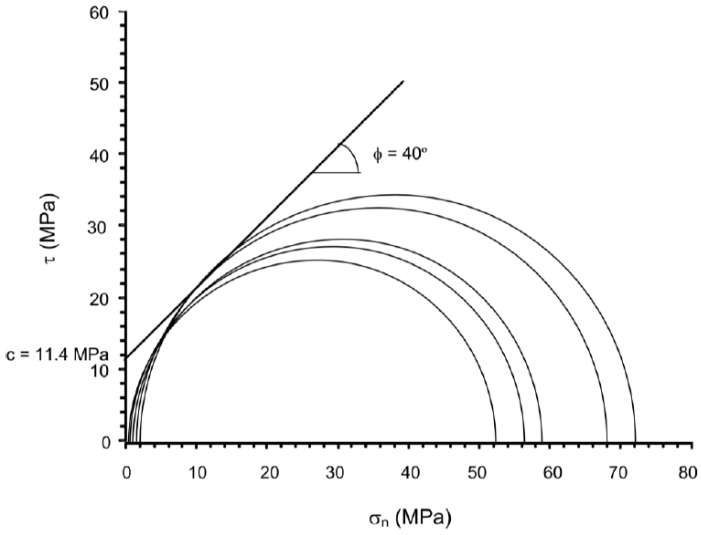

Conclusions:

- The friction angle is 40 degrees.
- The cohesions is 11.4 MPa.

References:

ASTM D7012-04. Standard Test Method for Compressive Strength and Elastic Moduli of Intact Rock Core Specimens under Varying States of Stress and Temperatures1. In **Annual Book of ASTM Standards** (Vol. 04.08). Philadelphia: American Society for Testing and Materials.

Brown, E. T. (1981). **Rock Characterization Testing and Monitoring: ISRM Suggested Methods.** The Commission on Rock Testing Methods, International Society for Rock Mechanics, Pergamon Press.

Figure 3.11 Fiction angle and cohesion of limestone

Table 3.10 Result of triaxial test for cohesion and fiction angle

No.	Sample no	Depth (m.)	Rock type	Axial Load (kN)	σ_3 (MPa)	σ_1 (MPa)	c (MPa)	ϕ (Deg.)
1	DH-17/11-1		coal and fossil lamina	20.2	1	11.74	9.6	41.47
2	DH-17/11-2	51.05-51.50		76.6	3	44.34		
3	DH-17/11-3			154	6	89.52		
4	DH-17/9-1	50.00-50.45		195.3	15	112.09		
5	DH-19/6-1			58.6	6	34.96	5.75	54.81
6	DH-19/6-2	32.45-32.70		136.1	15	81.19		
7	DH-19/7-1	39.50-39.88		311.8	20	18360		
8	DH-19/11-1			70.9	1	41.22	15.36	39.98
9	DH-19/11-2	42.30-42.80		117.5	3	68.6		
10	DH-19/11-3			183	6	106.84		
11	DH-19/9-1	41.65-41.98		265	20	155.38		
Max				311.80	20.00	18360.00	15.36	54.81
Min				20.20	1.00	11.74	5.75	39.98
Mean				**144.45**	**8.73**	**1736.90**	**10.24**	**45.42**
SD				89.62	7.35	5513.41	4.84	8.17

3.6.6 RQD Determination

The RQD was initially introduced for civil engineering applications, and it has been quickly adopted in mining, engineering geology as well as geotechnical engineering. The success of the RQD is in great part, due to its simplicity. This paper investigates the usefulness of rock quality designation (RQD) on determination of the rock mass strength. The determination of rock mass strength using the technique of RQD can be performed in field or in the laboratory. RQD Rock mass quality ranking are as table below:

<25%	=	very poor	25-50%	=	Poor
50-75%	=	Fair	75-90%	=	Good
90-100%	=	Excellent			

The RQD was done on rock mass in PCB coal mine project was determination by rock type, limestone, mudstone, muddy and coal. Drilling number 19 at coal field was selected to represent for determination. Because it is in area of research and contain full all of rock type. The results imply has to lower than by depth. (Table 3.15). It very low RQD at coal and mudstone bud fair rock at limestone and muddy coal.

Table 3.11 Representative RQD overburden Limestone at drill hole DH 6

Depth interval (m)	Core length (m)	Total length (m)	%RQD
10-12	246	300	82.00
13-15	236	300	78.67
16-18	166.5	300	55.50
19-21	213	300	71.00
22-24	242.5	300	80.83
25-27	242	300	80.67
28-30	249	300	83.00
31-33	139.5	300	45.50
Limestone Burden			**72.15**

Table 3.12 Representative RQD of coal seam at drill hole DH 6

Depth interval (m)	Core length (m)	Total length (m)	%RQD
46-48	62	300	21
49-51	0	300	0
52-54	100	300	33
Coal Seam			**18**

CHAPTER IV

ROCK MASS CHARACTERIZATIONS

4.1 Introduction

This chapter describes the characterizations of rock mass in the proposed area for coal underground mining. The study was using rock mass classification systems which have been developing for over 100 years. Ritter (1879) attempted to formalize an empirical approach to tunnel design, in particular for determining support requirements. Rock mass classification systems evaluate the quality and expected behavior of rock masses based on the most important parameters that influence the rock mass quality.

Rock mass along the tunnel alignment is classified by three individual systems included rock mass rating system (RMR), NGI tunneling quality index (Q system), rock mass index (RMi). The required input parameters and engineering geological properties for the rock mass classification systems are described in Chapter 3.

4.2 Rock mass rating system (RMR)

The rock mass rating system is initially developed by Bieniawski (1973), otherwise known as geomechanics classification system. It was modified over the years as more case studies, became available and conforms to international standards

and procedures (Bieniawski, 1979). In this research, the 1989 version of the classification table has been used by considering the uniaxial compressive strength of intact rock (UCS), rock quality designation (RQD), discontinuity spacing, discontinuity conditions, groundwater conditions and discontinuity orientation are the utilized parameters of rock mass rating system. Based on rock mass rating system, the rating value and class of rock mass along the water tunnel alignment are shown in Table 4.1. Result of RMR classification has significant in RQD of rock type. It has very good quality in limestone, and fire rock in muddy coal, coal, and mudstone.

Table 4.1 RMR rock mass rating result at study area

Six Parameters Bieniawski	**Rock Mass Character and Ranking**							
	Limestone		**Mudstone**		**Muddy Coal**		**Coal**	
1. Uniaxial compressive strength	72-171 %	17	2-24 %	2	35-69 %	8	2 -24 %	2
2. Rock Quality Designation (RQD)	32.15	8	9.71	3	19.17	3	3.17	3
3. Joint spacing	0.3-1m	25	0.3-1m	25	0.3-1m	25	0.3-1m	25
4. Joint conditions	<1mm HDR	20	<1mm HDR	20	<1mm HDR	20	<1mm HD	20
5. Groundwater conditions	Dry	10	Dry	10	Dry	10	Dry	10
6. Joint orientation	Fair (parallel)	-5	Fair (parallel)	-5	Fair (parallel)	-5	Fair (parallel)	-5
Rating		75		55		61		55
Ranking	Good rock		Fair Rock		Fair Rock		Fair Rock	

Figure 4.1 Coal seam at DH 19 depth between 42-48m

Figure 4.2 Limestone at DH 19 depth between 33-38m

Figure 4.3 Muddy coal at DH 19 depth between 49-56m

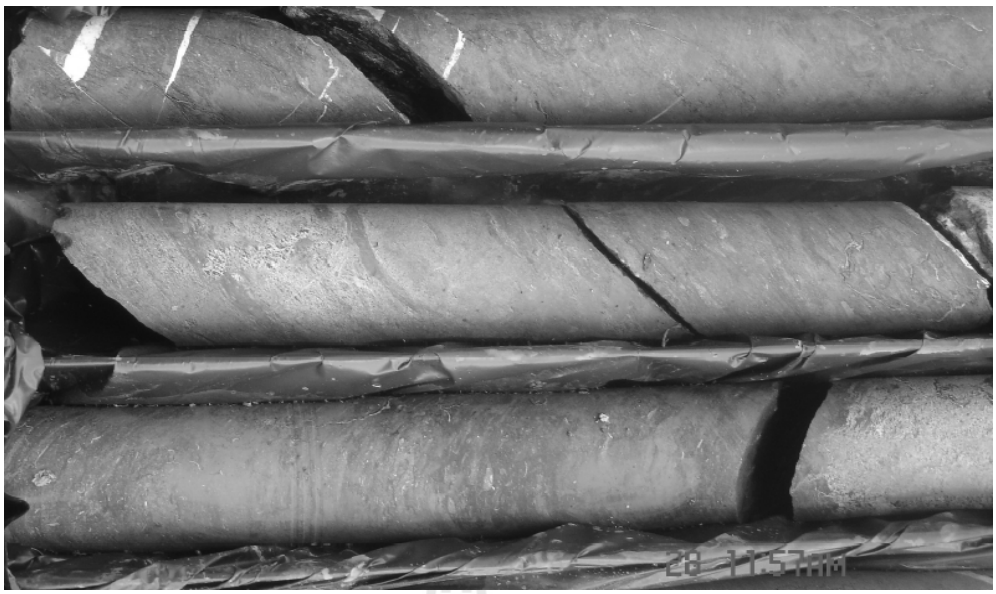

Figure 4.4 Fracture of rock mass

4.3 NGI tunneling quality index (Q system)

The Q system proposed by Barton et al. (1974) is a numerical description of the rock mass quality with respect to the tunnel stability and consists of six parameters, which are estimated from geological mapping, in-situ measurements and drilled core loggings. These six parameters are 1) rock quality designation (RQD), 2) joint set number (J_n), 3) joint roughness number (J_r), 4) joint alternation number (J_a), 5) joint water reduction number (J_w) and 6) stress reduction factor (SRF). The numerical value of Q index is defined by a function of these six parameters (equation 2.1 in Chapter 2). The Q index value and class of rock mass classified by Q system are presented in Table 4.2.

Table 4.2 Q index values rating result at study area

Six Parameters Barton, Lien and Lunde (1974)	Condition	Limestone	Mudstone	Muddy Coal	Coal Seam
1) RQD (0-100)	Poor - Fair	72.15	9.71	19.17	12.00
2) Number of Joint Set (Jn)	3 set	9.00	9.00	9.00	9.00
3) Roughness (Jr)	Rougness Planar	1.50	1.50	1.50	1.50
4) Degree of alternation (Ja)	Staining only; no alteration	1.00	1.00	1.00	1.00
5) Water Inflow (Jw)	Dry	1.00	1.00	1.00	1.00
6) Stress Condition (SRF - Stress Reduction Factor)	Rock at shallow depth (< 50 m) with clay-filled discontinuities	2.50	2.50	2.50	2.50
Q = (RQD/Jn) × (Jr/Ja) × (Jw/SRF)					
ROD/Jn		8.02	1.08	2.13	1.33
Jr/Ja		1.50	1.50	1.50	1.50
Jw/SRF		0.40	0.40	0.40	0.40
Q		**4.81**	**0.65**	**1.28**	**0.80**
Ranking		Fair Rock	Very Poor	Poor Rock	Very Poor

4.4 Comparison of the rock mass classification results

The rock mass classes along the study area room and pillar area are classified by four rock mass classification systems. There are summarized in Table 4.5. The three different rock class zones are defined by the results of four rock mass classification systems, Zone 1 is identified as fair rock, Zone 2 is very poor rock and Zone 3 is generally identified as good rock.

4.5 Rock mass engineering property

Laboratory experiments have been carried out to determine the physical and mechanical properties of intact rock. The rocks specimens of limestone and coal were selected from borehole number DH-17, DH-19 and DH-27. The tests are uniaxial compression (ASTM D2938-95), triaxial compression (ASTM D2664-95a), direct shear (ASTMD5607-95), and tilt test on discontinuity planes. The result test of uniaxial compressive strength (UCS) at natural moisture content of the rocks from

DH-17 and DH-19 are indicated. Results of confining and axial stresses of each sub-specimen from the triaxial compressive test have the shear strength parameters (cohesion, c and internal friction angle,ϕ) determining from the tests is also included. The limestone of dark colure, fine grain sand with some muddy coal laminar also gives a similar wide variation in shear strength parameters. The rock mechanic testing results were shown as below Table 4.1.

Table 4.3 Comparison of the rock mass classes between RMR and Q system (MGI)

RMR Rock Mass Classification									Rock Mass Classification by Q System					
Six Parameters Bieniawski (1974)	**Limestone**		**Mudstone**		**Muddy Coal**		**Coal**		**Six Parameters Barton, Lien and Lunde (1974)**	**Condition**	**Limestone**	**Mudstone**	**Muddy Coal**	**Coal Seam**
1. Uniaxial compressive strength	72-171 %	17	2-24 %	2	35-69 %	8	2 -24 %	2	1) RQD (0-100)	Poor - Fair	72.15	9.71	19.17	12.00
2. Rock Quality Designation (RQD)	32.15	8	9.71	3	19.17	3	3.17	3	2) Number of Joint Set (Jn)	3 set	9.00	9.00	9.00	9.00
3. Joint spacing	0.3-1m	25	0.3-1m	25	0.3-1m	25	0.3-1m	25	3) Roughness (Jr	Rougness Planar	1.50	1.50	1.50	1.50
4. Joint conditions	<1mm HDR	20	<1mm HDR	20	<1mm HDR	20	<1mm HDR	20	4) Degree of alternation (Ja)	Staining only; no alteration	1.00	1.00	1.00	1.00
5.Groundwater conditions	3000 l/sec	0	3000 l/sec	0	3000 l/sec	0	3000 l/sec	0	5) Water Inflow (Jw)	Dry	1.00	1.00	1.00	1.00
6. Joint orientation	parallel/35 Dreg(Fair)	-5	Pallalen/35 Dreg(Fair)	-5	Pallalen/35 Dreg(Fair)	-5	Pallalen/35Dreg(Fair)	-5	6) Stress Condition (SRF - Stress Reduction Factor)	Rock at shallow depth (< 50 m) with clay-filled discontinuities	2.50	2.50	2.50	2.50
Rating		**65**		**45**		**51**		**45**	**Q**		**4.81**	**0.65**	**1.28**	**0.80**
Ranking	**Good rock**		**Fair Rock**		**Fair Rock**		**Fair Rock**		**Ranking**		**Fair Rock**	**Very Poor**	**Poor Rock**	**Very Poor**

Table 4.4 Rock mechanic laboratory test results of pale grey limestone and Coal

Rock type	UCS strength ($\sigma_{c)}$ Mpa	Young's modulus (E) Gpa	Poisson's ratio (ν)	Unit weight (γ) MN/m3	Cohesion (c) Mpa	Internal friction angle (ϕ) degree	RMR Ranking	Q System Ranking
Limestone	30.20	10.90	0.25	2.64	11.44	40.00	75.00	4.81
Muddy Limestone	36.63	22.18	0.15	0.028	13.68	43.42	55.00	1.28
Coal Seam	22.80	15.03	0.29	0.027	5.75	39.98	61.00	0.80
Mudstone	13.66	0.00	0.00	2.56	10.24	45.24	55.00	0.64

CHAPTER V

NUMERICAL ANALYSIS

5.1 Introduction

This chapter will perform to primary design underground coal mine by room and pillar method. The criteria use for design are rock mechanic engineering and geological of coal deposit. The result of primary design was rechecked confirmable the built ability by safety analysis. Coal deposit information was collection data from 19 drilling holes. They were carrying out on year 2007 - 2010. The rock mechanic property was test by core collected sampling at drill hole (DH) number 6, 17 and 19. Because they are well represent for the study area. For detail of geological data and rock mass classification were showing at chapter 3 and 4.

Rock mechanics is the study of the properties and behavior of rock mass, the nature of the stresses about underground openings, and their relation in the design and support of mine workings and in the induced caving of rock in mine exploitation. All rock at depth is under stress due to the weight of the overlying rock (superincumbent load) and to possible stresses of tectonic origin. In addition, the presence of amine opening induces occur stresses in the rock mass surrounding the opening, and this rock (and the opening) will fail if the rock stress exceeds the rock strength (Obert et al. 1960). Thus the problem of designing a stable mine opening reduces to determining (1) the maximum stress approach to pillar and (2) the maximum of pillar strength.

Rock mechanics is often defined more broadly. The aspect described above-that concerned with time rates of loading that are very long in duration-is referred to as static rock mechanics. A different aspect related to rock attack under rates of loading of loading of short time duration and the corresponding behavior of rock is called dynamic rock mechanics. The latter includes rock penetration and fragmentation processes of all types, ranging from conventional means of drilling, blasting, and continuous mining to novel methods of applying energy to excavate rock such as fluid, thermal, and electrical attack

In this discussion, we shall be concerned with static rock mechanics only, because it is fundamental to a study of all rock mechanics and because the factor of safety and stability support design for underground openings are fundamental to mining itself. We remind ourselves that the ultimate expression of depth as a constraint in mining takes two forms and that one is the inexorable rise in rock stress. The other is the equally unrelenting climb in rock temperature.

Since our treatment of the subject of rock mechanics is abbreviated and restricted to the design of underground openings, a number of simplifying assumptions about rock prove helpful (Panek, 1951):

1. Rock is perfectly elastic (stress is proportional to strain).
2. Rock is homogeneous (there are no significant imperfections).
3. Rock is isotropic (its elastic properties are the same in all directions).

While never perfectly true, these assumptions apply reasonably well to many rocks (igneous best, sedimentary least) at moderate depth. Causes of departure are the

complex, diversified, and temperature at great depth, the presence of water or solutions, and the effects of geologic structures (bed-ding, fractures, folding, joints, alteration, etc.).To a certain extent, uncertainties and departures from theory are compensated for in design by the use of factors of safety.

5.2 Conceptual of Primary Design

The applications of pillar mining have been discussed by Hamrin (1982) and Hittman Associates (Anon., 1976) among others. Suitable conditions include ore bodies that are horizontal or have a dip of less than 30°. A major requirement is that the hanging wall is relatively competent over a short period of time, or is capable of support by rock bolts that are used extensively in room and pillar mining. The method is particularly suited to bedded deposits of moderate thickness (6 to 20 ft, or 2 to 6 m) such as coal (the main application) salt, potash, and limestone.

Geology of this study area was comprises with two coal seams. They was consign name by upper and lower coal seam. The lower coal seam is target to selects for room and pillar mining method. It is a single bed but various in true thicknesses between 5.00 – 9.00 m, average 8.10m. The minimum 5 m was found at drilling number DH_6 and maximum total 9 m at number 19. Type section was use for primary design is on line of drill hole number 3, 6, 7 and 19. It appears an appearance thickness 11 m.

Coal seam dipping angle is this area is high validation. It observed effect from tectonic movement. The result from field joint measurement showing average 42 degrees (See Figure 3.10). Result measurement in core sample showing 33 degrees at

drilling number 6, about 36 degree at number 7 and 40 degree at number 19. The representative coal seam dip angle was select to design is 36 degree.

Direction of tunnel will parallel with coal strike. (Figure 5.5). It will plan to design by horizontal driving with difference depth. First pillar will be starting in 10 .00 m and the last is 60 meters from ground surface. Width of pillar was design equal with maximum span. High of room was available follow up with coal seam thickness It is less than 2 time. (See Figure 5.1 - 5.3)

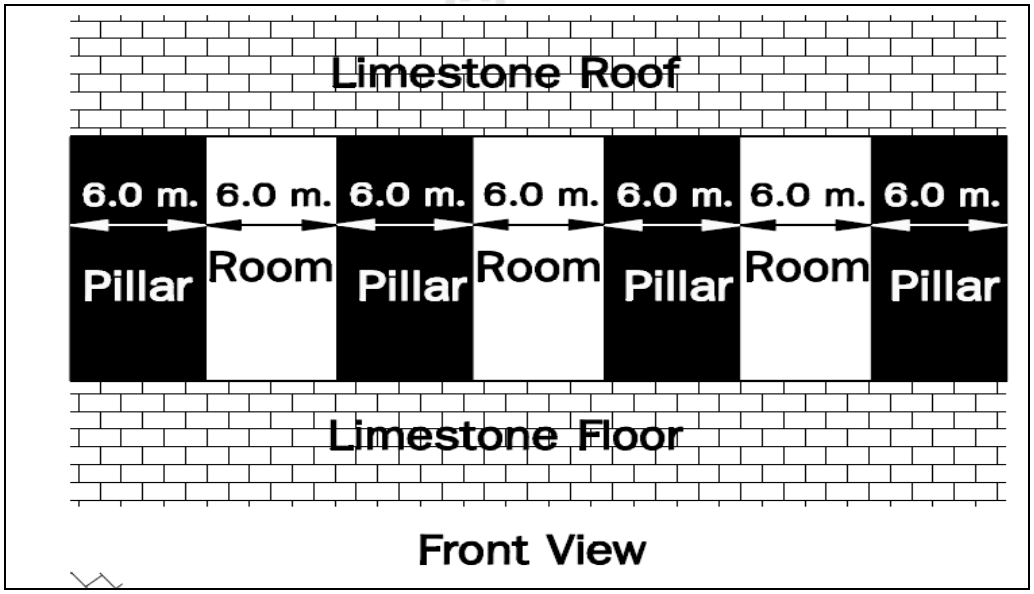

Figure 5.1 Front views of room and pillar conceptual design

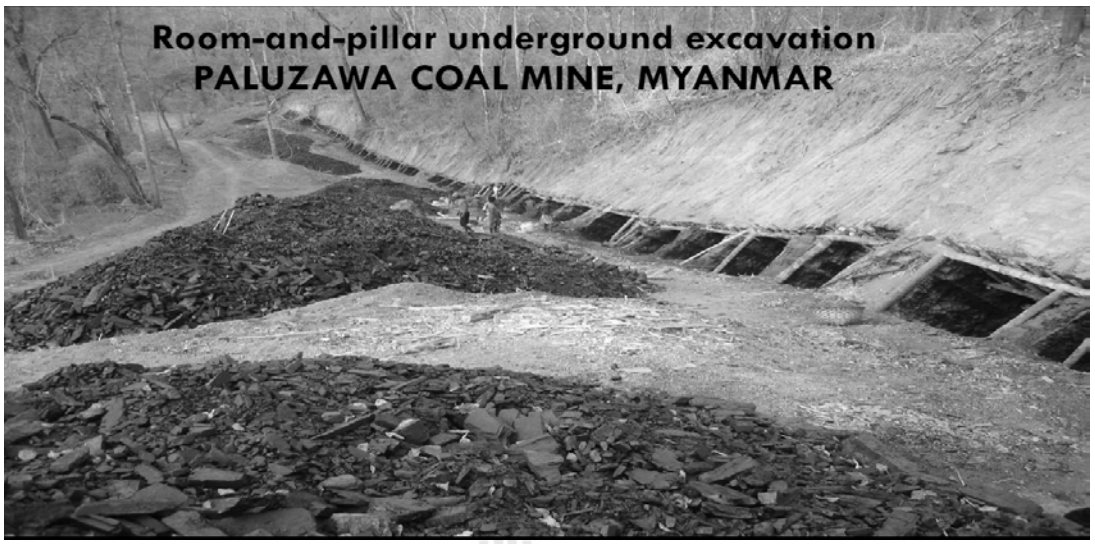

Figure 5.2 Similar conceptual designs for room and pillar underground coal mine (Paluzawa coal mine, Myanmar 2013)

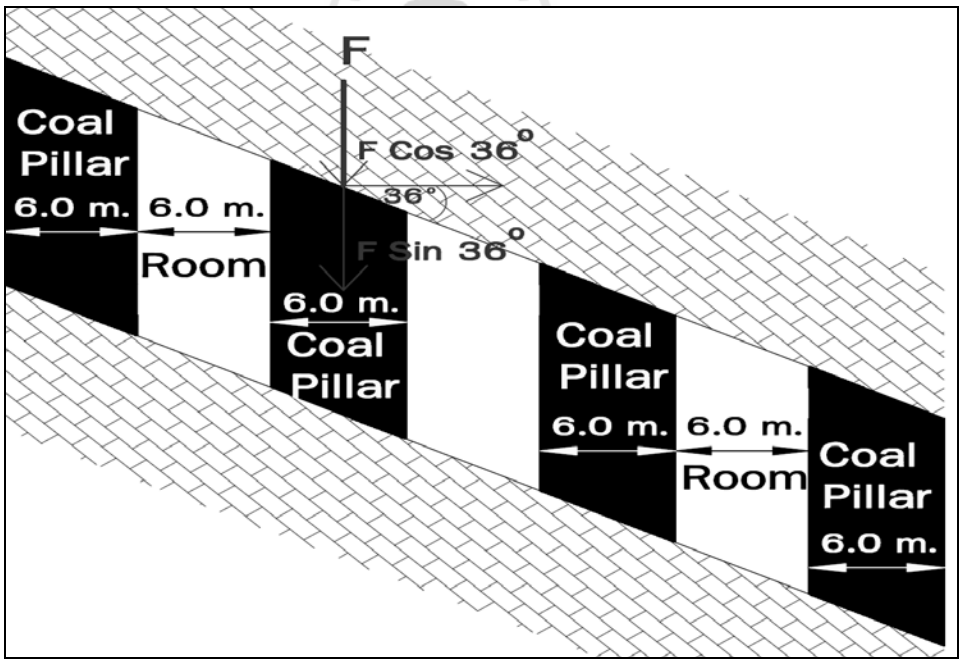

Figure 5.3 front and side views of room and pillar conceptual design

5.3 Maximum Unsupported Span

The typical geological of PCB coal deposit, is very poor coal seam was overlay by good rock of limestone. Coal seam has is single bed with true thickness 5-9 m and appearance along tunnel axis about 11.00 meters. Maximum unsupported span will be use limestone and coal will be pillar support. For high factor of safety, the maximum unsupported span will design by use Q value of limestone.

Barton et al. (1974), relating the Q index with the stability and support requirements of underground excavations, have defined an additional parameter that is called the Equivalent Dimension D_e of excavation. This dimension is obtained by dividing the span, diameter or wall height of excavation by a quantity called the excavation support ratio, ESR. Hence:

$$D_e = \frac{\text{Excavation span, diameter or height (m)}}{\text{Excavation Support Ratio, ESR}} \tag{5.1}$$

The value of ESR is the so-called excavation support ratio. It ranges between 0.5 and 5. For the diversion tunnel, the excavation support ratio, ESR is defined as 1.6. For Q value of limestone is 4.81, the maximum unsupported span was calculating result in 6.40 m. (See Figure 5.4)

Overall of mine planning for underground coal mine have 400m long and width 180m widths and maximum depth 60m. It is comprise with room and pillar total 11 rows by difference by depth. Road hauling was conceptual to horizontal driving of a few slop angle degrees. (See Figure 5.5)

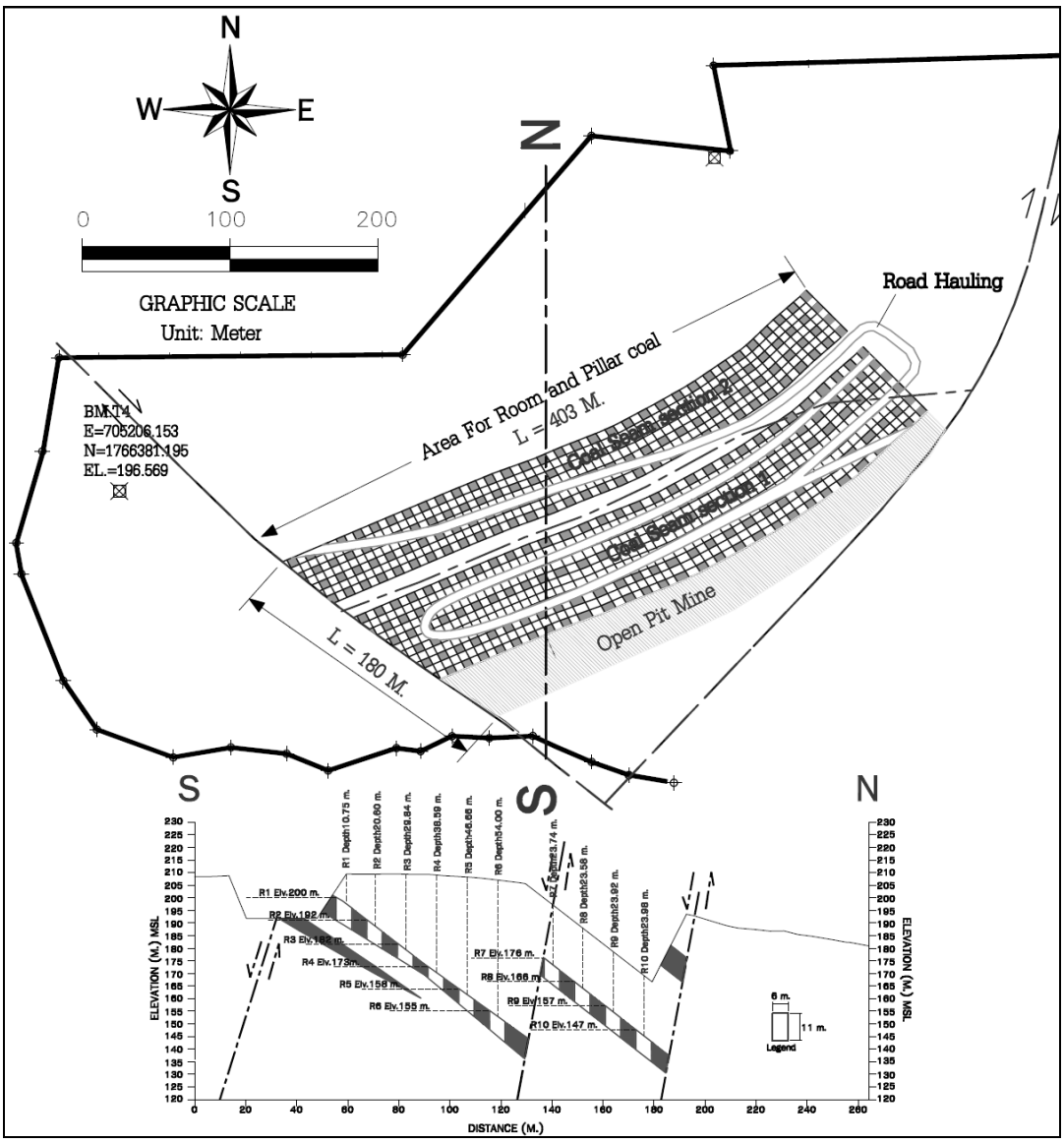

Figure 5.4 Results of maximum unsupported span of limestone

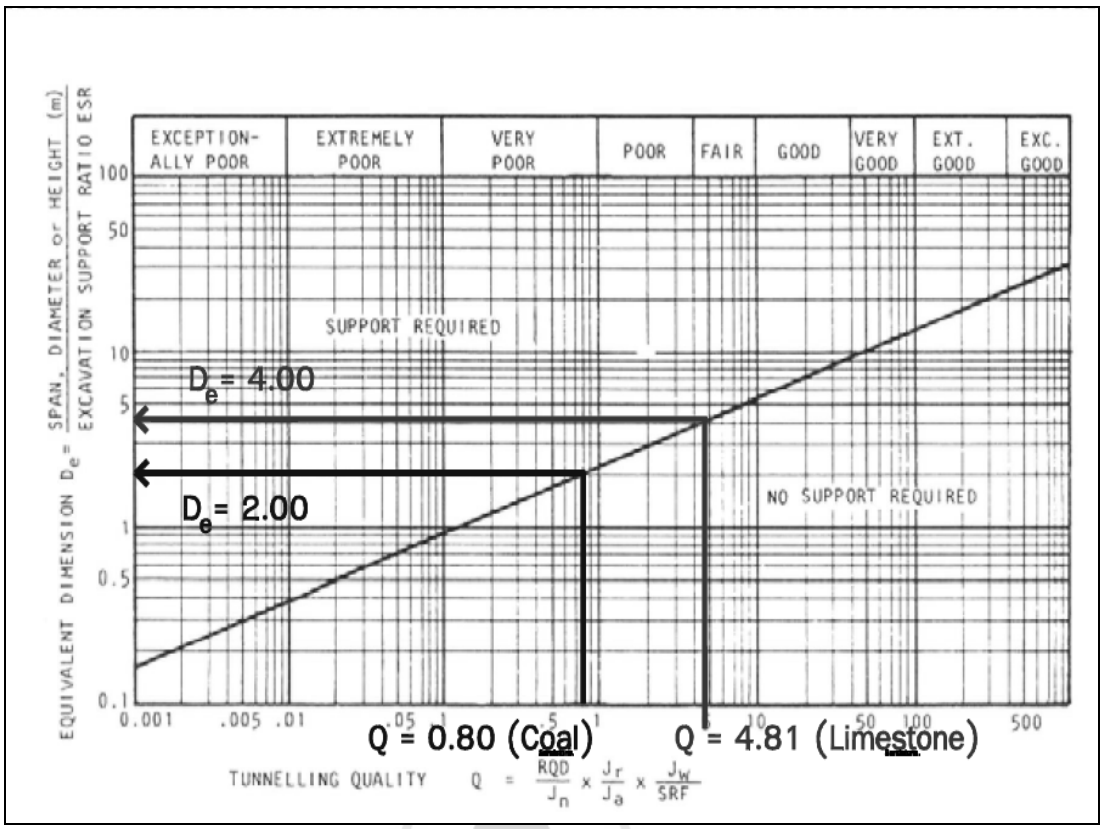

Figure 5.5 Map showing result of room-and pillar design by overview

5.4 Stress surrounding Room and Pillar

5.4.1 Stress approach and UCS Coal Pillar Strength(Intact Rock)

The major recent work on stresses acting on pillars has been carried out by Coates (1981). He started with the simplest and traditional statement of average pillar stress, known as the tributary area method. This assumes that each of the pillars left during excavation supports all the overlying strata that are “tributary” to their location. Then the average pillar stress for square pillars with rooms of consistent width is

$$\partial p = (At/Ap) \times \partial v \qquad (5.2)$$

Where At and Ap are width of the pillar and room, respectively (5.7), and is the geostatic or pre mining stress acting normal to the plane of excavation.

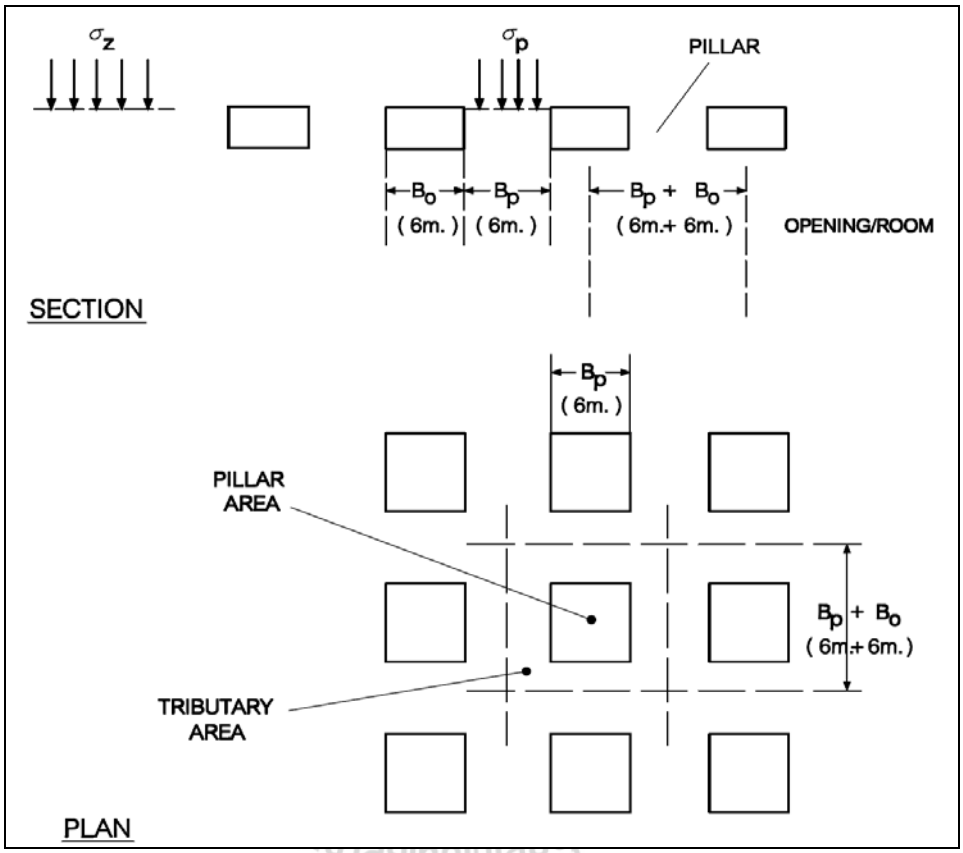

Figure 5.6 Section and plan of room and pillar with widths and dimension for simple analysis

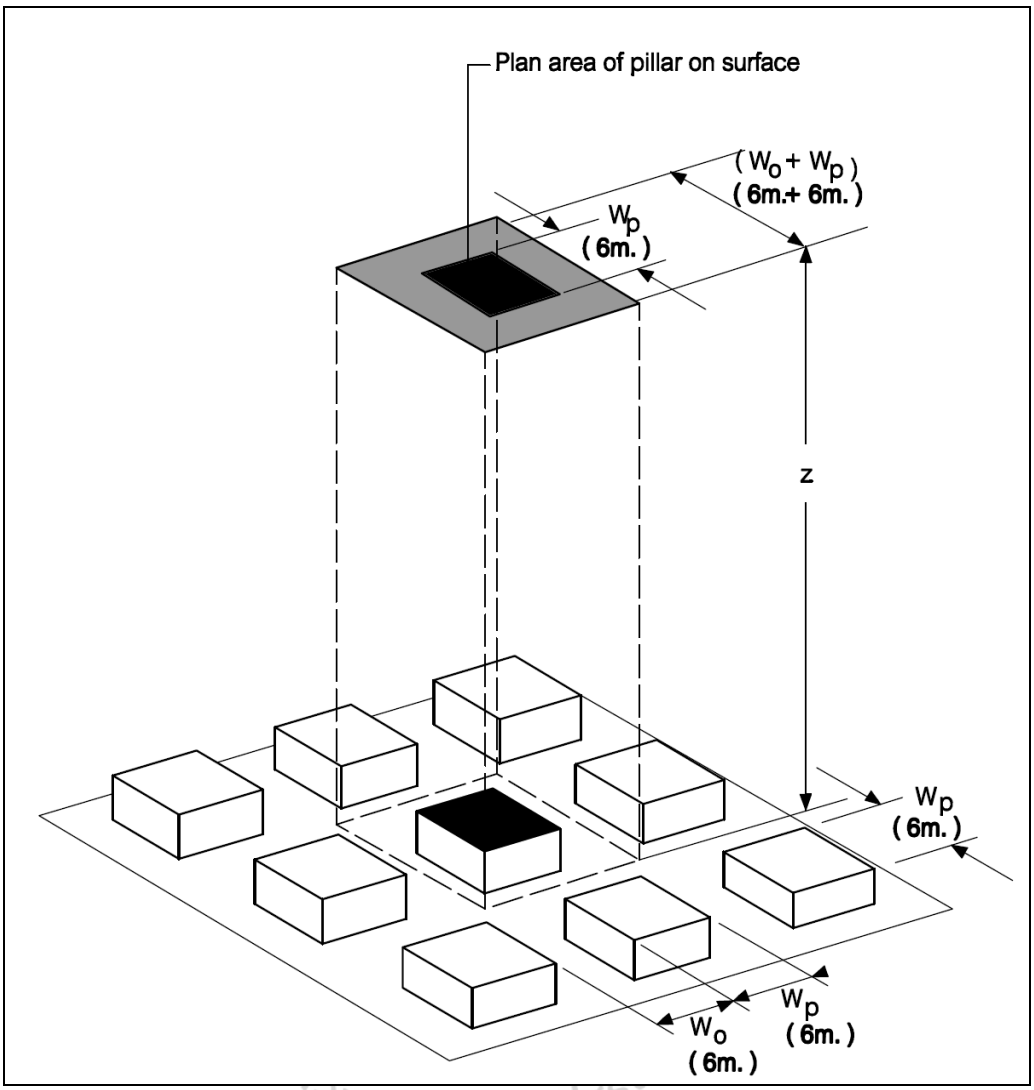

Figure 5.7 Three dimensions of room and pillar for simple analysis

There is a large literature on pillar strength, much of it empirical. The most complete work is by Salamon and Monro (1967), and the best summaries by Bieniawski (1981) and Tsur- Lavie and Denekamp (1982). The basic problem with pillar strength is that in a brittle rock, strength is dependent upon the size, and to a lesser extent, the shape of a test specimen. This means that the conventional method

of pillar design, relating rock strength to pillar stress through a factor of safety is unacceptable in brittle rocks, although it may be acceptable in more ductile rocks.

Figure 5.8 is shows cross section along room and pillar. It was use to measurement depth of each pillar from ground surface. This depth was used to calculate the vertical load upon roof of pillar and average stress approach on pillar. The results of each row of pillar are showing in Table 5.1

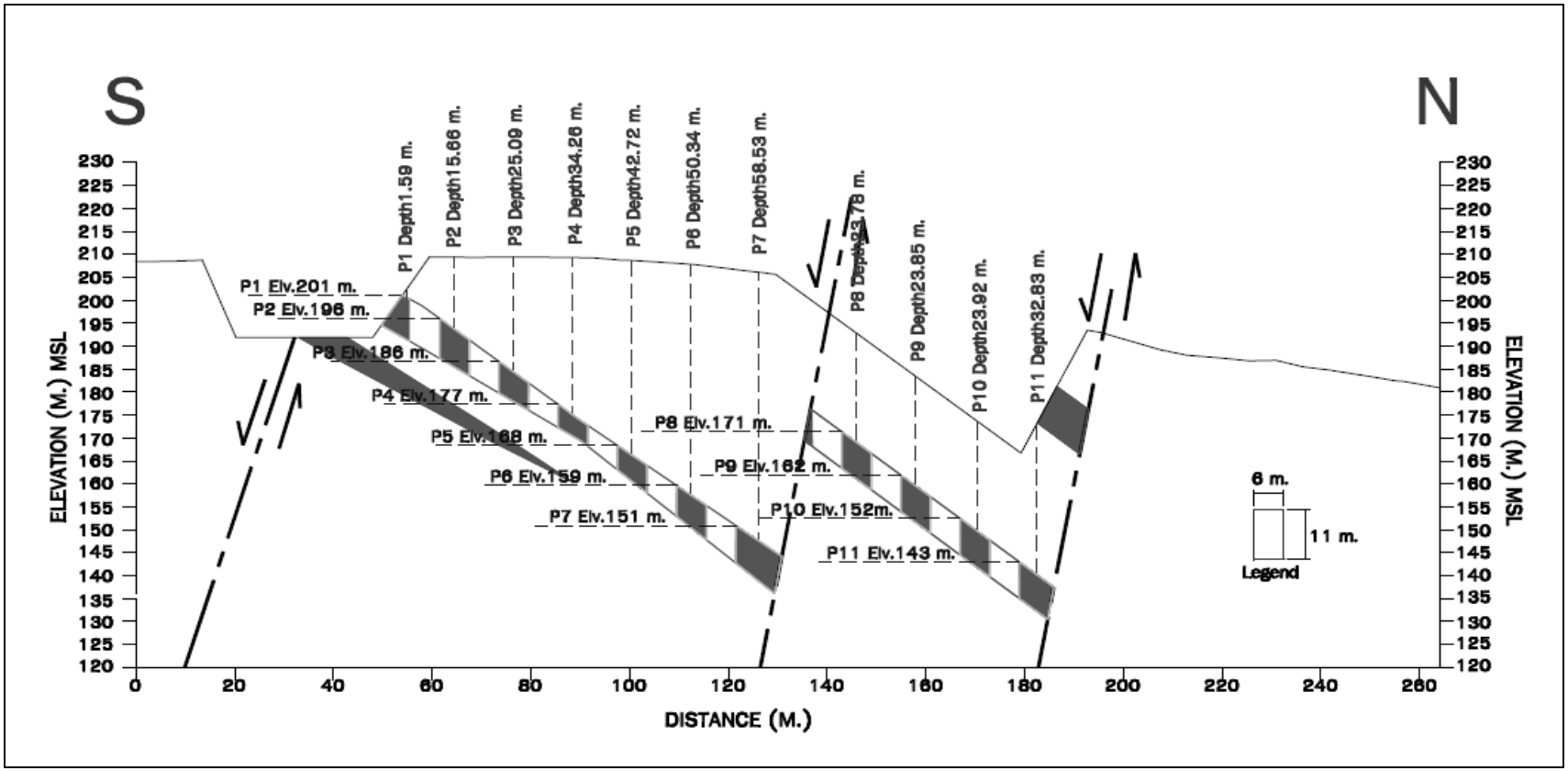

Figure 5.8 Cross section for depth of roof pillar for safety factor analysis at PCB underground coal mine

Table 5.1 Results of stress acting upon pillar and factor of safety analysis

Pillar level number	Depth of pillar Roof (H)	Area of Coal pillar and roomm		Stress Acting On Pillar Roof				USC Coal Pillar Stress by Intact rock
				γ	Stress per unit Depth of OB (SOB)	Vertical stress before Tunnel (SOB x H)	Average Vertical acting stress on pillar (At/Ap x ∂v)	
		W_P	$W_P + W_r$		∂_v	∂v	∂P	∂c
	m	m	m	g/cc	Mpa/m	Mpa	Mpa	Mpa
P1	1.59	6.00	12.00	2.64	0.027	0.043	0.172	22.80
P2	15.66	6.00	12.00	2.64	0.027	0.423	1.691	22.80
P3	25.09	6.00	12.00	2.64	0.027	0.677	2.710	22.80
P4	34.26	6.00	12.00	2.64	0.027	0.925	3.700	22.80
P5	42.72	6.00	12.00	2.64	0.027	1.153	4.614	22.80
P6	50.34	6.00	12.00	2.64	0.027	1.359	5.437	22.80
P7	58.53	6.00	12.00	2.64	0.027	1.580	6.321	22.80
P8	23.78	6.00	12.00	2.64	0.027	0.642	2.568	22.80
P9	23.85	6.00	12.00	2.64	0.027	0.644	2.576	22.80
P10	23.92	6.00	12.00	2.64	0.027	0.646	2.583	22.80
P11	32.83	6.00	12.00	2.64	0.027	0.886	3.546	22.80

5.5 Stress Acting Upon Parallel Room and Pillar

Obert and Duvall (1987) report the result of photo elastic studies carried out to determine the stress distribution in room and pillar between a numbers of parallel tunnels. The type of plate model which could be used in such study is illustrated in Figure 5.6 show that the average vertical stress at the mid height of pillar is given by;

$$\partial p = (1 + Wo/Wp)/Pz \quad (5.3)$$

In case of room and pillar coal mine at study area. The shape of parallel tunnel has width equal with Long (Wo/Wp=1). The maximum pillar strength (∂c) and average pillar stress (∂ps) given equation 5.4 and 5.5. Result of calculation showing in Table 5.2

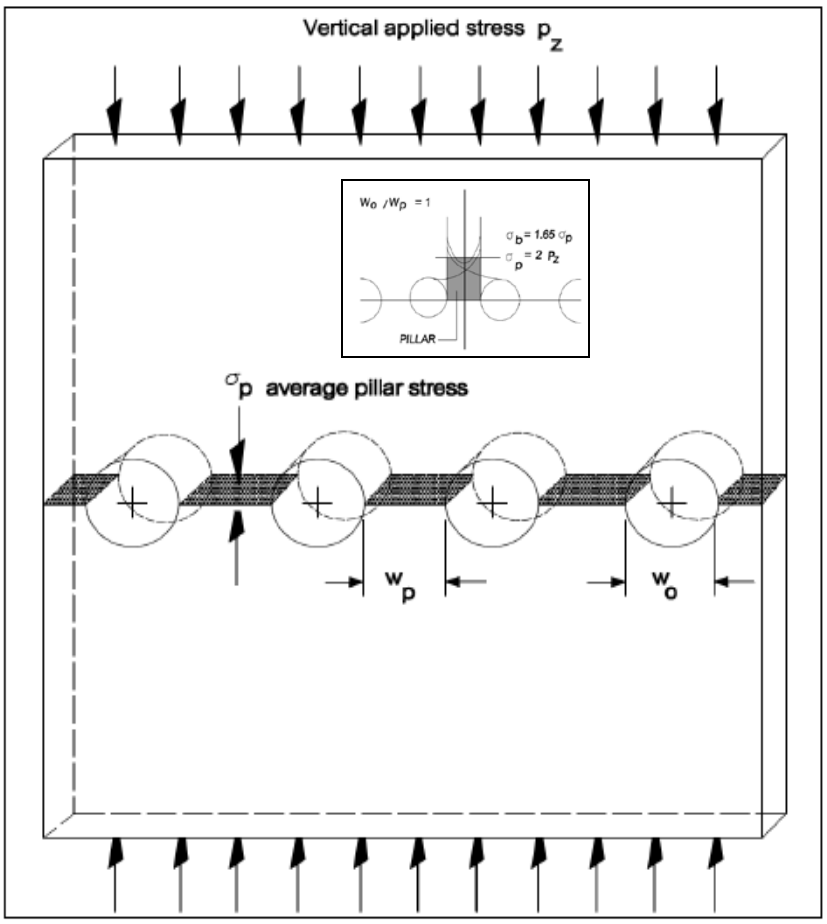

Figure 5.9 Rock plate model and stress in room and pillar between parallel circular tunnels after Obert and Duvall (1967)

$$\partial b = 1.65 \partial p \tag{5.4}$$

$$\partial p = 2\,Pz \tag{5.5}$$

Result of average stress acting upon parallel of pillar and factor of safety analysis given in Table 5.4

5.6 Factor safety analysis

5.6.1 Stresses independent of elastic constants

The equations presented in figure 5.1 show that the stresses around the circular hole are dependent upon the magnitude of the applied stresses and the geometry or shape of the stressed body. The elastic constants E (Young's modulus) and v (Poisson's ration) do not appear in any of the equations and this means that the stress pattern is independent of the material used, provided that this is a linear elastic material.

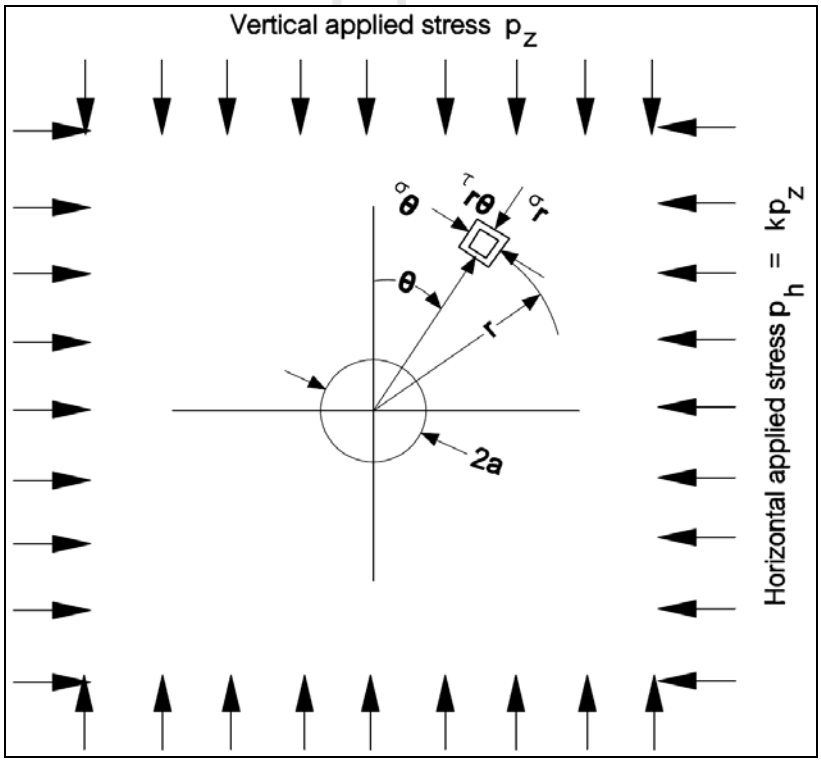

Figure 5.10 Equation for the stress in the material surrounding a circular hole in stresses elastic body

Radial $\sigma_r = \frac{1}{2}Pz[(1+k)\left(1-\frac{a^2}{r^2}\right)+(1-k)\left(1-\frac{4a^2}{r^2}+3a^4/r^4\right)Cos\,2\theta]$ (5.6)

Tangential $\sigma_{\theta=}\frac{1}{2}Pz[(1+k)(1+a^2/r^2)-(1-k)(1+3a^4/r^4)Cos\,20)$ (5.7)

Shear $\tau_{r\sigma=}\frac{1}{2}Pz\,[-(1-k)(1+2a^2/r^2-3a^4/r^4)Sin\,2\theta)$ (5.8)

Principal stresses in plane of paper at point (r,θ)

Maximum $\sigma_{1=}\frac{1}{2}(\sigma_r+\sigma_\theta)+(\frac{1}{4}(\sigma_r-\sigma_\theta)2+\tau_{r\frac{2}{\theta}})^{\frac{1}{2}}$ (5.9)

Maximum $\sigma_{2=}\frac{1}{2}(\sigma_r+\sigma_\theta)-(\frac{1}{4}(\sigma_r-\sigma_\theta)2+\tau_{r\frac{2}{\theta}})^{\frac{1}{2}}$ (5.10)

Inclinations to radial direction Tan $2\alpha=2^{\tau}r\theta/(\sigma_\theta-\sigma_r)$ (5.11)

This has been utilized by a number of researchers who have studied the distribution of stresses around excavations by means of photoelasticity this technique involves viewing a stressed glass of plastic model in polarized light. The stress pattern which appears under these conditions is related to the difference between the principal stresses ∂1 and ∂2 (∂3 if smaller principle stress in tensile) in the plane of the model. Since these stresses do not depend upon the properties of the material, as discussed above, the Photoelastic stress pattern can be used to calculate the stresses around an opening or openings of the same shape in hard rock. Photoelastic techniques are seldom used for this purpose today because stresses around underground excavations can be calculated more rapidly and more economically.

5.6.2. Influence of excavation Size

It is important to note that the equations for the stresses around a circular hole in an infinite rock mass given in figure 5.90 do not include terms in the

radius of the tunnel(hole radial =a, r = radial distance) but rather, include terms in the dimensionless parameter a/r. This means that the calculate stress level at the boundary of the excavations are independent of the absolute value of the radius.

This has led to considerable confusion in the past. Some underground excavation designers have concluded that, because the stresses induced in the rock around an excavation are independent of the size of the excavation, the stability of the excavation is also independent of its size.

If the rock mass were perfectly elastic and completely free of defects, this conclusion would be reasonably correct, but it is not valid for real rock masses which are already fractured. Even if the stresses are the same, the stability of an excavation in a fractured and jointed rock mass will be controlled by the ratio of excavation size to the size of the blocks in the rock mass. Consequently, increasing the size of an excavation in a typical jointed rock mass may not cause an increase in stress but it will almost certainly give rise to a decrease in stability.

5.6.3 Influence of Parallel Excavation on Pillar Strength

The shapes of a pillar between two adjacent excavations depend upon the shape of the excavations and their distance apart. The shape of a pillar has a major influence upon the stress distribution within that pillar. Figure 5.1 shows the principle stress distribution in the rock surrounding two adjacent excavations aligned normal and parallel to the stress direction.

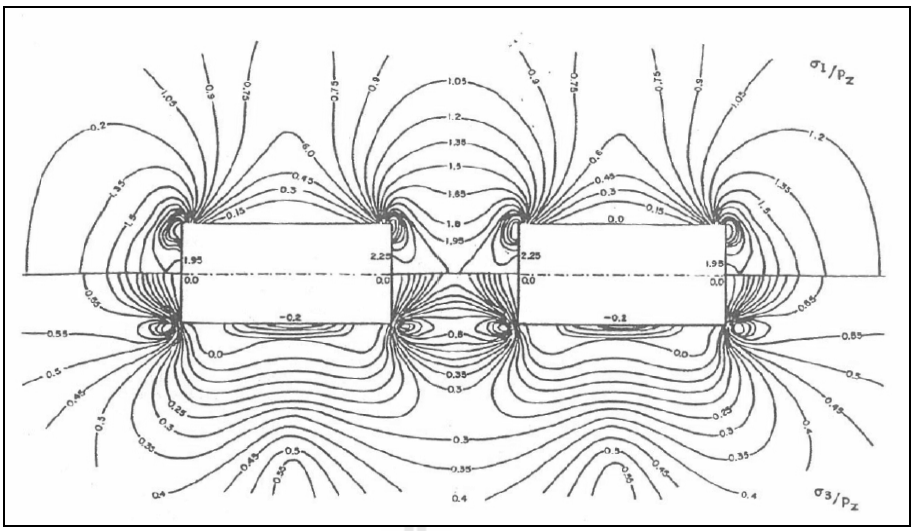

Figure 5.11 Principle stress distribution in the rock surrounding two adjacent excavations aligned normal and parallel to the stress direction

5.6.4 Influence of width to height ratio on pillar strength

It has long been recognized that the shape of a pillar has a significant influence upon its strength. Since most room and pillar mining is carried out in coal, most of this literature deals with the strength of coal pillars in horizontal seams.

The strength of coal pillar will start from result of uniaxial compressive strength (UCS) of intact rock which, testing by lab scale. The maximum of coal pillar rock mass strength (∂m) will calculate from UCS but relating with size ration of pillar. In this case study the ratio pillar high and width is 1:1. The maximum of pillar strength is:

$$\partial ps = (0.875 + 0.25\ W/H) \times (h/hc)^{1/2} \cdot \times \partial c \qquad (5.12)$$

The results of calculated of each pillar was showing in table 5.3. Principle stress distribution see figure 5.12

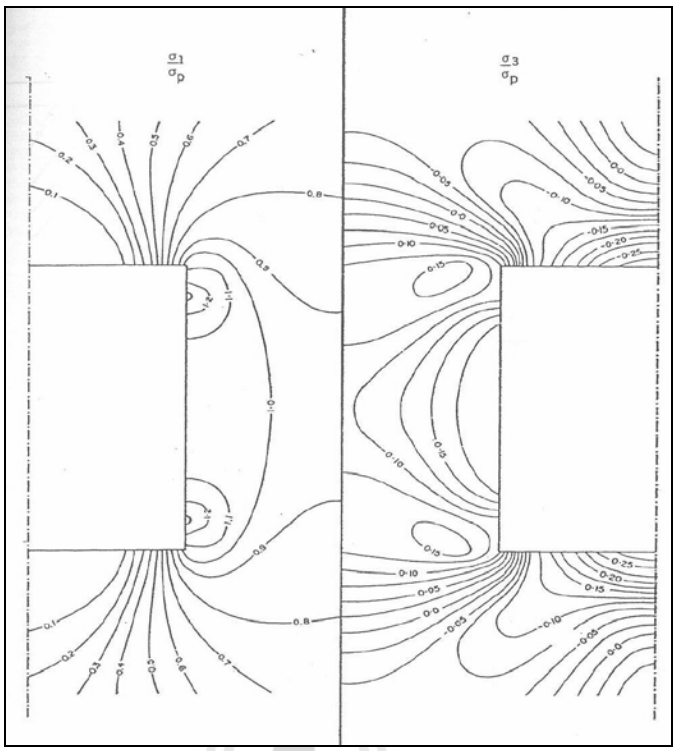

Figure 5.12 Principal stress distribution in room and pillar defined by ratio pillar high and width = 1. The contour values are given by the ratio of major and minor principal stress to average pillar stress

5.6.5 Influence of ore body inclination

In the preceding discussion on pillar strength, is distributions in the pillar are symmetrical about line through the Centre of the pillar. This situation illustrated in figure 5.13 and 5.14 shows that these assumptions longer valid in the case of an inclined ore body and pronounced when the excavations are close to influenced by stress gradients due to that pillar failure follows the same sequence pillar, namely that failure initiate.

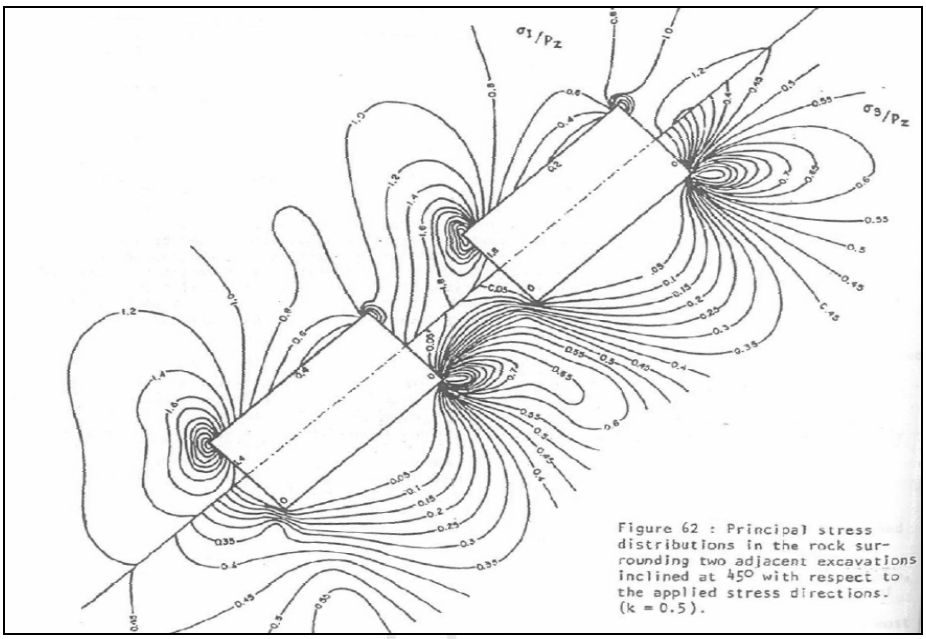

Figure 5.13 Principal stress distribution in the rock surrounding two adjacent excavations incline 45 degree with respect the apply stress direction

PCB case study, coal pillar was show that, vertical stress acting upon pillar is non-perpendicular with vertical surface area. Because of coal seam was incline by appearance dipping angled about 36 degrees. Horizontal stress acting to pillar is various depend on depth with magnitude equal with $\partial v Cos\Theta$. This stress driven pillar sliding fall drown to room same as wage. The factor of safety in this research will use Amonton's law (Jaeger and Cook, 1979) for the relation of vertical (Normal) strength and share force. Newton's given equation;

$$\text{Horizontal Force (Fh)} = \partial v \times \cos\Theta \qquad (5.13)$$

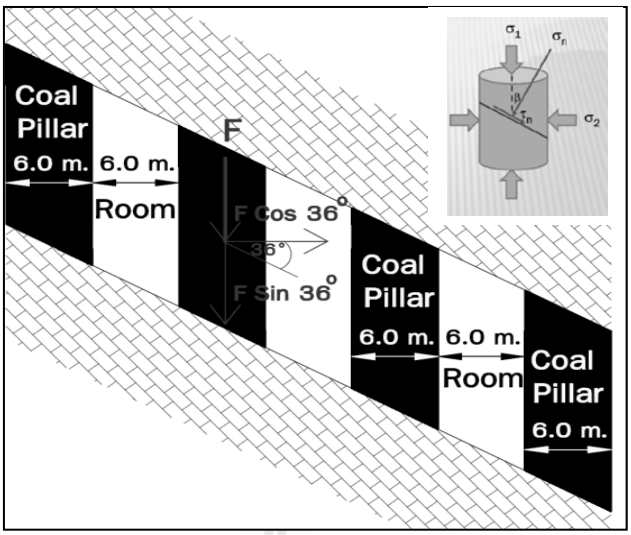

Figure 5.14 Inclination stress approach to pillar

Force calculate the shear strength was use Coulomb's law (Jaeger and Cook, 1979) for coal pillar shear strength, given pillar shear strength stress as this;

$$\tau = Cp + \partial x \tan\phi_p \quad (5.14)$$

$$\tau = Cp + (\partial v \sin\theta) \times \tan\phi_p \quad (5.15)$$

where Cp is cohesion, τ is maximum shear strength and Θp is angle of of maximum shear. The factor safety of coal pillar from shear stress will carry out by comparison between horizontal diving force and shear strength of pillar by each depth. The rock property will use result of lab rock mechanic testing as table 5.1. Results of calculated of average shear stress acting to pillar each pillar, case of parallel opening was showing in Table 5.5 .

5.6.6 Influence of injection between Discontinuity and Driving

The results of representative joint analysis at study area on Figure 5.15 show the major of discontinuity is orientated in 354/69 and 254/42 is bedding plan is 245 / 42 and 080/26 is rock fracture or fault plan. The axis of excavation (room) was design to run parallel strike direction. It was driven pass into three line of intersection of joint sets. Assume that, these joint area uniform space interval 1 m. These criteria of this geological structure and tunnel direction will influence to occur wedge on roof with half one square meter size.

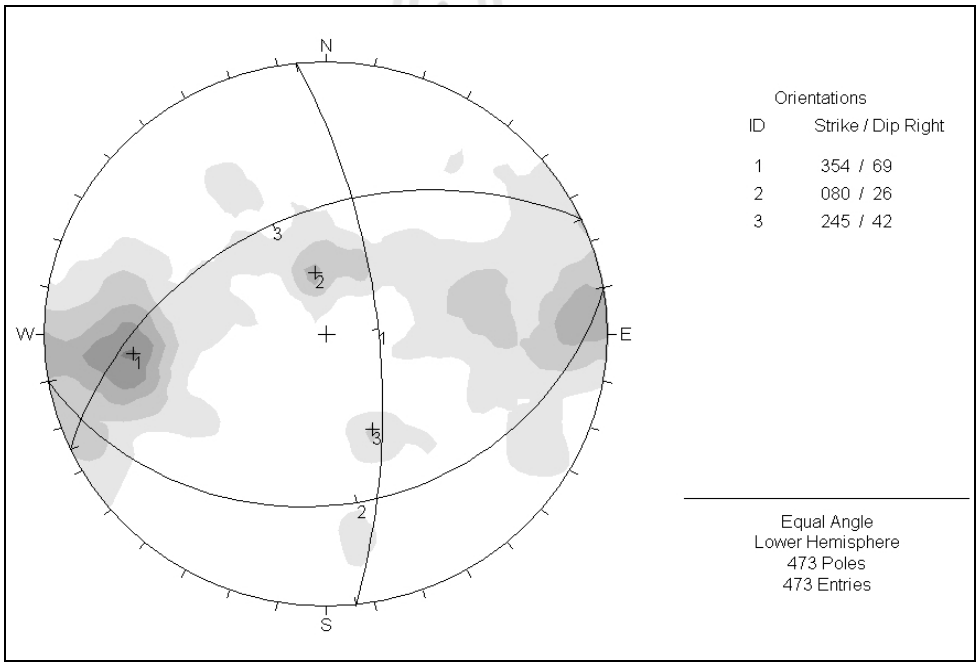

Figure 5.15 Representative fractures at PCB coal mine project. Attitude 245/42 is bedding plan of coal seam

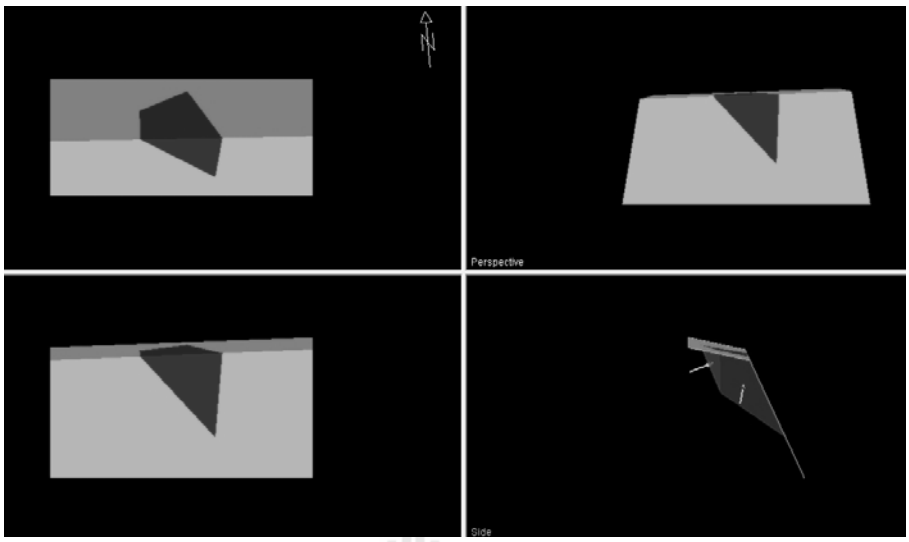

Figure 5.16 Computer simulations the discontinuity for 3D wage shape

5.7 Support design

Where a bolt is used to restrain a single block in the roof of an entry, the volume and hence the weight of the block and where necessary its direction of sliding can be determined by stereographic analysis of the kinetics of sliding. This method is outlined in Farmer and Shelton (1980) and in Farmer (1985). Methods of support based on the common requirement that bolt spacing should be half the bolt length are discussed in the same sources. In coal mining, the design of bolts is usually based on Panek's (1962a, b) analysis. The most simple assumption for design purposes is to consider a sagging roof plate or beam of thickness *L*, span *B*, and length *X*, supported by rows of bolts with separation *a* between rows and spacing *S*. Then the bolt tension force *P* to support the roof will be given by:

$$p = \left(\frac{\gamma BXL}{\left(\frac{\chi}{\alpha}+1\right)\left(\frac{B}{S}+1\right)} \right) \tag{5.16}$$

Cases of PCB project, rock quality of roof of room and Q system value indicate by (Grimstad and Barton, (1993), reproduced from Palmstrom and Broch, (2006)) accept to support. For empirical support design showing in figure 5.17

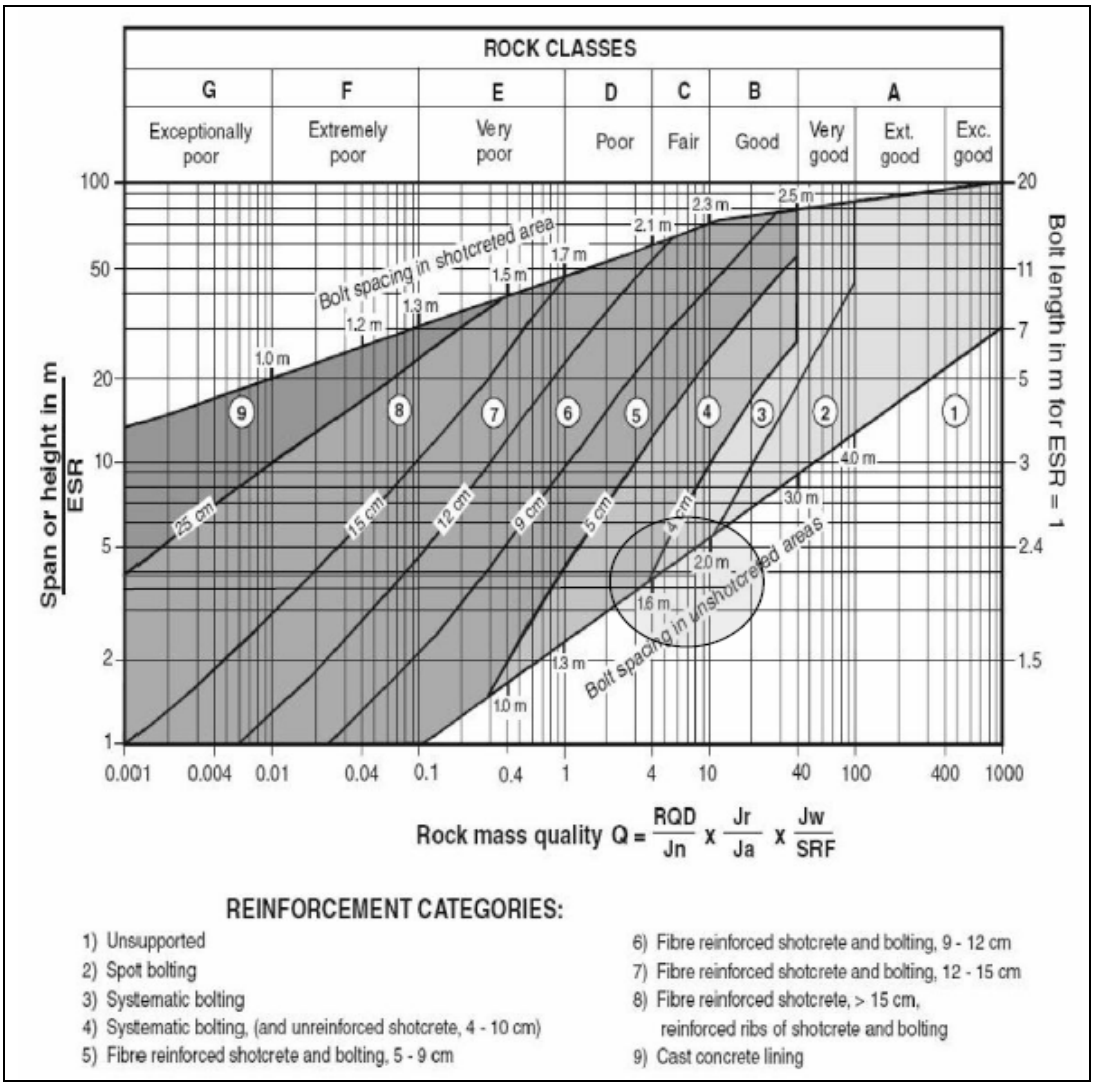

Figure 5.17 Estimated support categories based on the tunneling quality index *Q* *(After* Grimstad and Barton, 1993, reproduced from Palmstrom and Broch, 2006).

Table 5.2 Results of calculate the acting stress upon room and pillar and factor of safety analysis

Pillar level number	Depth of pillar Roof (H)	Area of Coal pillar and roomm		Poisson ratio	Pillar Stress				USC Coal Pillar Stress by Intact rock	Maximum USC Coal Pillar Stress	Factor Safety (∂ps/∂P)
					γ	Stress per unit Depth of OB (SOB)	Vertical stress before Tunnel (SOB x H)	Average Vertical acting stress on pillar (At/Apx∂v)			
		W_P	$W_P + W_r$			∂_v	∂v	∂P	∂c	∂ps	
	m	m	m		g/cc	Mpa/m	Mpa	Mpa	Mpa		
P1	1.59	6.00	12.00	0.25	2.64	0.027	0.043	0.172	22.80	7.99	46.517
P2	15.66	6.00	12.00	0.25	2.64	0.027	0.423	1.691	22.80	7.99	4.723
P3	25.09	6.00	12.00	0.25	2.64	0.027	0.677	2.710	22.80	7.99	2.948
P4	34.26	6.00	12.00	0.25	2.64	0.027	0.925	3.700	22.80	7.99	2.159
P5	42.72	6.00	12.00	0.25	2.64	0.027	1.153	4.614	22.80	7.99	1.731
P6	50.34	6.00	12.00	0.25	2.64	0.027	1.359	5.437	22.80	7.99	1.469
P7	58.53	6.00	12.00	0.25	2.64	0.027	1.580	6.321	22.80	7.99	1.264
P8	23.78	6.00	12.00	0.25	2.64	0.027	0.642	2.568	22.80	7.99	3.110
P9	23.85	6.00	12.00	0.25	2.64	0.027	0.644	2.576	22.80	7.99	3.101
P10	23.92	6.00	12.00	0.25	2.64	0.027	0.646	2.583	22.80	7.99	3.092
P11	32.83	6.00	12.00	0.25	2.64	0.027	0.886	3.546	22.80	7.99	2.253

Table 5.3 Results of calculate the acting upon two adjacent and parallel room and pillar and factor of safety analysis

Pillar level number	Depth of pillar Roof (H)	Area of Coal pillar and roomm				Poisson ratio	Pillar Stress					USC Coal Pillar Stress by Intact rock	Maximum USC Coal Pillar Stress	Factor Safety (∂ps/∂P)
							γ	Stress per unit Depth of OB (SOB)	Vertical stress before Tunnel (SOB x H)	Average vertical acting stress(2x∂v)	Maximum acting stress(1.65 x∂P)			
		W_P	$W_P + W_r$	Ap	At			∂_v	∂v	∂P	∂b	∂c	∂ps	
	m	m	m	mxm	mxm		g/cc	Mpa/m	Mpa		Mpa	Mpa		
P1	1.59	6.00	12.00	36.00	144.00	0.25	2.64	0.027	0.043	0.086	0.142	22.80	7.99	56.384
P2	15.66	6.00	12.00	36.00	144.00	0.25	2.64	0.027	0.423	0.846	1.395	22.80	7.99	5.725
P3	25.09	6.00	12.00	36.00	144.00	0.25	2.64	0.027	0.677	1.355	2.236	22.80	7.99	3.573
P4	34.26	6.00	12.00	36.00	144.00	0.25	2.64	0.027	0.925	1.850	3.053	22.80	7.99	2.617
P5	42.72	6.00	12.00	36.00	144.00	0.25	2.64	0.027	1.153	2.307	3.806	22.80	7.99	2.099
P6	50.34	6.00	12.00	36.00	144.00	0.25	2.64	0.027	1.359	2.718	4.485	22.80	7.99	1.781
P7	58.53	6.00	12.00	36.00	144.00	0.25	2.64	0.027	1.580	3.161	5.215	22.80	7.99	1.532
P8	23.78	6.00	12.00	36.00	144.00	0.25	2.64	0.027	0.642	1.284	2.119	22.80	7.99	3.770
P9	23.85	6.00	12.00	36.00	144.00	0.25	2.64	0.027	0.644	1.288	2.125	22.80	7.99	3.759
P10	23.92	6.00	12.00	36.00	144.00	0.25	2.64	0.027	0.646	1.292	2.131	22.80	7.99	3.748
P11	32.83	6.00	12.00	36.00	144.00	0.25	2.64	0.027	0.886	1.773	2.925	22.80	7.99	2.731

Table 5.4 Results of calculate the share stress acting upon coal pillar and factor of safety analysis

Pillar level number	Depth of pillar Roof (H)	Area of Coal pillar and roomm				Poisson ratio	Cp	Φp	Pillar shear Stress				Maximum Shear strength of coal pillar (Cp + (∂v sinΘ) x tanΦp)	Factor Safety (Pτm /τp)
									γ	Stress per unit Depth of OB (SOB)	Vertical stress before Tunnel (SOB x H)	average shear stress acting pillar (∂v cos 36)		
		W_P	$W_P + W_r$	Ap	At		Mpa	Deg		∂_v	∂v	τp	Pτm	
	m	m	m	mxm	mxm				g/cc	Mpa/m	Mpa	Mpa	Mpa	
P1	1.59	6.00	12.00	36.00	144.00	0.25	5.75	37.09	2.64	0.027	0.043	0.034	5.77	167.972
P2	15.66	6.00	12.00	36.00	144.00	0.25	5.75	37.09	2.64	0.027	0.423	0.338	5.94	17.547
P3	25.09	6.00	12.00	36.00	144.00	0.25	5.75	37.09	2.64	0.027	0.677	0.542	6.05	11.158
P4	34.26	6.00	12.00	36.00	144.00	0.25	5.75	37.09	2.64	0.027	0.925	0.740	6.16	8.318
P5	42.72	6.00	12.00	36.00	144.00	0.25	5.75	37.09	2.64	0.027	1.153	0.923	6.26	6.779
P6	50.34	6.00	12.00	36.00	144.00	0.25	5.75	37.09	2.64	0.027	1.359	1.087	6.35	5.836
P7	58.53	6.00	12.00	36.00	144.00	0.25	5.75	37.09	2.64	0.027	1.580	1.264	6.44	5.096
P8	23.78	6.00	12.00	36.00	144.00	0.25	5.75	37.09	2.64	0.027	0.642	0.514	6.03	11.743
P9	23.85	6.00	12.00	36.00	144.00	0.25	5.75	37.09	2.64	0.027	0.644	0.515	6.03	11.710
P10	23.92	6.00	12.00	36.00	144.00	0.25	5.75	37.09	2.64	0.027	0.646	0.517	6.03	11.677
P11	32.83	6.00	12.00	36.00	144.00	0.25	5.75	37.09	2.64	0.027	0.886	0.709	6.14	8.657

5.8 Computer Simulation for Safety Analysis.

The Universal Distinct Element Code (UDEC) is a two-dimensional numerical program based on the distinct element method for discontinue modeling. UDEC simulates the response of discontinuous media subjected to either static or dynamic loading. The discontinuous medium is represented as an assemblage of discrete blocks. The discontinuities are treated as boundary conditions between blocks; large displacements along discontinuities and rotations of blocks are allowed. Individual blocks behave as either rigid or deformable material.

Deformable blocks are subdivided into a mesh of finite-difference elements, and each element responds according to a prescribed linear or non-linear stress-strain law. The relative motion of the discontinuities is also governed by linear or non-linear force-displacement relations for movement in both the normal and shear directions. UDEC has several built-in material behavior models, for both the intact blocks and the discontinuities, which permit the simulation of response representative of discontinuous geologic. UDEC is well-suited to model the large movements and deformations of a blocky system.

Computer simulation was use for rock displacement analysis after mine. The result will utilize to roof support design. Result of simulate at PCB coal mine project have maximum displacement about 18.44m. It need to installation the supported rock bolt length 2.5 m and spacing 1 m. This support suggests that reduce a maximum displacement from 18.44 to 4.62m and roof of tunnel steady safety. For diagram for simulation was showing in Figures 5.18 and 5.19

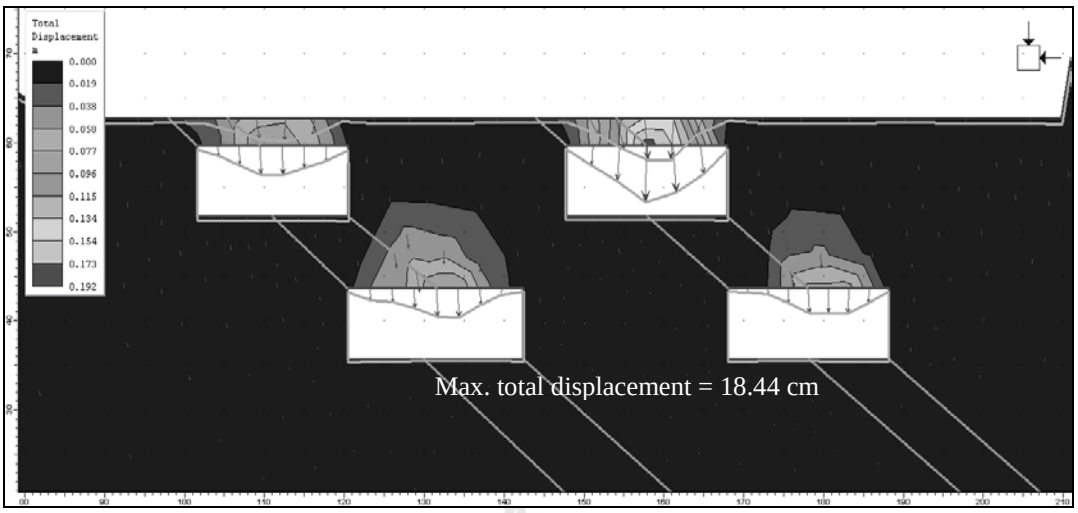

Figure 5.18 Result of simulate for displacement. It is significant, upper level has the displacement more than lower opening in coal seam, cause of shallow depth room has more tension The opening has main effect from vertical loading.

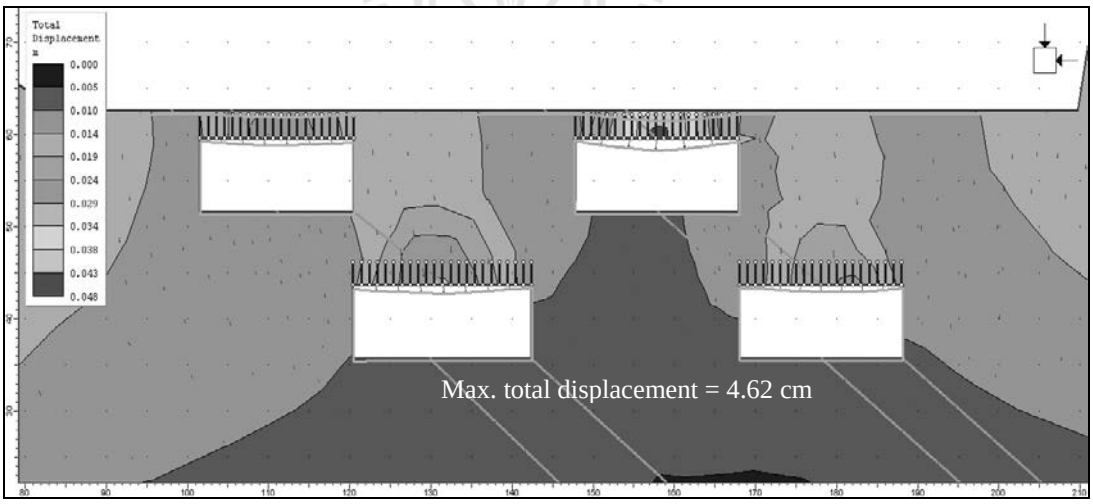

Figure 5.19 Maximum total displacement and displacement vectors and deforming boundary for unsupported for pillar. This numerical method provides rock bolt support has a length 2.5 m and spacing 1 m. It reduce a maximum displacement from 18.44 to 4.62m

5.9 Summary of factor of safety

The safety factor analysis was calculate the stress approach to pillar follow both of Obert and Duval (1967) and Hoek and Brown (1980) was global say that achieve to safety all level of room and pillar when compare with empirical standard at Salamon and Munro in South Africa. The final result of safety factor for PCB room and pillar coal mine project was summary and given in Table 7.1 and cure in Figure 5.19 of this report.

Table 5.5 Summary final results the safety factor analysis

Pillar level number	Depth of pillar Roof (H)	Area of Coal pillar and roomm				Maximum USC Coal Pillar Stress	Pillar Factor Safety (∂ps/∂P) (Obert and Duvall (1967))	Paralellel Tunnel Factor Safety (∂ps/∂P) (Hoek and Brown (1980))	Factor Safety (Pτm /τp) (Jaeger and Cook, 1979)
		W_P	$W_P + W_r$	Ap	At	∂ps			
	m	m	m	mxm	mxm				
P1	1.59	6.00	12.00	36.00	144.00	4.79	46.52	56.38	167.97
P2	15.66	6.00	12.00	36.00	144.00	4.79	4.72	5.72	17.55
P3	25.09	6.00	12.00	36.00	144.00	4.79	2.95	3.57	11.16
P4	34.26	6.00	12.00	36.00	144.00	4.79	2.16	2.62	8.32
P5	42.72	6.00	12.00	36.00	144.00	4.79	1.73	2.10	6.78
P6	50.34	6.00	12.00	36.00	144.00	4.79	1.47	1.78	5.84
P7	58.53	6.00	12.00	36.00	144.00	4.79	1.26	1.53	5.10
P8	23.78	6.00	12.00	36.00	144.00	4.79	3.11	3.77	11.74
P9	23.85	6.00	12.00	36.00	144.00	4.79	3.10	3.76	11.71
P10	23.92	6.00	12.00	36.00	144.00	4.79	3.09	3.75	11.68
P11	32.83	6.00	12.00	36.00	144.00	4.79	2.25	2.73	8.66

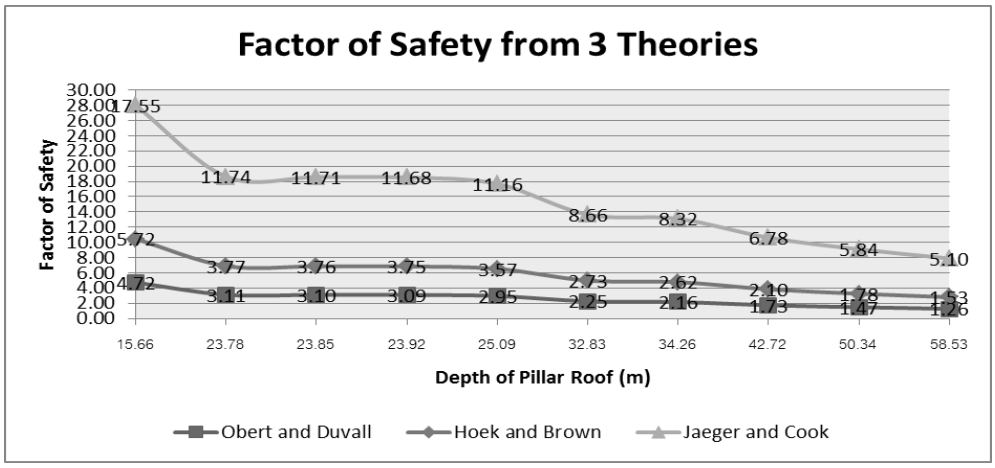

Figure 5.20 Relation between depth of pillar and factor of safety

CHAPTER VI

COMPARISION

6.1 Introduction

This chapter performs a comparison of the results obtained from empirical methods design in this research with the design results from other mine sites that have similar geological and topographic environments to optimize the final design. The research achievement would provide technique support for safety mining under similar condition in PCB coal mine project mining district.

The other underground exaction that has similar geology character and design condition is mine of Wongawilli Mining Area in Shallow Close Distance Coal Seams. It was illustrate by ZHU Wei-bing XU Jia-lin KONG Xiang XUAN Da-yang QIN Wei, School of Mines, China University of Mining and Technology, Xuzhou Jiangsu 221116, China State Key Laboratory of Coal Resources and Mine Safety, China University of Mining and Technology, Xuzhou Jiangsu 221116, China. This paper was presentation on the 6th International Conference on Mining Science & Technology

6.2 Empirical design of Wongawilli Mining

Wongawilli mining area pillars in shallow close distance coal seams in Bulianta coalmine, the influence of Wongawilli coal pillars' stability in upper coal seam on lower working face is studied by three-dimensional simulation and fiel

measurement. The results of finite element software FLAC3D was shows that, the maximal vertical stress in Wongawilli coal pillars is 32 MPa, and the stress concentration factor is 4.8 but the pillars in Wongawilli mining area are stable. The results of on-site surface subsidence and rock pressure appearance shows that, the surface subsidence value corresponding to Wongawilli coal pillars is much less than old gob area, and the rock pressure appearance of mining face is always normal, so the result indicates that Wongawilli coal pillars are not unstable and the safety of extraction of 32301 working face is ensured. The research achievement would provide technique support for safety mining under similar condition in Shendong mining district.

Shendong mining district has always being paid attention to scientific mining and exploring actively by new mining technology and methods suitable for the distribution condition of coal seams in Shendong. Wongawilli mining method was introduced from Australia in the 1990 to solve the problem of mining bound and unstable coal seams by conventional mining methods and it improved the mining rate of difficult coal seams greatly. Based on the “room and pillar method”, Wongawilli mining method is a new-style effective method combined with short wall and pillar. It has these features: continuous mining the coal seam with coal cutter; continuous transportation of the coal; roof management with entire caving; and the goaf supported by remaining pillars. The pillars in the Wongawilli mining area are mainly 0.5~0.9 m width for separating excavating roadways, and pillars with the width of 15~25m used to separate different areas are kept after several roadways are excavated with the purpose of supporting the coal roof effectively.

6.2.1 Basic condition of the working face

Bulianta coalmine, which has a yearly capacity of 20.0 Mt, is one of the main mines in Shendong Corporation of Shenhua Group working face 32301 is the first face of the third panel in 2-2 coal seam with a length of 301 m and an advancing distance of 5,220 m. Its coal structure is simple, the angle of coal seam is 1~3°, and the thickness of Aeolian sand in the unconsolidated layer is 5~20 m. The thickness of coal seam is 6.7~7.5 m with an average thickness of 7.1 m, and the average mining depth is 260 m. Fully-mechanized mining method is used with a whole cutting height at a time. The designed mining height is 6.1 m while the cutting supports are 6.3 m. Roof control method is entirely caving.

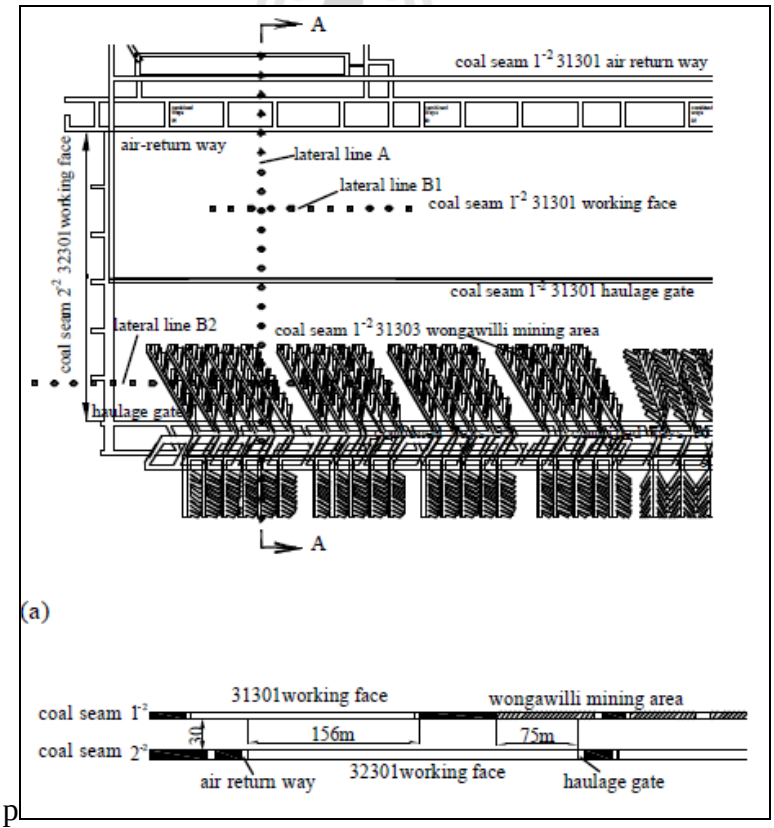

p

Figure 6.1 Position relationship of 32301 working face (a) plan (b) section view of A-A

The working face has a set of equipment as follows: ZT10800/28/55D style supports produced by Zhengzhou coal mining machinery Group Co.Ltd with a rated working resistance of 10800kN, SL1000 Shearer produced by Eickhoff Corporation, and scraper conveyor by DBT Corporation. Because longwall mining method and Wongawilli mining method are applied to upper 1-2 coal seam, 32301 working face is now located under three different areas, and along the head–to- tail direction of the conveyor, they are virgin coal area using Wongawilli mining method, solid virgin coal area and old goaf area. The 156 m range of 32301 working face away from the air return way is under the old goaf caused by 31301 longwall face in upper seam, while the 75 m range of 32301 working face away from the haulage drift is under Wongawilli mining area. The position relationship is shown in Figure 6.1 and the combined column is section map of the third panel is shown in Figure 6.2.

level number	thickness	buried depth	lithology	columnar
1	14.41	14.41	aeolian sand	
2	4.48	18.89	siltstone	
3	7.92	26.81	sandy mudstone	
4	3.53	30.34	fine-sandstone	
5	8.56	38.9	sandy mudstone	
6	3.5	42.4	siltstone	
7	16.97	59.37	sandy mudstone	
8	2.5	61.87	siltstone	
9	23.63	85.5	sandy mudstone	
10	13.06	98.56	fine-sandstone	
11	31.86	130.42	siltstone	
12	9.85	140.27	sandy mudstone	
13	16.72	156.99	siltstone	
14	7.5	164.49	fine-sandstone	
15	13.53	178.02	medium-Sandstone	
16	3.98	182	fine-sandstone	
17	0.7	182.7	mudstone	
18	0.84	183.54	non-number 1	
19	2.9	186.44	sandy mudstone	
20	4.14	190.58	fine-sandstone	
21	4.59	195.17	1^{-2}coal	
22	3.95	199.12	fine-sandstone	
23	11.64	210.76	medium-sandstone	
24	0.7	211.64	non-number 2	
25	3.95	215.41	siltstone	
26	5.66	221.07	medium-sandstone	
27	16.22	237.29	fine-sandstone	
28	1.4	238.69	sandy mudstone	
29	6.18	244.87	2^{-2}coal	

Figure 6.2. Combined columnar section

6.2.2 Calculation Model and Simulation Program

Calculation model FLAC3D has been widely used in the simulation of geological materials and geotechnical engineering with nonlinearity, large deformation and instability, especially the plastic flow of the materials reaching the yield limit and the gradual destruction together with caving of tracking materials. FLAC3D modeling is based on the principle of the use of Mohr-Coulomb yield criterion to determine the damage of rock mass and reflect the strain-softening model, after the destruction of coal deformation with the development gradually reducing the residual strength of character. Based on the geological conditions and mining technology of the mining face, the level model is established (see Figure 6.3). The model's strike length is 1008 m, and inclined length is 615 m, and height is 137 m with a total of 361 148 units block and 406 375 grid nodes. The bottom and the side border in the model use displacement constraints, and the vertical loads are imposed on the top of model to simulate the weight of overlying strata. The development of numerical simulation of the mechanical parameters of materials is shown in Table 6.1.

Table 6.1 Development of numerical simulation of the mechanical parameters of materials

Lithology	Density	Bulk Modulus	Shear Modulus	Cohesion	Friction Angle	Tensile Strength
Sandy Mudstone	2300	8.33e9	3.85e9	3e7	34	6e6
Mudstone	2200	1.43e9	1.30e9	2e6	25	5e6
Siltstone	2350	1.11e9	8.33e9	8e6	35	8e6
Medium Sandstone	2500	2.28e9	1.84e9	1.5e7	38	9e6
Fine Sandstone	2500	2.78e9	2.08e9	2e7	40	1e7
Coal	1400	1.67e9	3.57e8	1e6	20	3e6

According to actual mining situation to 2-2 coal seam at field, we put forward a calculation scheme as below: firstly, mine longwall face and Wongawilli mining area in 1-2 coal seams, then excavate the two crossheadings at working face 32301 in 2-2 coal seam. At last, we calculate exploitation process of working face 32301. When mining the working face 32301, we are excavating pace of 4 m in the model. Every pace is calculated with 800 time stepping.

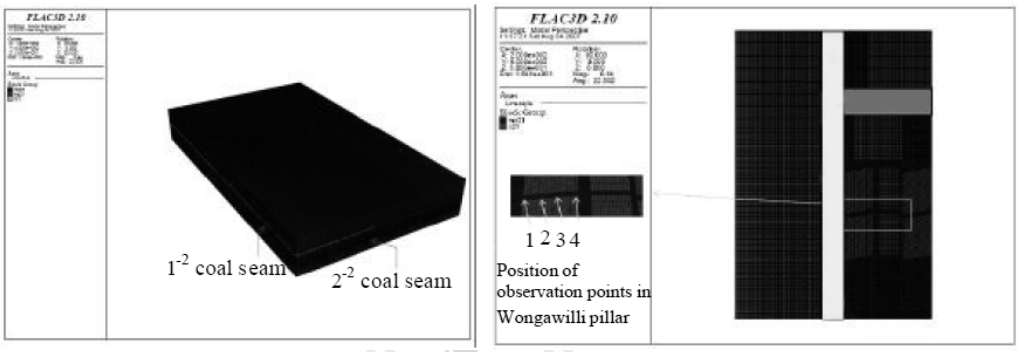

Figure 6.3 Three-dimensional numerical simulation model diagram (a) model diagram (b) Pillar survey line measuring point position.

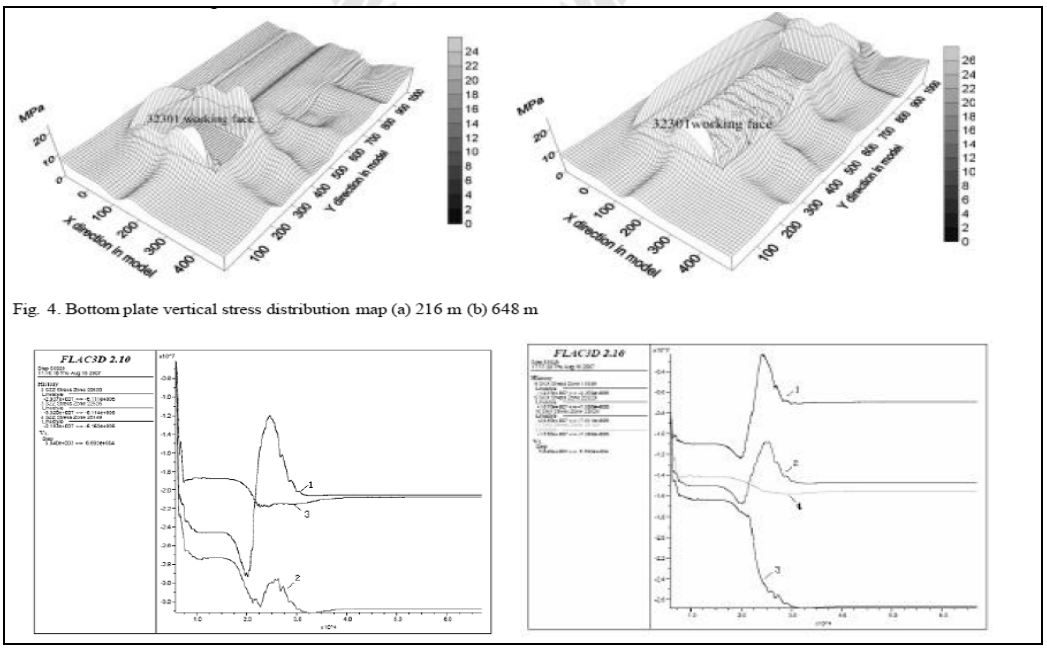

Figure 6.4 Stress change curve drawing of monitoring point on Wongawilli pillar (a) vertical stress (b) horizontal stress with X direction

6.2.3 Simulation results and analysis

In the simulating mining process, extract vertical stress contour map at 2-2 coal seam floor after every excavation (see Figure 6.4). The conclusion is: when the working face advances, there will appear stress increasing zone on both sides of 32301 working face, especially above the Wongawilli mining area pillar, trend and strike direction pillar where would form large stress concentration.

Figure 6.5 is the stress change curve of monitoring point in Wongawilli pillars. From it we can see that: when the working face excavates the coal pillars in Wongawilli mining area, the load of Wongawilli mining area experiences from small to large and then decreases. The bearing stress have larger change in a short time , the maximal vertical stress in Wongawilli coal pillars is 32 MPa, and the stress concentration factor is 4.8. The pillars in Wongawilli mining area are stable before excavating; even there is elastic rock body in the coal pillars of Wongawilli mining area. It shows that the roof destruction is not severe. During the mining of 32301 working face, the coal pillars in Wongawilli mining area are subjected to the tension and damaged, but the pillars are not unstable suddenly and prevent roof accident.

6.2.4 Result analysis of surface subsidence

When mining 32301 working face, we uses GTS -7001i total station to observe elevation and plane coordinate from August 4, 2007 to October 10, 2007, lasting for 68 days. During this time, the working face advanced from 126m to 752m, and was observed totally 25 times. The working face excavated about 10 m every day from August 4, 2007 to August 24, 2007. We observed comprehensively every day to master the upper coal pillars' stability in Wongawilli mining area at initial mining stage. Fig6.6 is the tendency observation line of dynamic subsidence curve.

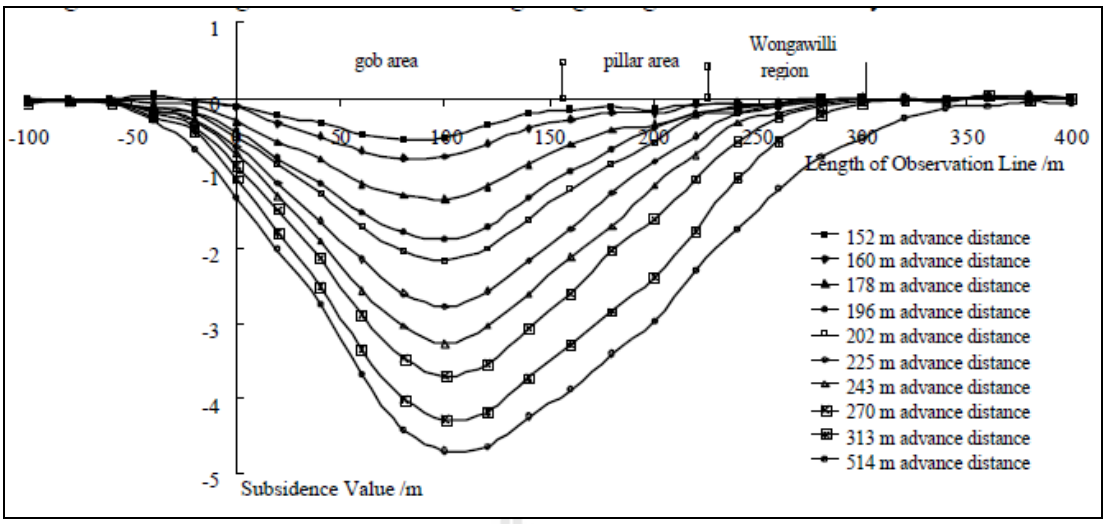

Figure 6.5 Tendency observation line of dynamic subsidence curve

From Figure 6 we could know that on August 16, 2007 when the working face advanced 202 m, namely advanced 52 m from the tendency observation line, the surface subsidence corresponding to return way of working face 32301 was 0.514 m, and the maximum surface subsidence corresponding to 1-2 coal long wall old goaf was 2.169 m. While, the surface subsidence corresponding to haulage gate of working face 32301 was 0.011 m, and the maximum surface subsidence corresponding to the Wongawilli mining area was 0.249 m. If lower coal was mined, it could lead to the instability of 1-2 upper coal pillars in Wongawilli mining area. Working face 32301 was being mined as total under 1-2 coal long wall old goaf, and its fitting subsidence curve was corresponding to the Figure 6.7. At this time, the surface subsidence corresponding to haulage gate of working face 32301 increased 0.503 m, and the surface Subsidence corresponding to the place 75 m away from haulage gate of working face 32301 increased 1.797 m. On September 20, 2007, when the working face advanced 514 m, namely advanced the tendency observation line 364 m, the regional overlying strata movement and surface subsidence corresponding

to its tendency observation line had become steady. Working face 32301 return way's surface subsidence was 1.324 m, the maximum surface subsidence corresponding to 1-2 coal long wall old goaf was 2.038 m. While, the surface subsidence corresponding to haulage gate of working face 32301was 0.546 m, and the maximum surface subsidence corresponding to the total Wongawilli mining area was 2.038 m. If mining the lower coal could lead to the instability of 1-2 upper coal pillars in Wongawilli mining area. From the fitting subsidence curve in Figure 6.7, we could see that the surface subsidence corresponding to haulage gate of 32301 working face should be increased 0.778 m, and the surface subsidence corresponding to the place 75 m away from haulage gate of working face 32301 should be increased 2.097 m.

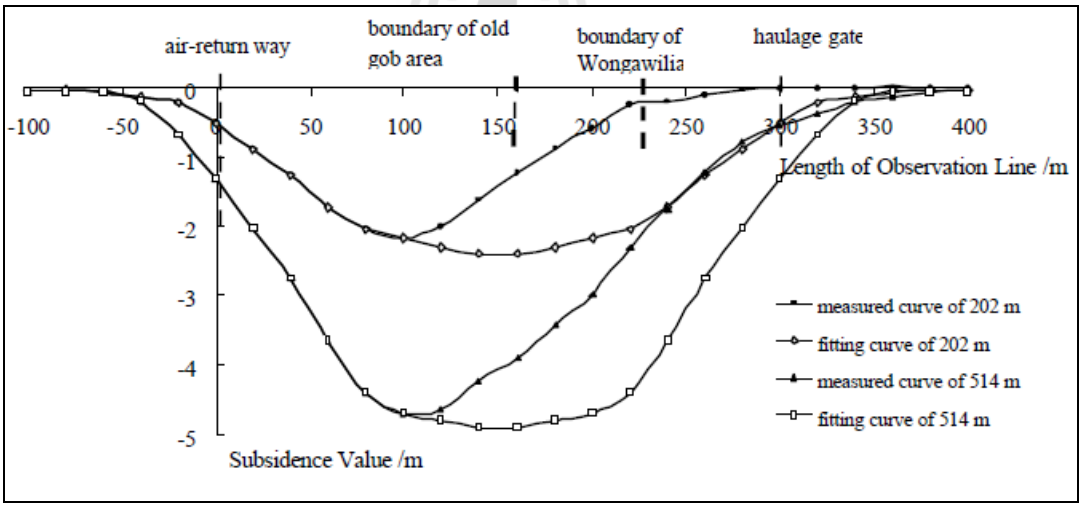

Figure 6.6 Tendency observation line fitting subsidence curve

According to the analysis mentioned above, considering the surface subsidence characteristics in shallow close distance coal seams during first mining on Shendong mining district, we could obtain that the Wongawilli coal pillars in 1-2 coal seam are not unstable; if Wongawilli coal pillars have instability, the tendency

observation line fitting subsidence curve should be similar to the fitting subsidence curve in Figure 6.7. In fact, pillars in Wongawilli Mining area corresponding to the surface subsidence are much smaller than the fitting subsidence curving. It indicated that Wongawilli mining area and its upside rock mass global motion is stable. Mining area corresponding to the surface did not have clearly sidestepped and cracked .It shows that pillar in 32301 working face in mined mining area is stable. This is also proved by field strata behaviors. During the 32301 working face was advancing, it did not have roof fall, impulsion pressure, hurricane and others for upside coal legacy pillar instability.

6.3 Comparison

Wongawili and PCB are similar in geology character. They are coal deposit and mine by underground room and pillar method. Wongawilli is under existing as current. PCB is under mining design. Coal thickness is averaged 7.10 and 8.10. Wongawilli has the angle gentle more than PCB is 2 and 36 degree. The over burden of Wongawilli is soft rock of argillaceous sedimentary rock but PCB is competent limestone. The result of room and pillar design, Wongawilli and PCB is same long and width but difference in high of room production. Wongawilli have the high of room 6.10m but 11.10 in PCB. This ratio is difference from dipping angle of coal seam. For detail given in Table 7.1

Result of comparison between PCB empirical design and Wongawilli underground coal mine in china have two difference parts. One is the maximum of coal pillar strength is more difference. Wongawilli is 32 MPa but PCB is 7.99 MPa in coal rock mass a while 22.80 MPa at intact rock. (see Table 6.2) The second is depth

of underground from ground surface. Wongawilli is 260m and 60m at PCB. It mean that, Wongawilli have vertical stress approach to pillar more than PCB a while rock mass quality at overburden is very low strength (Unconsolidated rock and siltstone, sand stone.)

Table 6.2 Maximum coal pillar strength and stress concentrate at PCB coal mine project

Pillar level number	Depth of pillar Roof (H)	Area of Coal pillar and roomm		Poisson ratio	Pillar Stress			USC Coal Pillar Stress by Intact rock	Maximum USC Coal Pillar Stress
					γ	Vertical stress before Tunnel (SOB x H)	Average Vertical acting stress on pillar (At/Apx∂v)		
		W_P	$W_P + W_r$			∂v	∂P	∂c	∂ps
	m	m	m		g/cc	Mpa	Mpa	Mpa	
P1	1.59	6.00	12.00	0.25	2.64	0.043	0.172	22.80	7.99
P2	15.66	6.00	12.00	0.25	2.64	0.423	1.691	22.80	7.99
P3	25.09	6.00	12.00	0.25	2.64	0.677	2.710	22.80	7.99
P4	34.26	6.00	12.00	0.25	2.64	0.925	3.700	22.80	7.99
P5	42.72	6.00	12.00	0.25	2.64	1.153	4.614	22.80	7.99
P6	50.34	6.00	12.00	0.25	2.64	1.359	5.437	22.80	7.99
P7	58.53	6.00	12.00	0.25	2.64	1.580	6.321	22.80	7.99
P8	23.78	6.00	12.00	0.25	2.64	0.642	2.568	22.80	7.99
P9	23.85	6.00	12.00	0.25	2.64	0.644	2.576	22.80	7.99
P10	23.92	6.00	12.00	0.25	2.64	0.646	2.583	22.80	7.99
P11	32.83	6.00	12.00	0.25	2.64	0.886	3.546	22.80	7.99
Maximum	58.53						6.321	22.80	7.99

Table 6.3 Result of comparison between Wongawili and PCB coal mine by room and pillar method

Description	Unit	Wongawilli China	PCB Coal Mine Project
Rock type Over burden		silt /sand	Limestone
Rock mass		Unconsolidated	Hard Bedding
Angle of coal seam	Degree	2	36
Average Thickness	m	7.1	8.1
Maximum Depth	m	260	60
Pillar rock type		Coal	Coal
Density		1.4	
RMR Ranking			61
Q System Ranking			0.8
USC strength	Mpa		22.8
Young Modulus	GPa	1.6	15.03
Share Modulus	GPa	0.35	
Tensile Strength	MPa	3	
Poission Ration			0.29
Unit Weight	MN/m		0.03
Cohesion	MPa	1	5.75
Fiction Angle	Degree	40	39.98
Pillar Width		6	6
Mining High	m	6.1	11.1
Maximum Vertical Stress	Mpa	**32**	**7.99**
Stress concentrate factor		**4.8**	**6.32**
Factor Of safety			>1.2
Cutting support	m	6.3	
Coal Capacity	Mton/year	20	0.3
Result		Damage subsidence	Indicate Subsidence

CHAPTER VII

CONCLUSIONS AND DISCUSSIONS

7.1 Conclusions

Phetchaboon coal mine project (PCB) is located 300 km north of Bangkok. It was located at Lamtanen village, Nongphai district Phetchaboon provinces. Coal was deposited two main seams in competent limestone Permian age with depths ranging from 5 to 90 m, 10-30 m appearance thickness

Room and pillar mine was researched by conceptual use room in competent bed of limestone and pillar support is in coal seam. Q value of limestone is 4.81 and ESR 1.6 was related with maximum unsupported span 6.00 m and coal pill is design equal size with room. Each room has difference elevation belong with dip angle of coal seam which has 36 degree. The first room starts at 2m and the end is 60 m from ground surface. Height of room has height is belonging coal is 11 m. This design has coal recovery 75 % by calculation

The safety factor analysis was calculate the stress approach to pillar with Influence of Parallel Excavation on Pillar Strength, width to height ratio on pillar strength, Ore Body Inclination and wage occur from discontinuity. The result of factor of safety analysis follow both of Obert and Duval (1967) and Hoek and Brown (1980) was global say that achieve to safety all level of room and pillar when compare with empirical standard at Salamon and Munro in South Africa.

The room at depth more than 50 m has safety factor less than 1.6. They are request to more modify the size of pillar to increase the strength of coal rock mass. Wage stability indicated occur fall drown in room safety factor (SF) value should be do identify and design the support. The computer simulation for subsidence was indicated that, have potential to inducement to surface displacement after mine. More research in shallow rock subsidence for preventive is good recommenced by next step

7.2 Discussions

7.2.1 Standard of Safety Factor Room and Pillar Coal Mine

As recent (2014) Thailand is not having yet for room and pillar safety factor. Factor of safety for slope stability by normal must more than 1 but in mining and civil work was definition between 1.2 -1.5. In this thesis the factor of safety will use 1.6, as an alternative to the stress analysis approach to pillar design, several authors have adopted. The one typical approach will be considered. Salamon and Munro carried out a study on 98 stable and 27 collapsed pillar areas in South Africa. The data included in their study are listed in below.

	Stable	Collapsed
Depths below surface, z feet	65-720	70-630
Pillar heights, h feet	4-16	5-18
Pillar heights, Wp feet	9-70	11-52
Width/height ratios, Wp/h	1.2-8.8	0.9-3.6
Extraction ratios, e=1 – (Wp/(Wo+Wp))	0.37-0.89	0.45-0.91

Salamon and Munro assumed that the pillar strength could be represented by an equation of the form:

$$\partial ps = Kh^{a} x \ Wp^{b} \tag{7.10}$$

where K is the strength of a unit cube of coal for a 1 ft cube of coal (k in lb/in for n a 1 ft cube or a 1 meter cube) and a and b area Constance. For square pillars, the average pillar stress ∂p is given by

$$\sigma_p = \gamma z\left(1 + w_o/w_p\right) \quad ^2=\gamma z/(1-e) \tag{7.11}$$

The factor of safety of pillar is given by

$$\text{F.S.} = \frac{\sigma_{ps}}{\sigma_p} = \frac{kh^a wp^b (1-e)}{\gamma z} \tag{7.12}$$

In order to determine the values of K, a and b, Salamon and Munro carried out a statistical study on the 27 collapsed pillar cases and adjusted the values of K, a and b until a mead factor of safety of 1.0 was obtained for these case. A histogram of factor of safety obtained by Salamon and Munro is reproduced in figure 5.2. The values used in calculating this histogram were k=1320 lb/ in^2 or k= 7176 kPa and a= -0.66, b=0.46.

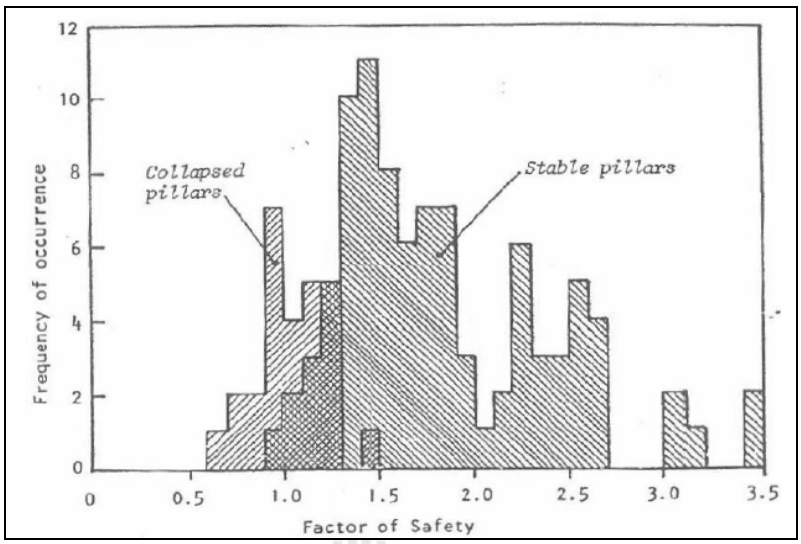

Figure 7.1 Histogram of factors of safety for coal pillar in South Africa Analyzed by Salamon and Munro

Also included in Figure 5.2 is a histogram of the factors safety for the 98 stable pillar cases studied by Salam on and Munro. Because of the wide range of factors of safety include in this study(no generally accepted pillar design rules had been used in South Africa up to that time), Salamon and Munro decided to consider only that 50% of the stable pillar population which fell in the densest cluster between factors of safety of 1.31 and 1.88 The mean factor of safety for these 49 cases was 1.57 and Salam on and Munro suggested that a factor of safety of 1.6 is an appropriate design value for pillars similar to those studied.

In rock slope engineering, factors of safety range from about 1.2 for temporary mine slope to about 1.5 for slopes in which failure could have serious economic and safety consequence. In view of the potential for a domino effect failure in pillar, the authors consider that the factor of safety should be the same range as that

for critical slope. Hence, the factor of safety of 1.60 suggested by Salamon and Munro is considered to be a reasonable value for permanent pillar design

7.3 PCB room and pillar factor of safety

7.3.1 Factor of safety event

Result of factor of safety for room and pillar for primary design at PCB coal mine project by use method follow both of Obert and Duval (1967) and Hoek and Brown (1980) was global say achieve to safety all level room.(Table 7.1) The room at depth more than 50 m has safety factor less than 1.6. They are request to more modified the size of pillar to increase the strength of coal rock mass.

7.3.2 Wedge unsafe condition in room

The study of the stability of the wedges was carried out focusing only the shape of the joints. The influence of the persistence on the safety factor (SF) value should be do identify and design the support. Cohesion and fiction angle and share strength index by each facture in limestone roof and coal pillar is importance to do as well.

7.3.3 Shallow subsidence indicated

The computer simulation for subsidence was indicated that, have some displacement by vertical direction in room of coal production. These displacements will induct to surface displacement after mine. Figure 7.1 showing linear relations between depth of pillar and factor of safety. It pronounces that, safety factor was deceases if more depth distance of pillar. It means that, room and pillar in shallow distance, the safety is depending on vertical stresses which come from overburden weight. This criterion indicated that, if pillar damage the surface subsidence will be pronounced occurs.

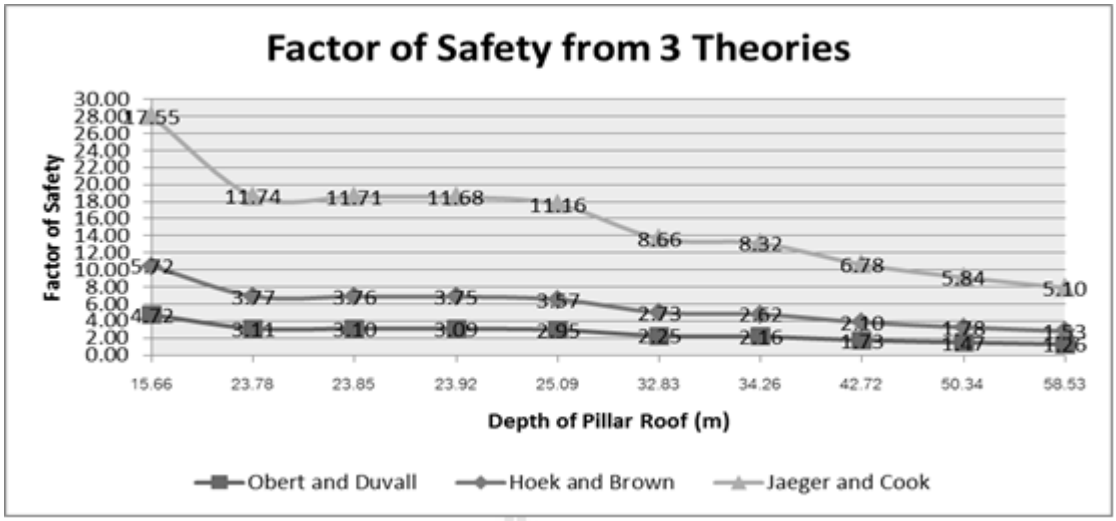

Figure 7.2 Relation between depth of pillar and factor of safety

REFERENCES

Barton, N. (2002). Some new Q-value correlations to assist in site characterization and tunnel design. **International Journal of Rock Mechanics and Mining Sciences.** Vol. 39, pp 185-216.

Barton, N., Lien, R. and Lunde, J. (1974). Engineering Classification of Rock Massess for the Design of Tunnel Support. **Rock Mechanics,** Vol. 6, No. 4, pp. 189-236.

Başarır, H. & Özsan, A. (2002). Support Capacity Estimation of a Diversion Tunnel in Weak Rock, **Engineering Geology**, Elsevier publication, Vol. 68, pp. 319-331.

Bieniawski. Z. T. (1973). Engineering Classification of Jointed Rock Masses. **Transactions, South African Institution of civil Engineer,** Vol. 15, No. 12, pp. 335-344.

Bieniawski. Z. T. (1978). Determining rock mass deformability: Experience from case histories. **International Journal of Rock Mechanics and Mining Science & Geomechanics Abstracts**, Vol. 15, pp. 237-247.

Bieniawski. Z. T. (1979). The Geomechanics Classification in Rock Engineering Applications. **Proc. 4th Int. Congr. Rock Mech., ISRM, Montreux,** Vol. 2, pp. 41-48.

Bieniawski. Z. T. (1983). The Geomechanics Classification (RMR System) in Design Applications to Underground Excavations. **Proc. Int. Symp. Eng. Geol. Underground Constr., LNEC. Lisbon,** 1983, Vol. 2, pp. II.33-II.47.

Bieniawski. Z. T. (1986). Rock Mass Classification in Rock Engineering. **Exploration for Rock Engineering,** ed. Z. T. Bieniawski, A.A. Balkema and Johannesburg, Vol. 1, pp. 97-106.

Bieniawski. Z. T. (1989). Engineering Rock Mass Classifications: **Geomechanics Classification (Rock Mass Ration System).** John Wiley & Sons, New Yoke, 251 pp**.**

Daniele Peila'v · Claudia Guardini", and Sebastiano Pelizza (2008). **Geomechanical design of a room and rib pillar granite mine**. Journal of University of Science and Technology Beuing Volume 15, Number 2, April 2008, Page 97

Fuenkajorn, K.,(2003). **Fundamentals of Rock Mechanics.** The University of Suranaree, Nakhronratsima , Thailand. 210 pp.

Ghafoori, et al. (2006). Comparison of predicted and actual behaviour and engineering geological characterization of the Kallat tunnel, Iran. **The Geological Society of London**, 8 pp.

Grimstad, E. and Barton, N. (1993). Updating of the Q-system for NMT. **International Symposium on Sprayed Concrete. Fagernes, Proceeding,** pp. 46-66.

Hoek, E. (2004). Hoek's Corner. **www. rocscience.com**; accessed December 2004.

Hoek, E. and Brown, E. T. (1980). **Underground Excavations in Rock.** Institution of Mining and Metallurgy, London. 527 pp.

Hoek, E. and Diederichs, M. S. (2005). Empirical Estimation of Rock Mass Modulus. **International Journal of Rock Mechanics and Mining Sciences**, Vol. 43 pp. 203-215.

Hoek, E., Marinos, P. and Benissi, M. (1998). Applicability of the Geological Strength Index (GSI) Classification for Very Weak and Sheared Rock Masses. The Case of the Athens Schist Formation. **Bull. Engg. Geol. Env.** Vol. 57, pp. 151-160.

Howard, L., Hartman. (1987). **Introductory Mining Engineering.** The University of Alabama Tuscaloosa, Alabama , USA. 633 pp.

Kockar, M.K. and Akgun, H. (2003). Methodology for tunnel and portal support design in mixed limestone, schist and phyllite conditions: a case study in Turkey. **International Journal of Rock Mechanics & Mining Sciences**. 40:173-196.

Mahtab, M. A. and Grasso, P. (1992). **Geomechanics Principles in the Design of Tunnels and Caverns in Rocks**. Elsevier publish, New York, 250 pp.

Marinos, P and Hoek, E. (2000) GSI: A Geologically Friendly Tool for Rock Mass Strength Estimation. **Proc. GeoEng2000 Conference, Melbourne.** PP. 1422-1442.

Marinos. P. and Hoek, E. (2001). Estimating the Geotechnical Properties of Heterogeneous Rock Masses such as Flysch. **Bulletin of the Engineering Geology & the Environment (IAEG),** Vol. 60, pp. 85-92.

Palmstrom, A. (1995). **RMi – A Rock Mass Characterization System for Rock Engineering Purposes.** Ph.D.Eng. Thesis, University of Oslo, Norway.

Palmstrom, A. (2009), Combining the RMR, Q, and RMi classification systems. **www.rockmass.net**, 25p.

Palmstrom, A, and Broch, E. (2006). Use and Misuse of Rock Mass Classification Systems with Particular Reference to the Q-system. **International Journal of Tunnels and Underground Space Technology.** Vol. 21, pp. 575-593.

Palmstrom, A. and Stille, H. (2008). Ground behaviour and rock engineering tools for underground excavations. **Tunnelling and Underground Space Technology**. 22: 363-376.

Read, S. A. L., Richards, L. R. and Perrin, N. D. (1999). Applicability of the Hoek–Brown Failure Criterion to New Zealand greywacke rocks. **Proceeding 9th International Society for Rock Mechanics.**

Rocscience, (1998). **Phase^2 User's Guide.** Rocscience Inc, Toronto, Ontario, Canada.

Serafim, J. L. and Pereira, J. P. (1983). Considerations of the Geomechanics Classification of Bieniawski. **Proceedings International Symposium Engineering Geology and Underground Construction, Balkema, Rotterdam,** vol. 1, pp. 1133-1142.

Sonmez, H. and Ulusay, R. (1999). Modifications to the Geological Strength Index (GSI) and their Applicability to Stability of Slopes. **International Journal of Rock Mechanics and Mining Sciences,** Vol. 36, pp. 743-760.

Tugrul, A. (1998). The application of rock mass classification systems to underground excavation in weak limestone, Ataturk dam, Turkey. **Engineering Geology**. 50: 337-345.

ZHU Wei-bing, XU Jia-lin, KONG Xiang, XUAN Da-yang, QIN Wei (2009). **Study on Pillar Stability of Wongawilli Mining Area in Shallow Close Distance Coal Seams.** The 6th International Conference on Mining Science & Technology

APPENDIX

PUBLICATION

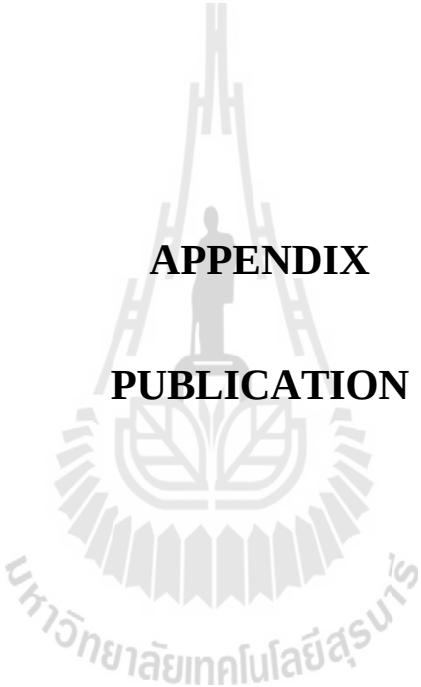

Publication

Choochang, S., Boonbatr, A. and Fuenkajorn, K. (2009). **Stability Analysis and Design of the Final Pit Walls of SCCC Limestone Quarry**. Proceedings of the Second Thailand Symposium on Rock Mechanics, 12-13 March 2009, Chonburi, pp. 293-308.

Rock Mechanics, Fuenkajorn & Phien-wej (eds) © 2009. ISBN 978 974 533 624 7

Stability analysis and design of the final pit walls of SCCC limestone quarry

S. Choochang & A. Boonbatr
Siam City Cement Public Company Limited, Saraburi, Thailand

K. Fuenkajorn
Geomechanics Research Unit, Suranaree University of Technology, Thailand

Keywords: Rock slope, limestone quarry, friction angle, kinematic analysis

ABSTRACT: Geotechnical investigation, rock mechanics testing and numerical simulations are performed to design the safe maximum slope angles of the final pit walls for the Siam City Cement PLC Ltd. (SCCC) limestone quarry. The primary requirement is to ensure the long-term stability during and after site decommissioning while maximizing the limestone reserve. The rock masses along the pit boundaries are classified into two main groups: well-defined discontinuity rocks and heavily-fractured rocks. The maximum bench width and height are pre-defined as 6 m and 12 m. For the well-defined discontinuity rocks the maximum bench slopes are recommended between 70° and 80°, depending on the slope orientations and shapes. This results in working slopes between 49° and 56°. For the heavily-fracturing slope mass the recommended maximum bench angle is 60° with working slope angle of 43°. The recommended designs should be practiced with cushion blasting or with pre-splitting at and near the final wall boundaries. Uncertainty of the geology and rock conditions may encountered as the mine faces are progressed. The designs should be revised accordingly when new relevant data are available.

1 INTRODUCTION

Geotechnical investigation and numerical analyses have been performed to assist in the design of the final walls of the Siam City Cement PLC Ltd. (SCCC) limestone quarry. With an annual production rate of about 15.3 million tons, this is the largest pit quarry in Thailand. The primary objective is to ensure the long-term stability of the final pit walls during and after site decommissioning. The results will also be used to estimate the remaining limestone reserve. The main tasks involve field investigation, theoretical analyses, rock mechanics testing and numerical simulations. Relevant geological data obtained previously by SCCC and its' contractors have been used in this study as much as practical. These include for example mine layout, pit boundary, pit limit, borehole logs, detailed topographic maps and geologic maps. A finite difference computer code (FLAC) is used to verify the stability condition of the designed pit walls.

2 METHODOLOGY

Figure 1 shows the study plan for the analysis and design of the final pit walls of SCCC's limestone quarry. Field investigation is carried out to collect geotechnical data at 20

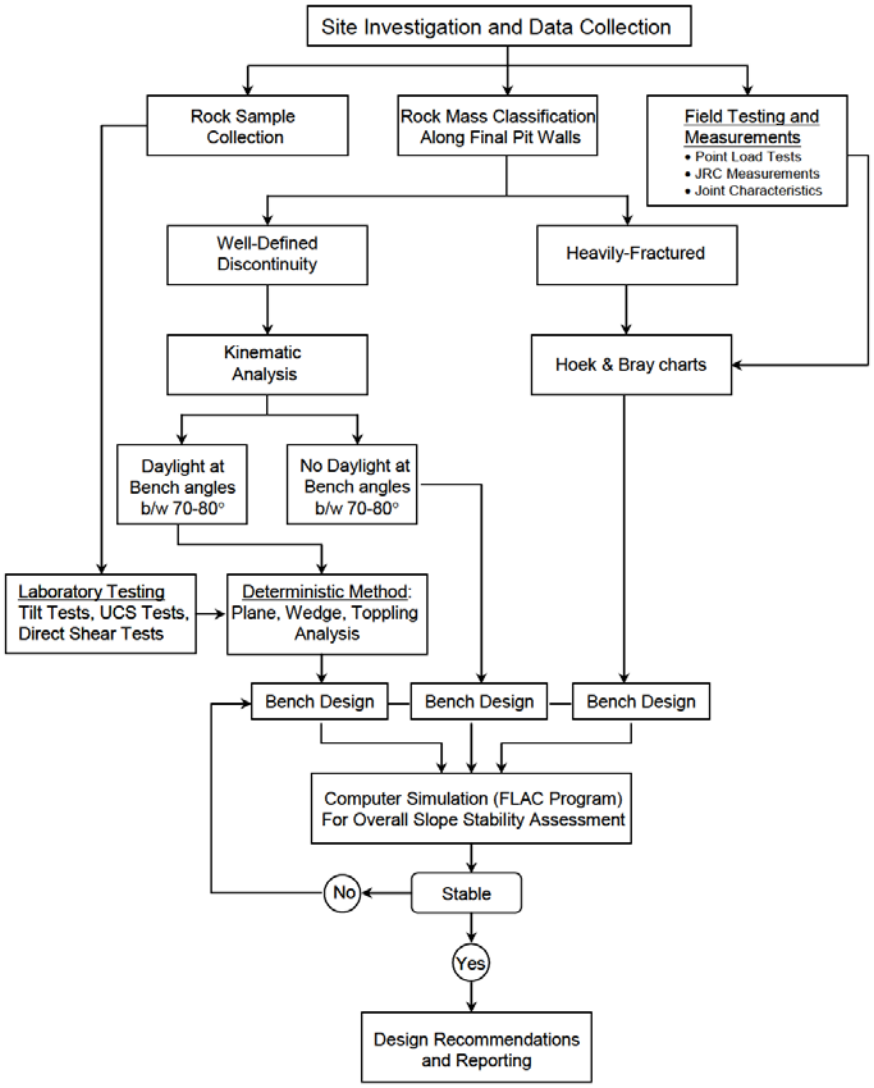

Figure 1. Study plan for determining safe maximum bench slope of the final walls of SCCC limestone pit quarry.

representative points as close as possible to the final pit boundary. Rock samples are collected from some representative points at the site for laboratory mechanical testing. Results from the field investigation are used to classify the rock mass in terms of the

Rock Mechanics, Fuenkajorn & Phien-wej (eds) © 2009. ISBN 978 974 533 624 7

geological engineering properties. Thirty-nine representative sections are defined around the 7.5 km long pit boundary to obtained vertical cross-sections of the final wall geometry and rock conditions. Kinematic analyses are performed on the slope mass with well defined discontinuities (joints and bedding planes). Hoek and Bray's circular failure charts are used to determine the stability condition of the slope mass exhibiting poorly-defined discontinuities and heavily-fracturing. For the kinematic analysis, the daylight conditions are determined for initial bench slope angles of 70° and 80° while considering the varied dip directions of each pit wall section. If no discontinuity is daylight, the bench angle of 70°-80° degrees is initially accepted as a safe maximum angle for that particular section. If any discontinuities show daylight condition, the stability condition (factor of safety) will be further determined by using Hoek and Bray's deterministic method for plane, wedge and toppling failures. These calculations use rock properties obtained from the laboratory and field testing, where applicable, including point load strength index tests, uniaxial compressive strength tests, tilt tests and direct shear tests. The bedding and joint characteristics measured from the field are also used in the factor of safety calculation, including joint roughness coefficient (JRC), apertures, spacing, filling materials and groundwater conditions. After the safe maximum bench slope angles for all pit wall sections are obtained, the stability of the overall pit wall is assessed by using computer simulation. The simulations use the rock mechanics parameters obtained above and the designed pit wall geometry and topographic profiles outside the pit boundary. If the initially-defined pit section geometry is proved to be safe, the design recommendations will be given. If not, the bench angle will be adjusted and the computer simulation will be repeated.

3 SITE INVESTIGATION

The SCCC's limestone quarry at Saraburi Plant composes mainly of limestone and silicified shale. Detailed geology of the site is presented elsewhere (Siam City Cement PLC. Ltd., 2005), and hence will not be repeated here. The general trend of the site geologic structures lies in the northwest-southeast direction. Figure 2 shows the pit boundary which also lies approximately in the northwest-southeast direction. There is a thrust fault lying close to the southwest boundary of the pit. The thrust fault has an average orientation of 145°/40° (strike/dip angle). Adjacent to the thrust zone on the hanging wall is a thin bed (about 30 m thick) of dark silicified shale which can be easily noticed on site. Well-bedded limestone lies on top of the shale. On the footwall, limestone adjacent to the thrust zone sometimes shows heavily fracturing. Away from the thrust zone most limestone mass shows well-defined discontinuities (bedding plane and joints). Along the pit boundaries, the rock near the natural ground surface sometimes exhibits poorly-defined discontinuities or heavily fracturing, and often with clay and silt filling. This is probably due to the weathering process and the local tectonic activity. These weathered zones are up to 15 m deep. Below these zones the limestone mass mostly shows well-defined discontinuities. This is also evidenced by the drill-hole logs obtained by Drillcorp South East Asia Limited (2000). Andesite sills with thickness ranging from 20-40 cm are seldom found in the limestone beds and joints. The andesite appears to be chemically unstable. It is easily disintegrated after exposing to the surrounding environment.

The site investigation is carried out specifically to obtain geotechnical data for rock mass classification, and to collect rock samples for laboratory mechanical testing. For this task a total of 20 stations (points) have been selected to represent the rock conditions around the final pit boundary, as shown in Figure 2. Criteria to select each representative point are: (1) it is as close as possible to the final pit wall, (2) it shows sufficiently large exposed rock surface

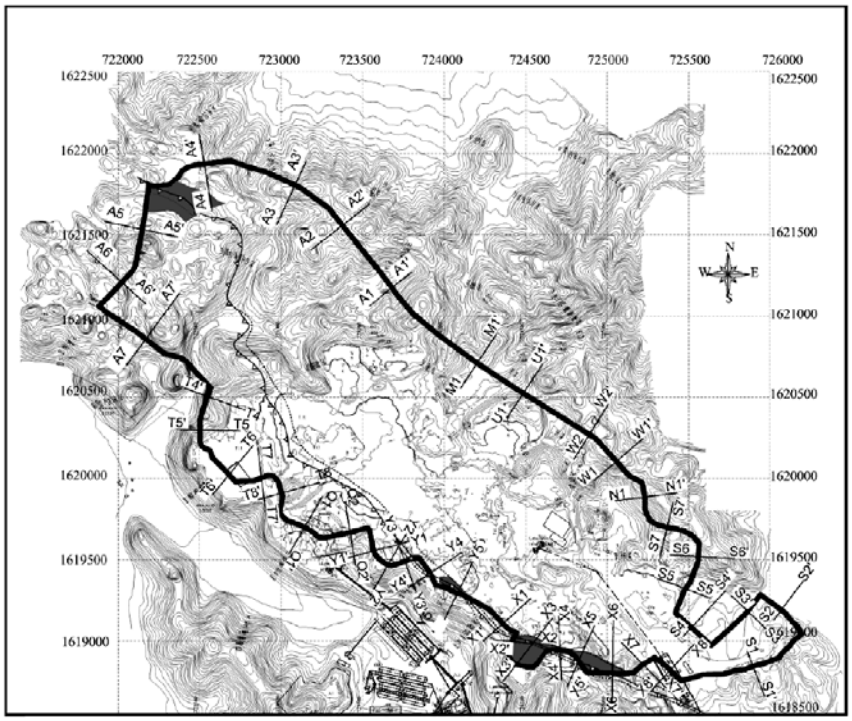

Figure 2. Representative sections defined along 7.5 km long pit boundary.

for geotechnical data collection, and (3) it allows repeatable and reliable rock sample collection. The names and numbers of these points are designated to coincide, as much as possible, with those used on SCCC pit layout. Several investigating points are concentrated along the southwest boundary due to the irregularity of the final pit outline and the exposure of the thrust fault.

The geotechnical data collected at each point include orientation (strike/dip angle) of discontinuities, joint roughness coefficient (based on Barton' roughness profiles), apertures, joint spacing (or bed thickness), joint conditions (apertures, continuity and types of in-filling materials), groundwater conditions. These measurements are made along a minimum traverse length of 50 meters for each representative point. Figure 3 and Table 1 give an example of the directional cosines calculations for the representative discontinuity at Point T11-1.

The rock mass at the representative points can be classified into 2 main categories: well-defined discontinuity rock mass (or blocky rock mass) and heavily-fractured rock mass. The well-defined discontinuity rock mass always comprises three sets of discontinuity: a bedding plane and two joint sets. The later includes poorly-defined discontinuity rock mass and weathered rock mass, usually showing scattered orientations of the discontinuities. The two

Rock Mechanics, Fuenkajorn & Phien-wej (eds) © 2009. ISBN 978 974 533 624 7

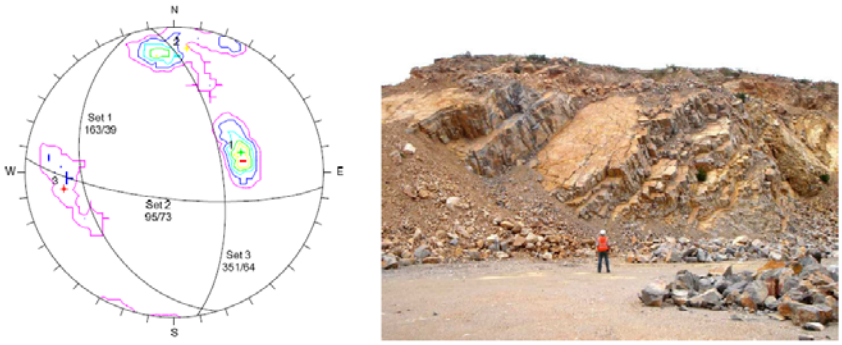

Figure 3. Example of contour and representative planes of discontinuity sets at Point T11-1 (left). Picture of Point T11-1 looking northeast (right).

Table 1. Example of directional cosines calculation for discontinuity Set 1 at Point T11-1.

Strike, α (degrees)	Dip Angle, ψ (degrees)	$l_i = \sin\psi \times \cos\alpha$	$m_i = \sin\psi \times \cos\alpha$	$n_i = \cos\psi$
135	37	-0.4255	0.4255	0.7986
140	44	-0.5321	0.4465	0.7193
140	39	-0.4821	0.4045	0.7771
144	35	-0.4640	0.3371	0.8192
145	40	-0.5265	0.3687	0.7660
155	37	-0.5454	0.2543	0.7986
155	45	-0.6409	0.2988	0.7071
160	40	-0.6040	0.2198	0.7660
163	35	-0.5485	0.1677	0.8192
165	38	-0.5947	0.1593	0.7880
165	40	-0.6209	0.1664	0.7660
165	42	-0.6463	0.1732	0.7431
166	42	-0.6493	0.1619	0.7431
167	37	-0.5864	0.1354	0.7986
168	36	-0.5749	0.1222	0.8090
172	39	-0.6232	0.0876	0.7771
178	53	-0.7981	0.0279	0.6018
180	36	-0.5878	0.0000	0.8090
181	40	-0.6427	-0.0112	0.7660
181	38	-0.6156	-0.0107	0.7880
184	42	-0.6675	-0.0467	0.7431
Summation		-12.3765	3.8883	16.1044

$\overline{R} = [(\Sigma l_i)^2 + (\Sigma m_i)^2 + (\Sigma n_i)^2]^{1/2} = 20.6797$

$l_R = \frac{\Sigma l_i}{\overline{R}} = -0.5985,\ m_R = \frac{\Sigma m_i}{\overline{R}} = 0.1880,\ n_R = \frac{\Sigma n_i}{\overline{R}} = 0.7788$

Mean orientation (Set 1):

Dip angle: $\psi_R = \cos^{-1}(n_R) = 39$ degrees, Strike: $\alpha_R = +\cos^{-1}(l_R / \sin\psi_R) = 163$ degrees (for $m_R \geq 0$)

main categories will therefore be analyzed separately for the bench slope design. The groundwater level of the site is below the pit limit (final pit bottom). This is suggested by the previous SCCC's groundwater investigation. All discontinuities on the slope mass observed here are well-drained and dry.

Table 2 summarizes the results of field investigation and lists the characteristics of the discontinuity conditions. These data will be later used in the stability analysis of the bench slopes and the overall final wall slopes in the following sections.

4 ROCK MECHANICS TESTING

The uniaxial compressive strength of the intact rock and the joint shear strength are needed in the stability analysis and design of the safe maximum bench angles and overall pit angles. Both parameters will be used to develop shear strength criteria for slope stability calculation and computer simulation. Two test methods are used here to obtain the intact rock strength: point load strength index testing and uniaxial compressive strength testing (UCS).

The frictional strength of the discontinuities is determined by tilt testing and direct shear testing. The tilt test is a quick method to estimate the friction angle of discontinuity. The direct shear testing process is lengthy, but it can provide both cohesion and friction angles of the rock discontinuities.

4.1 Point Load Strength Index Testing

The point load strength index tests have been performed on-site. The test method and data reduction follow the standard practice (ASTM D 5731-95). Rock fragments (irregular lumps) with approximate sizes of 10×10×5 cm are loaded to failure. The point load strength index (I_s) is calculated by dividing the failure load by the fracture area. A total of 10 points have been tested with a minimum of 20 samples for each point. The point load strength index is correlated to the uniaxial compressive strength (σ_c) by using a multiplied factor of 24 as suggested by the ASTM standard. The results are summarized in Table 3.

4.2 Uniaxial Compressive Strength Testing

The uniaxial compressive strength tests are conducted at the Geomechanics Research Laboratory, Suranaree University of Technology. Blocks of limestone from six representative points (Points U, V7, T11-2, Q11, Y7 and K) are collected and transported to the laboratory. Sample preparation (drilling & cutting) is performed in accordance with the ASTM D 4543-85 standard practice. The test method and calculation follow ASTM D 7012-07 standard. Five samples have been tested for each selected point. Table 4 summarizes the test results for each point. Note that the strength results obtained here are slightly lower than those correlated from the point load strength index values in Table 3.

4.3 Direct Shear Testing

The direct shear tests are performed to determine the shear strength of the bedding planes of the silicified shale at Point Y6-3. Sample preparation, test method and data reduction follow the ASTM D 5607 standard practice. The normal stresses of 0.7, 1.4, 2.1 and 2.8 MPa are used, which correspond to the bench height range up to 12 meters. Both peak and residual shear stresses are measured. Figure 4 plots the shear stress as a function of the normal stress, showing the shear strength criteria for both peak and residual conditions.

Rock Mechanics, Fuenkajorn & Phien-wej (eds) © 2009. ISBN 978 974 533 624 7

Table 2. Rock mass characteristics obtained from field investigation of 20 representative points.

Station	Rock Type	Rock Mass Classification	Discon-tinuity Set	Orienta-tions (strike/dip)	JRC	Joint Spacing (cm)	Joint Aperture (mm)	Filling Materials
Point U	Limestone	Well Defined Discontinuity	1	130/56	11	50	2.5-10	-
			2	270/69	11	50	0.5-2.5	-
			3	29/71	11	100	2.5-10	-
Point M	Limestone	Heavily Fractured	1	-	11	-	-	Silt/Clay
			2	-	11	-	-	Silt/Clay
			3	-	11	-	-	Silt/Clay
Point V	Shale/ Limestone	Heavily fractured	1	-	11	5	0.5-2.5	Silt/Clay
			2	-	11	15	0.5-2.5	Silt/Clay
			3	-	11	15	0.5-2.5	Silt/Clay
Point V7	Limestone	Well Defined Discontinuity	1	100/69	13	15	2.5-10	-
			2	180/75	13	20	2.5-10	-
			3	325/62	13	100	2.5-10	-
Point T10	Limestone	Heavily Fractured	1	-	11	5	0.5-2.5	-
			2	-	11	10	0.5-2.5	-
			3	-	11	10	0.5-2.5	-
Point T11-1	Limestone	Well Defined Discontinuity	1	163/39	11	20	0.5-2.5	-
			2	95/73	11	50	2.5-10	-
			3	351/64	11	30	2.5-10	-
Point T11-2	Limestone	Well Defined Discontinuity	1	196/40	13	150	0.5-2.5	-
			2	115/71	13	30	0.5-2.5	-
			3	25/59	13	30	0.5-2.5	-
Point T11-3	Limestone	Heavily Fractured	1	-	15	20	0.5-2.5	-
			2	-	15	5	0.5-2.5	-
			3	-	15	10	0.5-2.5	-
Point Q10-1	Limestone	Heavily Fractured	1	-	15	15	0.5-2.5	-
			2	-	15	10	0.5-2.5	-
			3	-	15	10	0.5-2.5	-
Point Q10-2	Limestone	Heavily Fractured	1	-	5	5	0.5-2.5	-
			2	-	5	10	0.5-2.5	-
			3	-	5	10	0.5-2.5	-
Point Q11	Limestone	Well Defined Discontinuity	1	119/56	13	40	0.5-2.5	-
			2	25/80	13	80	0.5-2.5	-
			3	291/48	13	80	0.5-2.5	-
Point Y6-1	Limestone	Well Defined Discontinuity	1	131/64	13	30	2.5-10	-
			2	289/33	13	50	2.5-10	-
			3	218/77	13	50	2.5-10	-
Point Y6-3	Shale/ Limestone	Heavily Fractured	1	-	5	20	0.5-2.5	-
			2	-	5	10	0.5-2.5	-
			3	-	5	5	0.5-2.5	-
Point Y7	Limestone	Well Defined Discontinuity	1	130/54	11	150	2.5-10	-
			2	314/29	11	100	0.5-2.5	-
Point X7	Limestone	Well Defined Discontinuity	1	28/79	11	30	2.5-10	-
			2	274/32	11	50	0.5-2.5	-
			3	101/67	11	50	2.5-10	-

Table 2. Rock mass characteristics obtained from field investigation of 20 representative points (cont).

Station	Rock Type	Rock Mass Classification	Discon-tinuity Set	Orienta-tions (strike/dip)	JRC	Joint Spacing (cm)	Joint Aperture (mm)	Filling Materials
Point X14	Shale/ Limestone	Heavily Fractured	1	-	3	5	0.5-2.5	-
			2	-	3	10	0.5-2.5	-
			3	-	3	5	0.5-2.5	-
Point S4F	Shale	Heavily Fractured	1	-	3	5	0.5-2.5	-
			2	-	3	5	0.5-2.5	-
			3	-	3	5	0.5-2.5	-
Point S4	Shale	Heavily Fractured	1	-	7	5	0.5-2.5	-
			2	-	9	5	0.5-2.5	-
			3	-	9	10	0.5-2.5	-
Point K	Limestone	Well Defined Discontinuity	1	111/53	11	200	0.5-2.5	-
			2	2/70	9	100	2.5-10	-
			3	286/60	11	100	2.5-10	-
Point W	Limestone	Heavily Fractured	1	-	7	10	2.5-10	Silt/Clay
			2	-	7	5	2.5-10	Silt/Clay
			3	-	7	15	2.5-10	Silt/Clay

Table 3. Point load strength index testing results for SCCC limestone and silicified shale.

Station	Rock Types	Point Load Strength Index, I_s (MPa)	Uniaxial Compressive Strength, σ_c* (MPa)
Point M	Limestone	3.2 ± 1.2	76.8 ± 28.8
Point V	Limestone	3.4 ± 1.7	81.6 ± 40.8
Point T10-2	Limestone	2.5 ± 0.8	60.0 ± 19.2
Point T11-3	Limestone	3.5 ± 1.5	84.0 ± 26.0
Point Q10	Limestone	3.5 ± 1.4	84.0 ± 33.6
Point Y6-1	Silicified Shale	2.4 ± 1.5	57.6 ± 36.0
Point Y6-3	Limestone	3.9 ± 1.6	93.6 ± 38.4
Point X14	Silicified Shale	4.8 ± 1.9	115.2 ± 45.6
Point S4F	Silicified Shale	2.5 ± 1.2	60.0 ± 28.8
Point W	Limestone	2.5 ± 1.6	60.0 ± 38.4

Note: $\sigma_c^* = 24 \cdot I_s$ (from ASTM D5731-95)

Table 4. Uniaxial compressive strength testing results for SCCC limestone.

Station	Rock Type	Density (g/cc)	Uniaxial Compressive Strength (MPa)
Point U	Limestone	2.77	58.0 ± 8.3
Point V7	Limestone	2.79	64.9 ± 19.2
Point T11-2	Limestone	2.77	60.2 ± 10.4
Point Q11	Limestone	2.77	56.7 ± 1.9
Point Y7	Limestone	2.75	50.3 ± 9.3
Point K	Limestone	2.76	76.1 ± 14.6

Rock Mechanics, Fuenkajorn & Phien-wej (eds) © 2009. ISBN 978 974 533 624 7

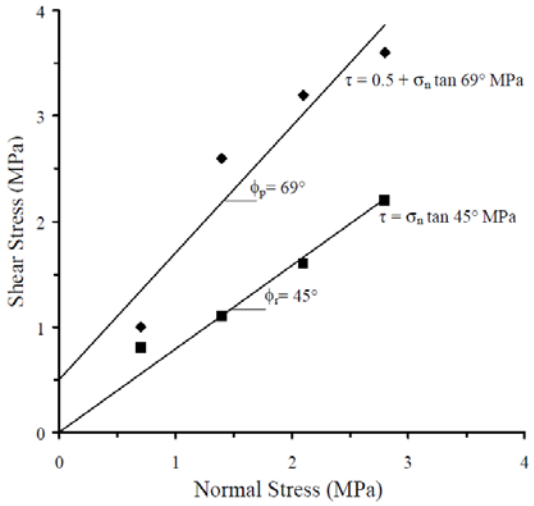

Figure 4. Shear stress as a function of normal stress for bedding plane in silicified shale from Point Y6-3.

4.4 *Tilt Testing*

The tilt tests are performed in the laboratory to obtain friction angles of the original bedding plane and joint in the limestone and shale. The values will be used to compare with those obtained from the Barton's shear strength criteria derived from the concept of basic friction angle and JRC values (to be discussed later). Ten rock blocks containing the discontinuity have been collected. The friction angles of the shale beds are averaged as 57 ± 7 degrees. The limestone beds and joints have friction angles varying from 42 to 63 degrees.

4.5 *Slake Durability Index Testing*

The slake durability index (SDI) test is performed on andesite to predict the durability (strength) of the rock as a function of time. The sample preparation and test method follow the ASTM D 4644 standard practice, except that up to six test cycles is performed, instead of two as suggested by the standard. Two sets of samples are prepared for testing under wet and dry conditions. The method to predict the rock durability uses the concept proposed by Fuenkajorn (2008). Figure 5 presents the ΔSDI as a function of test cycles and time. The results suggest that the andesite strength rapidly decreases after it has been exposed to the surrounding environment. Water and fluctuation of temperatures accelerate the strength degradation. Under wet condition, andesite changes from high durability rock to very low durability within 6 months. Under dry condition the rock changes from high to very low durability within a year.

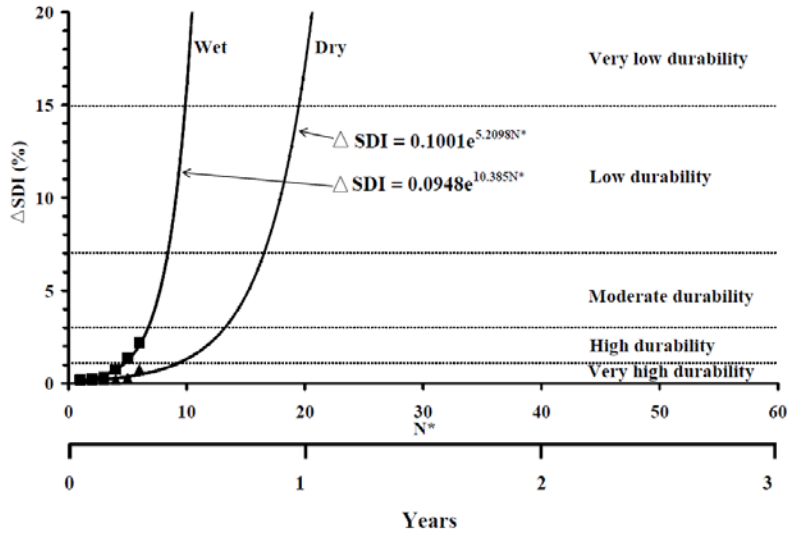

Figure 5. ΔSDI as a function of N* and time for slake durability testing of andesite. The conditions as collected are plotted at cycle no. 6.

5 KINEMATIC ANALYSIS

5.1 Correlation between Barton's and Coulomb's Shear Strength Criteria

The primary objective of this task is to determine the friction angle of the discontinuities for use in the kinematic analysis. First the Barton's shear strength criterion is defined for 18 representative points around the pit wall. The Barton's shear strength (τ) can be defined as follows.

$$\tau = \sigma_n \cdot \tan\left(\phi_b + \mathrm{JRC} \cdot \log\frac{\sigma_c}{\sigma_n}\right) \quad (1)$$

It has been found that the basic friction angle (ϕ_b) of limestones and marbles elsewhere tend to be consistent between 33° and 36° (Waltham, 1994; Grasselli & Eager, 2003; Kemthong, 2006). To be conservative the basic friction angle of 33° is selected here for the kinematic analysis. The JRC of discontinuities is obtained from geotechnical data collected during the field investigation. The uniaxial compressive strengths (σ_c) are taken from the point load and uniaxial strength tests of the rock samples from nearby representative points. Figure 6 gives example of the correlations for 2 representative points. A line fit for σ_n between 100 and 400 psi (normal stresses equivalent to the stresses at slope toe) are drawn to represent the equivalent Coulomb's shear strength criterion, and subsequently the friction angle (ϕ) and cohesion (c) can be determined from the gradient and intercept of that line, as follows.

Rock Mechanics, Fuenkajorn & Phien-wej (eds) © 2009. ISBN 978 974 533 624 7

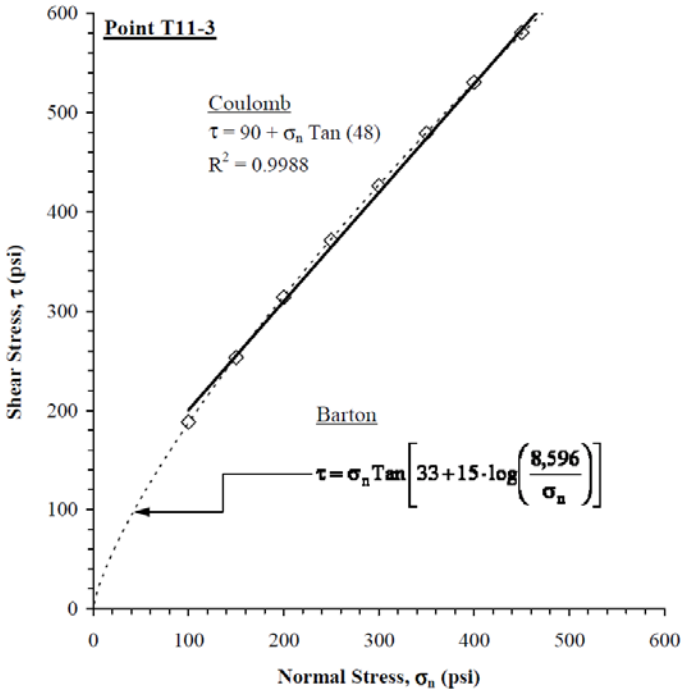

Figure 6. Example of Coulomb joint shear strength derived from Barton criterion at Point T11-3. Barton: $\phi_b = 33°$, JRC = 15, σ_c = 8,596 psi, Coulomb: $\phi = 48°$, c = 90 psi.

$$\tau = c + \sigma_n \cdot \tan \phi \quad (2)$$

where: τ = shear strength and σ_n = normal stress.

Table 5 summarizes the correlation results between Barton's and Coulomb's shear strength criteria for 18 representative points.

5.2 Results of Kinematic Analysis

Kinematic analysis is performed to determine whether the failure is possible (daylight condition) for the bench slopes with well-defined discontinuities. This task can be accomplished by presenting the friction angle, and orientations of the slope face and discontinuities in form of the stereo-graphic projections (Hoek & Bray, 1981). To obtain the orientations of the bench slope a total of 39 representative sections are assigned around the final pit wall boundary. This results in 39 cross-sections of the benches around the pit boundary, with different slope orientations and rock conditions. Since these sections are normal to the pit boundary, the strike or dip direction of the bench slope can be determined. Twenty out of 39 sections comprise well-defined discontinuities. The rest (19 sections) comprises heavily-fractured slope mass.

Table 5. Correlation results between Barton's and Coulomb's criteria.

Station	Barton's Parameters			Coulomb's Parameters	
	ϕ_b (degrees)	JRC	σ_c (psi)	c (psi)	ϕ (degrees)
Point U	33	11	8,410*	50	44
Point M	-	-	-	0	30***
Point V	33	11	11,940**	53	46
Point V7	33	13	9,410*	69	46
Point T10	33	11	21,040**	54	46
Point T11-2	33	13	8,730*	68	46
Point T11-3	33	15	8,600**	90	48
Point Q10-1	33	15	12,080**	102	50
Point Q10-2	33	5	12,080**	17	39
Point Q11	33	13	8,220*	67	46
Point Y6-1	33	13	11,800**	77	48
Point Y6-3	33	5	11,800**	17	39
Point Y7	33	11	7,290*	48	43
Point X7	25	3	16,530**	8	29
Point X14	25	3	16,530**	8	29
Point S4F	25	3	8,600**	8	28
Point S4	25	5	8,600**	8	28
Point K	33	11	11,020*	53	45
Point W	-	-	-	0	30***

Notes: * Obtained directly from uniaxial testing
** Calculated from point load testing ($\sigma_c = 24\ I_s$)
*** Friction angle of silt/clay filling (Waltham, 1994)

The friction angle for the kinematic analysis is taken from (1) results from the tilt testing, or (2) correlation between the Barton's and Coulomb's shear strength criteria. For representative sections that are close to the points where the tilt testing was performed the friction angle from the tilt test will be used. The rest of the representative sections where tilt test result is not available will use the friction angle determined from the correlation between Barton's and Coulomb's criteria. Figure 7 shows an example of the stereo-graphic projections for section Q2 with well-defined discontinuities.

6 ANALYSIS OF BENCH SLOPE USING DETERMINISTIC METHOD

The deterministic method of Hoek & Bray (1981) is used in the analysis of the bench slope on representative sections around the final pit wall. Seven sections with daylight conditions are analyzed to determine their safe maximum bench angle. Assessment of the plane and wedge sliding is performed on the seven slope sections. The circular failure analysis is performed on 19 sections with heavily fractured rock mass. All analyses assume dry condition. The maximum bench height is pre-defined by SCCC as 12 meters. Toppling failure is assessed on-site for all representative sections. It is concluded that large scale toppling failure is very unlikely because the spacing for the three observed discontinuity sets are relatively small and comparable.

Rock Mechanics, Fuenkajorn & Phien-wej (eds) © 2009. ISBN 978 974 533 624 7

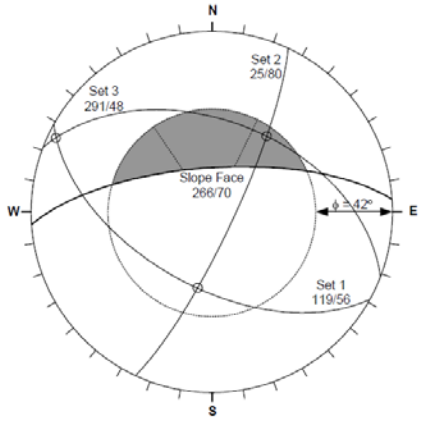

Figure 7. Example of kinematics analysis for bench slope at Section Q2. Discontinuity set 3 shows daylight condition.

7 COMPUTER SIMULATION FOR OVERALL SLOPE STABILITY

After the safe maximum bench angles have been designed for all representative sections, numerical simulation is performed to verify that the overall final pit wall at various sections will remain stable, and to ensure that large scale failure will not occur. The analysis uses finite difference code FLAC (Itasca, 1992). Physical and mechanical properties obtained from the test results from nearby point are used as data input. The results are calculated in terms of the factor of safety and distribution of displacement vectors in the slope mass. Figures 8 and 9 show examples of the simulations in terms of the slope profiles, displacement vectors, strain rate contours, and factor of safety for sections U1 and T5. It can be concluded that all slopes with the designed bench angle are safe, showing the factor of safety between 2.16 and 2.74. This suggests that a large scale failure is unlikely.

8 CONCLUSIONS AND DESIGN RECOMMENDATIONS

The results of the study lead to the design recommendations on the safe maximum final pit wall angles. The recommendations are based on the maximum bench height of 12 meters and minimum bench width of 6 meters. Three design schemes are recommended, as follows.

Scheme I: For sections T5-T7, Q2, Y1, Y2, Y4, Y5, X1-X6 and N1
Maximum bench angle = 80°
Maximum working pit slope = 56°

Scheme II: For sections U1, A1-A6, T8, Q1, Y3 and X7
Maximum bench angle = 70°
Maximum working pit slope = 49°

Scheme II: For sections M1, S2, S6, S7, W1 and W2
Maximum bench angle = 60°
Maximum working pit slope = 43°

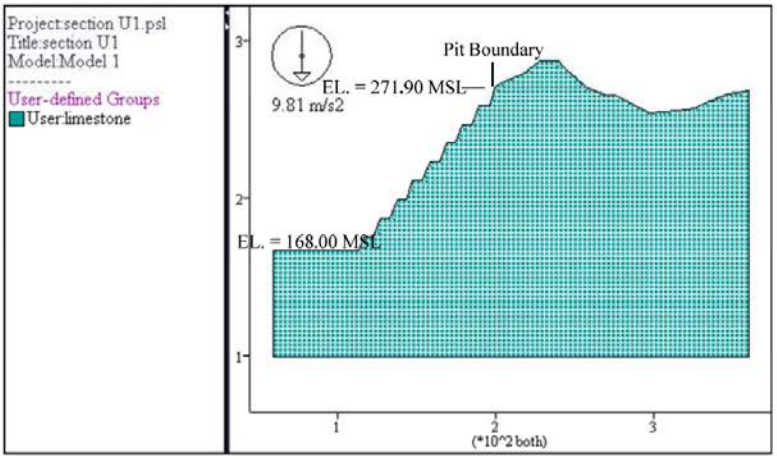

(a) Generated Mesh

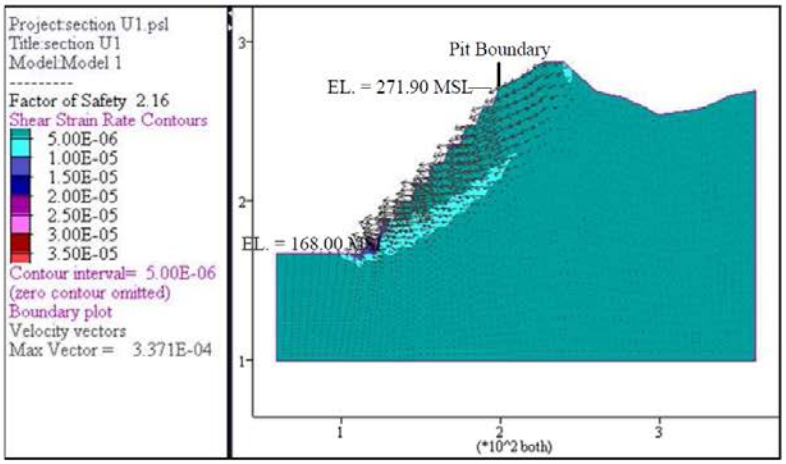

(b) Shear strain rate contour and displacement vector

Figure 8. Example of stability evaluation of overall slope for Section U1 using FLAC simulation. Bench slope = 70°, Bench width = 6 m, Overall slope = 49°, F.S. = 2.16.

Rock Mechanics, Fuenkajorn & Phien-wej (eds) © 2009. ISBN 978 974 533 624 7

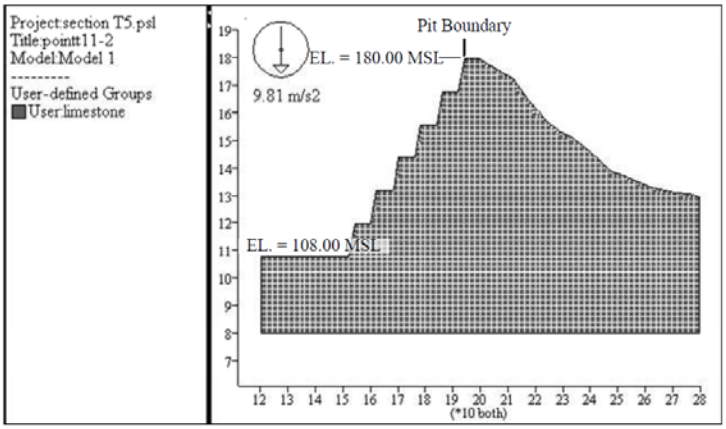

(a) Generated Mesh

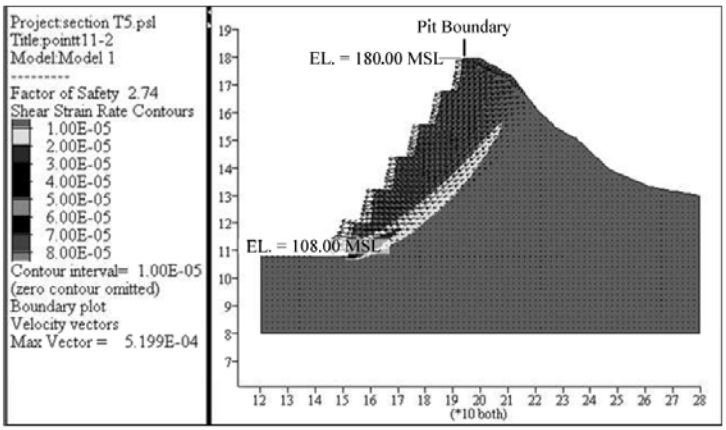

(b) Shear strain rate contour and displacement vector

Figure 9. Example of stability evaluation of overall slope for Section T5 using FLAC simulation. Bench slope = 80°, Bench width = 6 m, Overall slope = 56°, F.S. = 2.74.

The design recommendations are based on the available information and on the existing mine faces and outcrops at the time of the study. Uncertainty of the geology and rock conditions may encountered as the mine faces are progressed. A particular concern on this regard is the presence of andesite sill. As suggested by the test results here the andesite can quickly disintegrate with time, and hence may cause stability problem to the pit slope if it exposes under unfavorable position and orientation. The designs therefore should be revised accordingly when new information or relevant data are obtained.

ACKNOWLEDGEMENT

The authors would like to thank Siam City Cement PLC. Ltd. for the financial supports and for permission to publish this paper.

REFERENCES

ASTM D 4543-85. Standard practice for preparing rock core specimens and determining dimensional and shape tolerances. *Annual Book of ASTM Standards (Vol. 04.08).* Philadelphia: American Society for Testing and Materials.

ASTM D 4644-87. Standard Test Method for Slake durability of shale and similar weak rocks. *Annual Book of ASTM Standards (Vol. 04.08).* Philadelphia: American Society for Testing and Materials.

ASTM D 5607. Standard test methods for performing laboratory direct shear strength tests of rock specimens. *Annual Book of ASTM Standards (Vol. 04.08)*. Philadelphia: American Society for Testing and Materials.

ASTM D 5731-95. Standard test method for determination of the point load strength index of rock. *Annual Book of ASTM Standards (Vol. 04.08).* Philadelphia: American Society for Testing and Materials.

ASTM D 7012-07. Standard test method for unconfined compressive strength of intact rock core specimens. *Annual Book of ASTM Standards (Vol. 04.09).* West Conshohocken, PA: ASTM.

Barton, N.R., 1971. A relationship between joint roughness and joint shear strength. In *Proc. International Symposium on Rock Fracture*. Nancy, France. pp. 1-8.

Bieniawski, Z.T., 1978. Suggested Methods for determining the uniaxial compressive strength and deformability of rock materials. *International Journal of Rock Mechanics and Mining Sciences & Geomechanics Abstracts*. International Society for Rock Mechanics Commission on Standardization of Laboratory and Field Tests. pp. 35-140.

Drillcorp South East Asia Limited, 2000. Drillhole Summary and Geological Log of Drillhole. *Prepared for Siam City Cement PLC. Ltd.* Kaeng Khoi, Saraburi.

Fuenkajorn, K., 2008. Prediction of Long-Term Strength of Some Weak Rocks in Thailand. In *Proceedings of the First Southern Hemiphere Rock Mechanics Symposium, September 16-19*. Perth, Western Australia.

Grasselli, G. & Egger, P., 2003. Constitutive law for the shear strength of rock joints based on three-dimensional surface parameters. *International Journal of Rock Mechanics and Mining Sciences & Geomechanics Abstracts*. 40: 25-40.

Ground Data Probe Co., Ltd., 2007. *SCCC Exploration Campaign 2006 Quarry Rock Investigation Works*, Factual Report. Prepared for Siam City Cement Public Company, Limited.

Hoek, E. & Bray, J.W., 1980. *Rock Slope Engineering*. 3rd edition, London: Institute of Mining and Metallurgy.

Itasca, 1992. *FLAC – Fast Langrangian Analysis of Continua*. Version 4.0, User Manual, Itasca Consulting Group, Inc., Minneapolis, MN.

Kemthong, R., 2006 *Determination of rock joint shear strength based on rock physical properties*. M.Eng. Thesis, Suranaree University of Technology, Nakhon Ratchasima.

Siam city cement PLC. Ltd., 2005. Geological Map of SCCC. *Concession, Prepared by Sa-Nguan Choochany of SCCC*. Sheet no. AP-006/49.

Waltham, A.C., 1994. *Foundations of Engineering Geology*. 1st ed. Blackie Academic & Professional. Glasgow, London.

Wyllie, D.C., 1992. *Foundations on Rock*. Chapman & Hall, London.

BIOGRAPHY

Mr. Sa-nguan Choochang was born on the 20st of March 1977 in Kalasin province. He earned his Bachelor's Degree in Geology faculty of science in 1985 from the Khonkean University (KKU). For his post-graduate, he works in geologist both of private sector and government officer, as follow these;

- 1981 – 1982 Engineer Geologists: Department of Irrigation Officer
- 1982 – 1985 Project Managers: Siam Scope Mining Company
- 1985 - 1992 Division Managers: Department of Mineral Resources
- 1992 - 1999 Division Managers: Asia Cement Public Company.
- 1999 – 2003 Project Managers: Siam Carbon Lignite Company.
- 2003 - 2004 Senior Geologists: Italian Thai public Company.
- 2004 – 2007 Area Manager, Siam City Concrete Company.

Since, 2007 to recent (2014) he is division manager of raw material and fuel exploration at Siam City Cement Public Company. He has been responsible in geological exploration and production mine planning for raw material of limestone, Shale, Clay, Iron ore and Coal. He has published a technical papers related to rock mechanics as; in 2011, *"Room and Pillar design for Phetchaboon Coal mine project"* in the proceeding of the thirds Thailand symposium on rock mechanics, Cha-am, Thailand. He has taken the geologist license no 235 from Geological Society of Thailand.